MULTI SENSOR BASED DRILL WEAR MONITORING USING ARTIFICIAL NEURAL NETWORK

A Thesis Submitted

In Partial Fulfillment of the Requirements

for the Degree of

DOCTOR OF PHILOSOPHY

by

Mr. Sudhansu Sekhar Panda

Department of Mechanical Engineering

Indian Institute of Technology Guwahati,

Guwahati-781 039, INDIA

July 2007

MECHANICAL ENGINEERING DEPARTMENT

INDIAN INSTITUTE OF TECHNOLOGY GUWAHATI

GUWAHATI-781039

CERTIFICATE

It is certified that the work contained in the Thesis entitled **"Multi Senor Based Drill Wear Monitoring Using Artificial Neural Network"** submitted by **Mr. Sudhansu Sekhar Panda** to the Indian Institute of Technology Guwahati for the award of the degree of Doctor of Philosophy has been carried out under my supervision in the Department of Mechanical Engineering, Indian Institute of Technology Guwahati. This work has not been submitted elsewhere for the award of any other degree or diploma.

30th July 2007

(Debabrata Chakraborty)
Associate Professor
Department of Mechanical Engineering,
Indian Institute of Technology Guwahati,
Guwahati – 781 039

Dedicated to

My father late Sri Purna Chandra Panda

Mother Srimati Padmabati Panda

and

Loving Rudrakhya, Kunu, Papala, Niki and Mamuni

ACKNOWLEDGEMENTS

This thesis is the result of four years of work whereby I have been accompanied and supported by many people. It is a pleasant aspect that I have now the opportunity to express my gratitude for all of them.

I would like to express my greatest appreciation to Dr. Debabrata Chakraborty for his patient guidance and encouragement during the doctoral degree course. As my supervisor, his insight, observations and suggestions helped me to establish the overall direction of the research and contributed immensely to the success of the work. The research hadn't been possible without his invaluable support, advice and encouragement. I would like to appreciate to Dr. Surya Kanta Pal at Indian Institute of Technology Kharagpur, India for his time-to-time detailed comments and suggestions during the period of my research work.

I would like to thank my doctoral committee members, Prof P. S. Robi, Prof C Mohanta and Prof S Deb for their valuable discussions and help whenever I needed. I would like to render thanks to them for their question and discussion during my research. I am grateful to the Head of the Department of Mechanical Engineering, Professor U. S. Dixit for extending various facilities during the tenure of my Ph.D programme.

I would like to thank Prof R. K. Dutta, Head, Mechanical Engineering Department at Assam Engineering College, Guwahati for his detailed comments and suggestions during the period of my research work. I am also grateful to all the faculty members of mechanical engineering for giving me a comfortable and active environment for pursuing my research.

I am grateful to superintendent Mr. D. K Sharma, Mr. D. Deka and other technical staffs of mechanical workshop, Indian Institute of Technology Guwahati for their help to conduct the experiment. I would like to express my thanks Mr. A. K. Singh, Mr. S. Garg, Mr. A. Dutta and Mr. S. Panda (IIT Kharagpur) for their help in conducting the experiments. I would like to express my thanks all research scholar of Indian Institute of Technology Guwahati for their supports, advice and many helps.

I am grateful to my parents, brothers, sisters, relatives and friends for their constant encouragement and moral support. I would like to offer my thanks to them for their affection, tolerance, support and endless encouragement for which I could reach the present stage.

At last but not least I am grateful to Indian Institute of Technology Guwahati for providing me financial support to carry out the present thesis work during my Ph.D. period.

Sudhansu Sekhar Panda

30th July 2007

IIT Guwahati

ABSTRACT

Tool condition monitoring (TCM) is one of the most important activities in modern manufacturing activities. Proper implementation of TCM system not only prevents catastrophic failure of tool but also increases the productivity of the industries. Drilling is one of the most common machining operations used in industries and hence monitoring of the drill condition is of significant importance in industries. Among different causes of drill failure gradual wear of the drill is unavoidable and needs to be monitored to avoid sudden failure of the drill. The present work focuses on the possibilities of different strategies that could be adopted for development of an artificial neural network (ANN) based drill wear prediction systems. Combinations of different sensor signals and other parameters, which are influenced by the drill wear have been used to frame different strategies along with four different ANN architectures. Results indicates that the ANN based drill wear prediction systems can predict drill wear reasonably accurately when fused with appropriate sensor signals. Results from the comparative performances of different prediction system would be helpful in designing the appropriate drill wear monitoring system for a particular application.

CONTENTS

List of Figures

List of Tables

Nomenclatures

F	Thrust force
β	Point angle
M_{ch}	Chisel edge moment
I	Input vector
n	Number of nodes
W_{ji}	Layer weights matrix
x	Activation function
f	Transfer function
S	Logistic sigmoid function
N	Input patterns
d	Output vector
E	Mean square error
e	error at output layer
ΔW	Incremental weights matrix
T	Target output
η	Learning rate
α	Momentum coefficient
LR	Left and Right
μ_m	Degree of membership
α_1, β_1	Left and right spread parameters
CE	Centroid operation
ed	Euclidean distance
v	Center vector
σ	Width of center
M	Numbers of centers

CHAPTER 1
INTRODUCTION

This chapter describes the development of tool condition monitoring in general and the importance of drill wear monitoring in particular. The role of soft computing techniques in tool condition monitoring (TCM) has also been described in brief.

1.1 Development of manufacturing system

Manufacturing is the application of physical and chemical processes to alter the geometry, properties and appearance of a given starting material to make parts or products. Manufacturing industries consists of enterprises and organizations that produce and supply goods and services [1]. During the invention of machine tools, hand tools survived till several thousand years for their purpose. In late ninth century, gauges used in machine tool for serving the interchangeability of the product. In early twentieth century, transfer line played an important role in the manufacturing industry. During 1950-1970, applications of numerically controlled machine tools dominated the manufacturing industries. In late eighties, application of intelligent manufacturing induced the revolution in the economy, quality and productivity of the manufacturing industries. There are two distinct types of manufacturing processes that rely on the behavior of material past the yield point to form required shape of work piece. The first is a *deformation process*, which produces the required shape by plastic deformation of material while conserving mass, and the second one is the *machining process*, which forms the required shape of work piece by removing materials. Machining can also include *non-traditional processes* in which material is removed by other means such as electrically, chemically and optically. *Traditional machining* uses cutting tools to perform milling, drilling, sawing, turning and broaching operation. Hence, the study of metal cutting focuses on the features and behavior of work material that influences the efficiency and quality of cutting condition. Cutting conditions of a machining operation is improved by using the technology of other field of engineering and science appropriately. Higher productivity through faster material removal rate is one of the essential requirements in deciding the cutting condition and hence the cutting conditions can be optimized in order to enhance the economy of the manufacturing system through machining.

1.1.1 Flexible manufacturing system

Globalization of market, demand of customer and congenial environment for investment compelled the manufacturing system to adopt new technologies and new materials. Manufacturing industries are powerful contributors to the economy. The technology involved in manufacturing system (especially in metal cutting) has advanced with the developments in material selection, computer applications and sensor technology. One of the *states of art* in manufacturing system is the computer simulation of machining processes to acquire important information like knowledge of power requirement, cutting force, chip formation, signal analysis and to help precision manufacturing with less human intervention. Integration of computer in the form of computer controlled machine tools, jigs and fixtures with computer aided design (CAD), computer aided processing planning (CAPP), computer aided inspection (CAI), computer aided assembly (CAA), marketing, management task by the computer network have resulted in modern flexible manufacturing systems (FMS). Appropriate use of intelligent robots along with control systems to the FMS leads to intelligent manufacturing systems capable of better utilization of resources.

1.1.2 Features of flexible manufacturing system

(i) Minimum changeover cost and time

(ii) Maximum flexibility and quick turn around capability

(iii) Minimum down time for continuous maintenance attention

(iv) Maximum breadth of product range

(v) Ability to adopt a variation in materials and process

(vi) Ability to integrate new technologies into an existing system with minimum disturbance

(vii) Maximum adoption to variation in production volume

(viii) Ability to handle increasingly complex product design and technology

(ix) Allows for just in time manufacturing

1.2 Drilling

Drill is a tool designed to produce holes in metal parts quickly and easily. Drilling is a roughing operation and the primary items of interest are usually long life and high penetration rate. Very frequently drilling is a preliminary operation to reaming, boring or grinding where final finishing and sizing take place [2]. It was estimated that fourty percent of all the metal removal operations in the aerospace industry are by drilling [3]. Four major actions which take place during hole making operation are [2]

(i) A small hole is pierced by rotating the web (chisel)

(ii) Chips are formed by rotating the cutting edges

(iii) Chips are conveyed out of the hole in the form of helical flute

(iv) Drill is guided in the hole already produced by the margin

The geometry that is ordinarily provided on a drill represents a compromise of several conflicting requirements, which include [2]

(i) A small web to reduce thrust on the drill but a large web for greater resistance to chipping and greater torsional rigidity

(ii) Large flute to provide a large space for chip transport but small flute in the interest of torsional rigidity

(iii) An increase in helix angle to more quickly remove chip but a decrease in helix angle in the interest of greater strength of cutting edges

Twist drills are generally made of high speed steel (HSS) or carbon steel. Cemented carbide tipped drills are also used in mass production work. Process parameters in drilling viz. cutting speed, feed-rate and drill diameter are chosen depending on the material of the tool, the work-piece, desired hole quality, dimensional

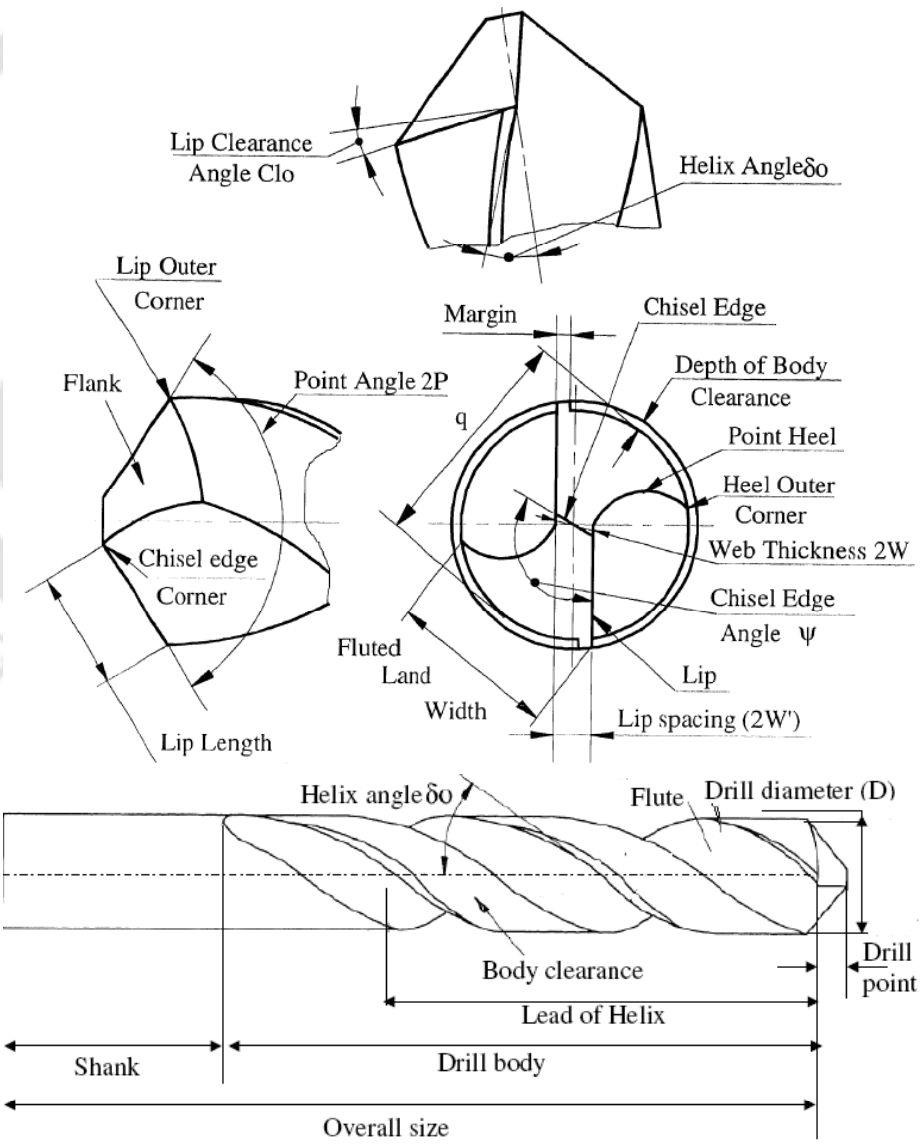

Figure 1.1 General geometry of the conventional twist drill

accuracy, capacity of the drilling machine and the cutting environment. Quality of hole produced by drilling operation mainly depends on the feed rate, spindle speed, work piece material, drill geometry and drill material. Drill geometry includes various cutting angles and linear dimension, which affect chip formation, tool strength, wear rate, cutting force, surface finish and tool chatter. Cutting fluids are used to improve surface finish and for reducing the friction at tool work-piece interface. Twist drills have complex geometry. Figure 1.1 [2,4] shows the geometry of conventional twist drill. Twist drill geometry includes various angles like rake angle, lip clearance angle, point angle and linear dimensions like flute length, lead of helix, lip length and body clearance diameter [2,4-6]. As shown in figure 1.1, drills have three general types of cutting edges viz. main cutting edges (lip), a chisel edge, and marginal cutting edges. The main cutting edges are formed by the termination of the flutes at the point. They remove most of the materials in the hole and typically account for almost all of the drilling torque. They contribute significantly to drilling thrust. The chisel edge is formed by the termination of the drill's central web at the point. It contributes substantially to the drilling thrust but due to its central position, relatively little to torque. It also determines the centering accuracy of the drill.

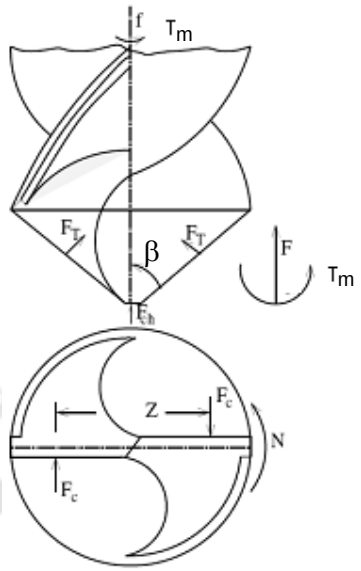

Figure 1.2 Developement of thrust force and torque

Various forces acting on a drill are shown in figure 1.2 [6]. The effect of all the forces acting on the drill can be represented by, a resisting torque (T_m) and a thrust force (F). The action at the chisel edge is not truly a cutting action, rather it is one which pushes into the material like a wedge. But the effect of the chisel edge on the torque is negligible as it is on the axis of rotation. The contribution of the chisel edge to the development of the thrust force is considerable.

The total thrust force can be expressed as [6]

$$F = 2F_t \sin\beta + F_{ch} + F_{friction} \tag{1.1}$$

Where

F_t = Cutting force component,

F_{ch} = Force from chisel edge,

$F_{friction}$ = Frictional force component,

β= Point angle,

Similarly, the total torque can be written as

$$T_m = F_c \times Z + M_{ch} + M_{friction} \tag{1.2}$$

where,

Z=Distance between the point of application of force,

M_{ch} = Moment from the chisel edge,

$M_{friction}$ = Moment due to the friction.

F_c = Cutting force component acts against the cutting speed

Force acting on the tool depends upon the material removal rate. Quantities influencing the torque and thrust to which a drill is subjected in producing a hole are work material, drill diameter, helix angle, length of chisel edge, point angle, number of cutting edges, feed rate and cutting fluid [7-9].

1.2.1 Failure mechanism of drill

Drills are designed to operate within limits specified by the environment in which they will be used. At the design stage, the strength of the drill is defined and appropriate material choices are made based on their properties. Drills are subjected to an extremely severe rubbing process during its operation. They are in metal-to-metal contact between the chip and work piece, under conditions of very high stress at high temperature. The situation is further aggravated due to the existence of extreme stress and temperature gradients at the cutting edges of drill. During drilling operation, drills remove materials from the component to achieve the required shape, dimension and surface roughness (finish). However, wear of the drill occurs during the cutting action, and it ultimately results in the failure of the drill. When the drill wear reaches a certain allowable limit, the drill or active edge has to be replaced to guarantee the desired cutting action. A drill is considered to have fail when it is unable to cut, consuming reasonable energy, and cannot produce an acceptable finish. The failure of drill may be due to one or combination of the following different modes are [4]

(i) Plastic deformation of drill due to high temperature and large stress

(ii) Mechanical breakage of drill due to large force and insufficient strength

(iii) Blunting of cutting edges of the drill through a process of gradual wear due to rubbing action at the cutting tool and work piece interface

By proper selection of drill material, drill geometry and cutting conditions, first two of the above mentioned modes of failure could be prevented. However, the gradual wearing process cannot be avoided which ultimately leads to the failure of drill [4-6].

1.2.2 Drill wear mechanism

Broadly cutting tool wear specific to drill can be classified into [10]

(i) Crater wear
(ii) Flank wear
(iii) Notch wear
(iv) Chipping
(v) Corner wear
(vi) Chisel wear
(vii) Margin wear

(i) Crater wear

The chip flows across the rake face, resulting in severe friction between the chip and the rake face. This phenomenon results a scar on the rake face. The crater wear increases the working rake angle, reduces the cutting force and reduces the strength of the cutting edge. The crater depth *KM* is the most commonly used parameter in evaluating the crater wear and is shown in figure 1.3.

Figure 1.3 Crater wear width

(ii) Flank wear

Wear on the flank (relief) face is called flank wear. Flank wear, most commonly results from abrasive wear of the cutting edge against the machined surface. Flank wear can be measured by using the average and maximum depth of wear size V_b and $(V_b)_{\max}$ as shown in figure 1.4. The criteria recommended by international organization for standardization (ISO) to define the effective tool life for high-speed steel tool is regularly worn flank wear V_b of 0.3mm or maximum flank wear $(V_b)_{\max}$ of 0.6mm [5,11]. Progress of the wear on the flank face is shown in figure 1.5. *Initial wear region* is caused by micro cracking, surface oxidation and carbon loss in layer, as well as micro roughness at the cutting tool tip. For a new cutting edge, the small contact area and high contact pressure

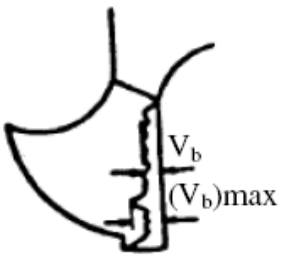

Figure 1.4 Flank wear

results in high wear rate. *Steady wear* region occurs after the initial (or preliminary) wear and happens to make the cutting edges round. In this region the micro roughness is improved, and the wear size is proportional to the cutting time. The wear rate is relatively constant. *Severe (catastrophic) wear* likely to initiate when the wear size exceeds a critical value. The surface roughness of the machined surface decreases, cutting force and temperature increase rapidly, the wear rate increases and the tool loses its cutting ability.

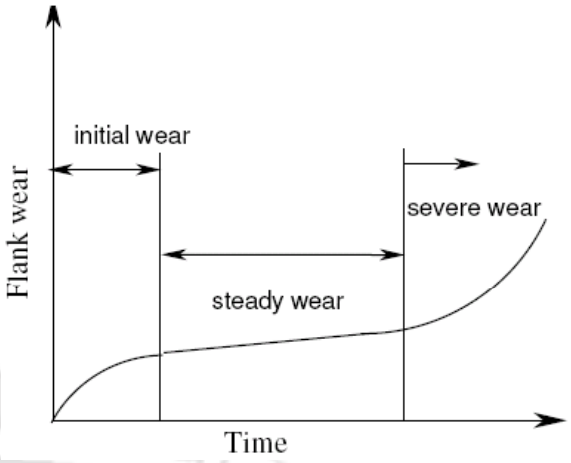

Figure 1.5 Progressive flank wear

(iii) Notch Wear

This is a special type of combined flank and rake face wear which occurs adjacent to the point where the major cutting edge intersects the work surface. The gashing (or grooving, gouging) at the outer edge of the wear land is an indication of a hard or abrasive skin on the work material. It is also common in machining of materials with high work-hardening characteristics.

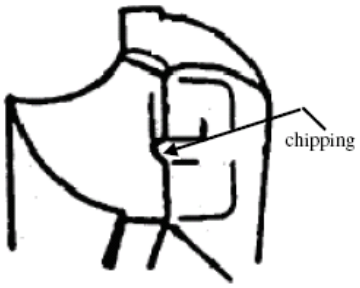

Figure 1.6 Chipping of drill

(iv) Chipping

Chipping of the tool, as the name implies, involves removal of relatively large discrete particles of tool material. Tools subjected to discontinuous cutting conditions are particularly prone to chipping. Chipping of the cutting edge is more like micro-breakages rather than conventional wear. Built-up edge formation also has a tendency to promote tool chipping. A built-up edge is never completely stable, but it periodically breaks off. Each time some of the built-up material is removed, it may take with it a lump (piece) of tool edge known as chipping is shown in figure 1.6.

(v) Corner wear

It specifically occurs at the corner of the drill point as shown in figure 1.7. This is due to high friction and impact forces between the drill and machined hole walls.

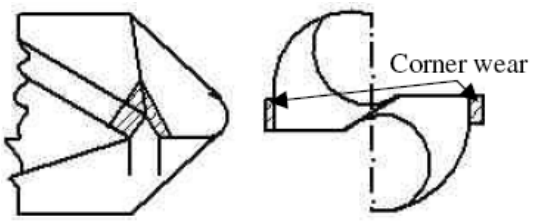

Figure 1.7 Corner wear

(vi) Chisel wear

Chisel wear normally occurs due to very high shear and compressive stresses in the flow zone of the tool work piece interface acting at high temperatures, which causes erosion of the chisel edge as shown in figure 1.8.

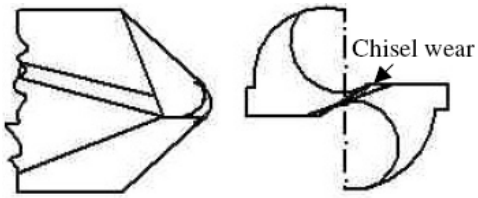

Figure 1.8 Chisel wear

(vii) Margin wear

Margin wear occurs due to rubbing of marginal cutting edges of drill with the work material resulting high temperature generation as shown in figure 1.9.

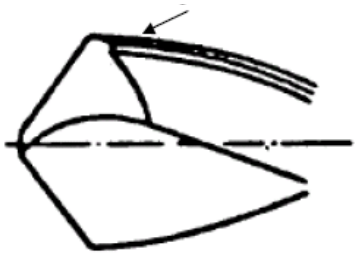

Figure 1.9 Margin wear

1.2.3 Causes of drill wear

Important tool wear mechanism [4-6] of cutting tool (drill), which is in contact with softer but deforming metal (work piece) sliding past the former at a fairly high speed are classified into following category

(i) Hard particle wear (abrasive wear)
(ii) Adhesive wear
(iii) Diffusion wear
(iv) Chemical wear
(v) Fracture wear

(i) Hard particle wear (abrasive wear) is mainly caused by the impurities or hard particle within the work piece material. These hard particles act as small cutting edges, which in due course is worn out through abrasion. In addition, these particles plough into the surface of hard tool metal, which intermittently get torn out and dragged along the tool surface. This is a mechanical wear, and it is the main cause of the tool wear at low cutting speeds.

(ii) Adhesive wear is based on the simple mechanism of friction. On account of friction, high temperature and pressure, particles of softer material adhere to a few high spots of harder material forming so-called built up edge which periodically breaks taking it with a piece of tool edge.

(iii) Diffusion wear is based upon the concept of atomic transfer at contacting asperities. When cutting tool is in sliding contact with a softer work piece material and the temperature at their interface is high, atomic transfer from cutting tool to work piece material occurs. This kind of wear strongly depends upon temperature.

(iv) Chemical wear occurs due to localized chemical reaction and hence weakens the tool material through formation of weak compound or dissolution of the bond between the binder and the hard constituent in the cutting tool.

1.2.4 Consequences of drill wear

Gradual wearing at the cutting edges of a drill deteriorates the performances of the drill during drilling. Cutting forces, surface finish of work piece, vibration and chatter, chip characteristics get affected by drill wear. Some of the significant consequences of drill wear are [7-9]

(i) *Cutting forces* usually increase with the increase in extent of wear

(ii) *Surface finish* produced in a machining operation usually deteriorates with wears

(iii) *Dimensional accuracy* gets affected by the flank wear

(iv) *Vibration and chatter* is another aspect of the cutting process, which is influenced by wear

(v) *Production efficiency and component quality* reduces due to drill wear

(vi) *Cost of component* increases due to wearing of tool

(vii) Tool wear leads to increase in power consumption resulting reduction in *economy*

1.3 Tool condition monitoring (TCM)

TCM is a field of technical activity in which selected physical parameters, associated with tool in operation, are observed for the purpose of determining tool condition. Although the technologist and application of tool condition monitoring is continually evolving, its conceptual basis can be traced back to the earliest development of machinery and the use of human senses to monitor the state of industrial equipment. The approach of looking, listening and using our senses of touch, smells and taste is still valid, although nowadays it is heavily augmented by scientific and sophisticated instrument. The use of such instruments allows us to quantify the health or the condition of the tool so that problems (if any) can be diagnosed and corrected by suitable maintenance or replacement before any catastrophic failure takes place. TCM therefore involves the design and use of sensing arrangement together with data acquisition and analysis system along with predictive and diagnostic methods with the objective of implementing tool maintenance in a planned way using actual knowledge of the tool condition.

Basic approaches for TCM are

(i) Detection provides a qualitative indication of presence of any defect in the cutting tool.

(ii) Classification provides about the type of defect.

(iii) Assessment provides an estimate of the extent of the defect.

(iv) Prediction offers the information about the safety of the product with knowledge of estimating the residual life of cutting tool.

1.3.1 Need for TCM

The material and geometry of cutting tools are generally so developed that cutting tool can be in service for reasonably long period of time. Cutting tool ultimately fails by slow growing of systematic wear. In spite of careful manufacture and selection, a cutting tool may often fail undesirably, randomly and catastrophically due to inadequate hot strength, hardness, excessive thermal stress, micro-cracks, mechanical breakage due to excessive stress. Such premature and random failures if occurs, it not only hamper production and enhance the tool cost, but also may cause severe damage to the work piece and machining system. Therefore attempts should be initially be made to avoid such rapid tool failure by taking all possible care during manufacturing, selection and use of cutting tools. Keeping in view maximum utilization of resources and prevention of random and catastrophic failure of cutting tool while working, the best strategy would be the continuous monitoring of condition (nature and extent of work, crack, wear etc) of cutting tool along with progress of machining and withdrawal of the tool at appropriate time i.e. just before the tool actually fails. Such tool condition monitoring, preferably on-line, is becoming an essential feature, particularly for sophisticated and expensive machining systems, which are increasingly used in modern manufacturing industries.

The back ground for the TCM is important due to the following reasons

(i) Increase in the tool availability and reliability

(ii) Improvement of operating efficiency

(iii) Improves the risk management (less down time)

(iv) Reduces maintenance costs (better planning)

(v) Improves safety

(vi) Improves knowledge of tool condition

(vii) Improves the customer relation

Hence cost effective unmanned production is the only possible in practice if there is a reliable method available for tool condition monitoring. In the absence of tool condition monitoring the quality of production will be poor as surface finish and dimensional accuracy are influenced by the condition of the tool. Gradual wear on a tool with machining time leads to the deterioration of the condition of the tool leading to the final failure. Hence

the extent of wear on the tool being an important parameter indicating the condition of the tool needs to be continuously monitored.

1.3.2 Techniques for TCM

Tool condition monitoring (TCM) is the domain of research and experimentation for determining in advance the impending tool failure during machining so that a planned tool change policy may be adopted. Primarily, the objective of TCM programme should be to predict tool failure on one side and also to identify the cause of failure among the variety of failure modes on other side. TCM application involves use of sensors to gain the knowledge of a machining process kept under surveillance. Because of noisy machining environment corrupting the useful signals informations, multiple sensors are used to supplement each other, aiming at retrieving the signals information. TCM may be accomplished broadly by two methods, viz. off-line and on-line. The off-line method has been the conventional technique over the years where machining activities are temporarily suspended to inspect the condition of the tool at certain intervals. Often the off-line methods help to some extent in indirect assessment of tool condition and deciding whether the tool should be withdrawn. However, it suffers from large down time of machining system causing substantial reduction in productivity and increase in production cost. Such limitation of off-line methods could be overcome by use of on-line methods where the tool condition is continuously monitored, preferably indirectly, without stopping the machining process. A great variety of monitoring methods are available for on-line tool wear monitoring. In principle, there are two possible approaches for on-line monitoring, i.e. direct methods and indirect methods. Direct methods measure tool wear directly. Unfortunately these direct methods are based on either visual inspection or computer vision have not become economically or technically advanced enough for use in industries. Instead of wear, indirect monitoring methods measure some other parameters, which must be a function of the extent of wear on the tool. Inherent problems associated with direct information and measurement of tool condition in on-line TCM could be avoided if the tool condition is indirectly evaluated on-line by monitoring and analysis other machining responses, which indicates the condition of the tool. Indirect monitoring techniques considered the different signals collected over time domain or frequency domain or both time-frequency domains to be analyzed to obtain the tool condition. A large variety of sensors are available for indirect on-line TCM among which force, vibration, sound, temperature, power, torque or motor current and acoustic emission measuring devices are found to be suitable for on-line TCM. The sensor output in the form of signal, generally is not the phenomenon considered to

interpret the tool condition. Instead, a systematic procedure is followed to process it and find meaningful parameters, which are sensitive to the condition and the type of failure of the tool expected in a specific machining process. In other words, after the signals are collected by sensors, those are analyzed by signal processing techniques to extract the features representing the signal behavior in most explicit manner. A number of such features are finally utilized in the framework of knowledge based decision systems to arrive at comprehensive idea about the tool condition. The prediction and classification of the tool state is done using a variety of statistical method such least square regression, response surface methodology, group method of data handling, time series model, frequency series model and wavelet technique. In recent time different soft computing techniques have been used by many researchers for prediction and classification of tool state.

1.4 Role of soft computing in TCM

Soft computing refers to a collection of new computational techniques in computer science, artificial intelligence, machine learning, and many applied and engineering areas where one tries to study, model and analyze physical phenomena. Generally speaking, soft computing techniques resemble human reasoning more closely than traditional techniques, which are largely based on conventional logical systems. The guiding principle of soft computing is to exploit the tolerance for imprecision, uncertainty, partial truth, and approximation to achieve tractability, robustness and low solution cost. Soft computing differs from conventional (hard) computing in that, unlike hard computing, it is tolerant of imprecision, uncertainty, partial truth, and approximation. Some of the important areas of soft computing which find application in TCM are fuzzy systems, artificial neural network (ANN) and evolutionary computation. ANN has been extensively used in TCM because of it's inherent advantages over other prediction tools.

1.4.1 Advantages of ANN in TCM

Neural networks can be seen as an attempt to automate the process of building a prediction system. In TCM, neural networks can be trained to model non-linear dependencies of manufacturing process parameters as well as sensor signals on the condition of the tool. Properties of artificial neural network (ANN) attractive in tool condition monitoring application could be summarized as follows

(i) It is like a device with adaptive and fault tolerance capability and can reduce the error apparent in the sensor signal to a low level and concentrate on recognizing tool wear state.

(ii) ANN is a data driven device and not a programme-driven as in conventional computer and can handle huge amount of data.

(iii) ANN can handle the data in noisy environment and can classify the pattern properly.

(iv) ANN is composed of highly parallel processing element and different learning strategies.

(v) ANN can handle the complex non-linearity in data and represent a complicated or poorly understood relationship between independent and dependent variables.

(vi) ANN models require less formal statistical training to develop.

(vii) ANN models have the ability to detect all possible interactions between predictor variables.

(viii) ANN can be developed using multiple different training algorithms

1.4.2 Advantages of fuzzy system in TCM

Fuzzy system exhibits immense potential for effectively solving the uncertainty in a problem. Fuzzy system provides a simple way to arrive at definite conclusions based on vague, ambiguous, imprecise, noisy, or missing input information. In a sense, fuzzy logic resembles human decision making with its ability to work from approximate data and find precise solutions. Some times fuzzy variables are used to train ANN for developing prediction systems useful for TCM. This kind of fuzzy ANN has the following advantages

(i) Fuzzy system is inherently robust since it does not require precise, noise-free inputs.

(ii) Since fuzzy system is user-defined rules governing the target output, it can be modified easily to improve system performance.

(iii) Fuzzy system allows the sensors to be inexpensive and imprecise thus keeping the overall system cost and complexity low.

(iv) Because of the rule-based operation, any reasonable number of inputs can be processed and numerous outputs generated, although system becomes complex if too many inputs and outputs are chosen for a single implementation

(v) Fuzzy system can control nonlinear systems that would be difficult or impossible to model mathematically. It has tendency to be used as an on-line controller.

1.5 Organization of the thesis

The present thesis has been organized as follows.

Chapter 1 introduces the significance of tool wear monitoring along with different techniques of tool condition monitoring in general and drill wear monitoring in particular.

In order to understand the state of art in the broad field of TCM and drill wear monitoring in particular, comprehensive literature review has been done and presented in chapter 2.

Chapter 3 presents theoretical description of ANN and fuzzy-neural network used in the present work.

Details of experimental set up used for conducting the experiments are described in chapter 4 of the thesis.

Chapter 5 described the experimental results, their analysis and important observations. Different TCM strategies and application of ANNs for prediction of drill wear used in the present work have been presented in chapter 6.

In chapter 7 fuzzy neural network based drill wear prediction methodologies have been presented and an overall comparison of all the possible strategies attempted in the present work has also been presented.

Chapter 8 concludes the thesis outlining the important conclusions drawn from the present work and it also discusses the scope for the future work.

CHAPTER 2

LITERATURE REVIEW

The problem of development of a decision based system and prediction of tool wear have attracted many researchers. There have been lots of efforts in the direction of prediction of wear using indirect methods. In this chapter review of existing literature in this area has been presented in four sections. The first section discusses the research carried out on deterioration and failure of drill. Second section presents the literature on multi sensor based tool condition monitoring. Third section represents different signal analysis techniques for tool wear monitoring. The last one reviews the application of soft computing techniques in the study of drill wear prediction. Motivation and the objective of the present work have been given at the end of this chapter.

2.1 Deterioration and failure of drill

The reason for acquiring the drill wear state information is to enhance the predictive capability to allow the machine operator to schedule tool change just in time to avoid under-use or over-use of tools, to avoid shutdown of machines due to damage, and to minimize scrap or rework. On the other hand, drill wear affects the ability of the hole cutting system to satisfy specified performance characteristics, such as hole roundness, centering, burr formation at drill exit and surface finish.

Kanai and Kanda [10] reported that several different types of drill wear could be recognized as outer corner wear, flank wear, margin wear, crater wear, chisel wear and chipping at the lip. Rehorn *et al.* [12] reported that drilling operation differs significantly from turning and face milling as drilling is a complex three dimensional material removal operations, unlike relatively simpler cases of orthogonal and oblique cutting. They also reported that drills have vastly different geometries compared to turning and face milling tools and observed that chip flow creates a significant friction between tool and work piece and hence changes the dynamic of the system causing the drill to break. The most widely tool failure modes in turning operation are flank wear, fracture, crater wear and plastic deformation as reported in some early works [13,14]. They also reported that flank and crater wear are generally accepted as the normal tool failure modes, as the others can be avoided by selecting the proper machining parameters. Wardany *et al.* [15] reported that mechanism of drilling is quite different from other machining operations due to the fact that the two points of the drill wear alternately until they both have zero clearance at the margin, and become lodged

within work piece. Thangaraja and Wright [16] reported that drill wear is an accelerating process that takes place at the outer margin of the flute of drill due to intimate contact and elevated temperature at tool work piece contact. In their study, they reported three distinct zone of progressive drill wear as initial wear zone, moderate wear zone and excessive wear zone.

Inasaki [17] reported that the detection of tool breakage or chipping and the determination of the cutting tool state is problematic in multipoint cutting tools due to non constant chip thickness throughout the cut and the fact that more than one cutting edge might be active at the same time. Hong [18] studied failure of drill due to outer corner wear, flank wear, asymmetry, difference in lip height, margin wear crater wear breakage; chisel edge wear, chipping at lip. He also reported that manufacturing process has many inherent factors which affect the criteria in judging drill wear or breakage, such as drill size, drill material, drill geometry, work piece material, cutting speed, feed rate, material microstructure, hardness distribution, etc. Rubenstein [19] proposed the equivalence of spade drill with twist drill based on chip deflection and the chip thickness ratio. Average width of crater as well as maximum depth of flank wears as criteria for tool failure in turning operation have been reported in some early works [20-21]. Nouari *et al.* [22] reported necessary information about the main factors influencing the hole quality i.e. cutting speed, temperature, feed rate, geometrical parameters as well as the influence of the cutting conditions and the temperature on the tool life in drilling. They reported the improvement of surface quality and a dimensional accuracy of the holes at large cutting speed values and a weak feed rate.

Elanayar and Shin [23] suggested that crater wear prediction is seen to be poor in contrast with flank wear. They reported that variable feed machining was superior to constant feed machining with respect to tool life, burr height, and surface roughness. Lin [24] reported the maximum tool life at optimize feed rate and speed. He also reported that the dominant wear is at the cutting edge and the outer corner when drilling stainless steel using TiN-coated curved cutting edge carbide drills. Some researcher [25-26] studied on the principle of tool wear in drilling and developed an approach to model flank wear using various techniques and discussed the influence of various wear modes like adhesion, abrasion and the influence of temperature. Morin *et al.* [27] reported that feed rate affects drilling forces and wear, but cutting speed has no significant effect over the range of speeds. They also reported that both drilling torque and thrust vary linearly with flank wear, so that a measurement of either may be used to estimate wear.

Zhou *et al.* [28] reported that passive force exhibits a higher sensitivity to the tool wear than main cutting force in turning operation. Gao *et al.* [29] suggested chip deformation cut by the inner edge is the largest in the three cutting edges of the boring and trepanning association (BTA) drill. They also reported that the chip deformation increases when the feed rate increases, and decreases when the rake and cutting speed increases. Some of the early works [30-31] reported that the tool breakage is a major cause of unscheduled stoppage in a machining environment, and is costly not only in terms of time lost, but also in terms of capital destroyed in milling operation. Yeo *et al.* [32] reported that cutting speed, feed rate, depth of cut, cutting forces, the force ratios as well as reflectance of chip surface are indicative parameters of the flank wear of a tool in turning operation.

2.2 Multi sensor based tool condition monitoring

The metal cutting process is highly nonlinear involving such phenomena as plastic deformation, fracture, impact, continuous and intermittent multi contact points, friction and wear. Direct visual inspection of the cutting edges during machining is not feasible because the work piece and chips obstruct the view. Due to the complexity of the cutting process, it is often not possible to obtain a mathematical description of the relevant dynamics of the process. To overcome this difficulty, indirect methods are required. Sensors are needed in these systems to identify unexpected failure. Sensory systems are increasingly playing a pivotal role in the realization of advanced automated manufacturing systems. However, it is difficult to decide on the best parameters to measure, and on the analysis methods to adopt for the system under investigation. The cost of the sensory system is another important consideration and should be accounted for when designing an industrial monitoring system. Drill wear affects the ability of the hole cutting system to satisfy specified performance characteristics, such as hole roundness, centering, burr formation at drill exit, and surface finish. An alternative approach in engineering applications is the utilization of more than one sensor signal, from different sources to detect the same parameter. Sensor fusion can enhance the quality of the quantity under investigation to yield a better outcome.

Micheletti *et al.* [33] discussed various types of sensors for in-process measurement of tool wear in metal cutting operation. Azouzit and Guillot [34] reported that the sensor selection and fusion method assisted the experimenter in determining the average effect of each sensor on the performance of detecting surface finish in a turning operation. Sensor based approach for tool condition monitoring is categorized into four sub section viz. force sensor and motor current sensor, vibration and sound sensor, acoustic emission sensor.

2.2.1 Torque, force and motor current

The forces in drilling are known as feed force and thrust forces. As with all other machining operations, the forces on drill increases as the drill edges and its cutting edges become dull. Thangaraj and Wright [35] measured only the thrust, or axial, component of force for TCM in drilling operation, although Braun *et al.* [36] used all drilling forces and spindle torque simultaneously. They reported another commonly measured quantity for TCM applications is the cutting torque, as it is related directly to the cutting forces. Thrust force and torque can be difficult and expensive to monitor; thus spindle current is measured in some of the early works [3,37-39] instead of thrust force and torque and they reported the use of drive variables such as spindle current and power have proven to be useful for the detection of breakage and the determination of wear in drilling. Ramamurthi and Hough [40] used the spindle and feed motor current as inputs for the machining influence diagram-based TCM system. They also used spindle motor and feed motor current together with thrust force to predict tool failure. One purpose of their study was actually to test whether current sensor would be sufficient for drill wear monitoring since it is cheaper and easier to use than other methods.

Elhachimi *et al.* [41] reported that drill torque and drill thrust forces for sharp drills varied with feed rate in the same way they do for classical materials. They also reported that feed rate affects the drilling forces and wear, but cutting speed has no significant effect on drilling force and wear. Lin and Ting [42] used the force signal to monitor online drill wear. They used the least square method for determining the thrust force, and torque as a function of spindle speed, feed rate, drill diameter and average flank wear. Many researchers [43-52] used thrust force and torque as a good indicator of tool wear and tool breakage in turning as well as in drilling operations. Liu and Chen [53] have extracted eight indices from thrust force for correlating drill wear. Szecsi [54] reported that close relationship exists between the axial force and the flank wear of the cutting tool and described the ratio of incremental force to incremental depth of cut as the best feature for flank wear estimation in turning operation. Wang *et al.* [55] suggested that mean of power consumption of spindle motor is sensitive to tool wear in turning operation.

Some literatures [56-60] reported that spindle motor and feed motor current are sensitive to burr formation and drill wear in drilling and reported good results for either in tool breakage or in tool wear estimation. Kumar *et al.* [61] reported that time series force signal produces better co-relationship with tool wear compared to the time series vibration signal. Damodarasamy and Raman [62] used the combination of the radial force, feed force and

acoustic emission (AE) signals in predicting the tool flank wear in a turning operation. Lee *et al.* [63] reported that dynamic characteristics of cutting force signals could interpret the tool wear state more efficiently in turning.

Jemielniak [64] had used strain gauges to measure three component of force in turning operation. Franco-Gasca *et al.* [65] used spindle drive current to study the dynamics of drilling process and to monitor the cutting tool condition. They reported that the wavelet transform is helpful in monitoring the condition of tool. They also reported that asymmetry algorithm can distinguish between a worn and a usable drill with high reliability and also provides an accurate estimate of drill wear under different drilling conditions. Shi *et al.* [66] reported that sensory signals viz. surfaced-mounted strain sensors, transverse strain sensors and integrated force sensors, correlate with the dynamometer signal very well in broaching operation. They also reported that these sensor signals are sensitive to detect tool wear and tool chipping.

2.2.2 Vibration and sound

The drill is assumed to vibrate freely at the tip and is only restricted by the radial forces. Vibration is most widely used measuring method in condition monitoring of rotating machinery. Vibration is measured both in the transverse and axial direction. The vibration signals are considered to contain reliable features for monitoring drill wear and breakage. The natural frequencies of the transverse and axial modes of the work piece drill system are basically insensitive to drill cross sectional size. Vibrations in the radial and feed directions are influenced by the torque and thrust force.

Abu-Mahfouz [67] reported that accelerometer when properly shielded have good resistance against coolants, chips, electromagnetic or thermal influences. He reported that accelerometers are easily replaceable and are very cost-effective in drilling. Vibration monitoring techniques applied to the detection of drill failure, have been reported by several investigators [68-69]. Hong *et al.* [70] used multiple sensor integration for identifying the mode of drill failure. They used vibration signals for identifying the symmetry and non-symmetry portion of drill cutting edges. Scheffer and Heyns [71] used eight different features extracted from vibration signature as input to the self-organizing map (SOM) for wear classification in turning operation.

Prateepasen *et al.* [72] studied the coherence function between the acceleration signals at the tool tip in the tangential and feed directions in turning. They identified coherence function in the frequency ranges 2.5-5.5 kHz and 18-25 kHz. Hayashi *et al.* [73] reported that the frequency range in vibration measurements is typically from about 1 Hz to about 10

kHz (or 20 or 16 kHz is used as a limit); in sound measurements the range is from 20 Hz to 20 kHz, which is the range a young person can hear; in ultrasonic vibration the frequency range is from 20 kHz to about 80 kHz. Weller *et al.* [74] reported that the vibration signatures of machining processes, including low-frequency vibrations of tooling systems have potential sources for monitoring of the condition of the tool in a metal cutting operation. Lee *et al.* [75] reported that signals carry a great deal of information about the originating sources and travel rapidly through the machine structure and hence, an appropriate sensor located remotely from the environmentally hostile cutting zone can potentially monitor even the very short events of the cutting process that cannot be monitored by any other means.

Tageia *et al.* [76] investigated the mutual relationship between tool wear and vibration power spectrum over a frequency range of 0.5 Hz to 30 kHz. They recorded the vibration energy spectra from several series of very carefully controlled machining experiments through an accelerometer attached to the tool holder. Bahr *et al.* [77] combined an on-line, indirect technique (tool fracture detection based on vibration signals) with an offline, direct technique (wear area measurement by means of a CCD camera) in turning operation. A somewhat different approach for use of vibration signals for monitoring drill wear was developed some workers [78-79]. In this system, an accelerometer was mounted on the work piece and the vibration signal was analyzed in the time domain. Successive segments of vibration signal equivalent to one full revolution of the drill bit were analyzed and if the amplitude exceeding a pre-selected level was detected then drill bit was considered worn beyond its useful life. Lim [80] in his work correlated the flank wear of tool with the acceleration amplitude of vibration signature in turning operation and he concluded that vibration acceleration produces two-peak amplitudes just before tool failure.

Haber *et al.* [81] reported that time domain of cutting force and vibration signals signatures relevant for tool-wear monitoring in high-speed machining processes. They also reported that the mean and peak values of cutting force and the vibration signal exhibit the best performance for tool-condition monitoring. Dimla [82] reported that cutting forces (static and dynamic) and vibration (acceleration) are most widely applicable parameters for tool wear monitoring in turning operation. Dimla and Lister [83] reported that vertical components of both cutting forces and the vibration signatures were most sensitive to tool wear. They also reported that nose wear is the most useful indicator of tool failure in turning. Dimla and Lister [84] again reported that depth of cut is most sensitive and cutting

speed is least sensitive parameter among the cutting parameters for tool wear monitoring in turning operation.

Therefore vibration monitoring presents a unique and attractive opportunity for monitoring the details of a cutting process. Various components of cutting forces fluctuate rapidly. These fluctuating conditions are reflected in the vibration spectra of the cutting tools and machine components. Most of the energy of the noise associated with this vibration is within the audible range of frequencies and therefore the sound of machine vibration is one of the most sensitive sources of information available to a machine operator for the prediction of the condition of the machine.

2.2.3 Acoustic emission

The term acoustic emission (AE) refers to the elastic stress wave generated as a rapid release of strain energy within a solid material in association with the deformation and fracture generated during metalworking processes. It was rediscovered by manufacturing engineers as a very promising signature to detect an emerging tool failure. Liang and Dornfeld [85] pointed out that the possible sources of AE during metal cutting processes are

(i) Plastic deformation and shear of work material

(ii) Deformation and sliding friction at the chip-tool surface

(iii) Sliding friction at the tool flank-work piece interface

(iv) Chip breaking and their impact on the cutting tool or work piece

(v) Normal and abnormal wear of the tool

(vi) Mechanical and thermal crack of the tool

Hayashi *et al.* [86] reported that in addition to mechanical vibration up to 20 kHz, a higher frequency range has been used for monitoring drill wear i.e. vibration measurement in the frequency range 20-80 kHz is called ultrasonic vibration. Farrelly *et al.* [87] reported that in order to achieve a good signal to noise ratio, the sensor should be placed as close as possible to the machining point. They also reported the shift of the curve towards lower levels due to increasing levels of wear as a result AE activity reduces. Beggan *et al.* [88] suggested that the AE value is taken as the value below which 20 percent of the root mean square value of AE data points lies and is a more useful quantity of acoustic emission for providing information on the cutting mechanisms in turning. This is attributable to the fact that it is less influenced by the occurrence of burst events, which are most often due to non-cutting events such as chip breakage and chip collisions.

Everson and Cheraghi [89] reported that the AE signal is influenced by the location of the hole being drilled in the coupon. They reported that this affects an adjacent hole and small

variations in material heat treat do not significantly affect the AE signal. They also reported that energy was the best and most consistent determining factor of lip height variations between drill bits. Kannatey-Asibu [90] explored the possibility of applying pattern recognition technique to monitor the condition of tool in cutting operation using AE signals. Dong *et al.* [91] reported that the maximum AE during each drilling cycle usually occurred at increased depths, probably caused by the chips jamming inside the drill's flutes. Koenig *et al.* [92] reported that with growing flank and corner wear, there was an appreciable increase in the overall magnitude of the AE-signal in drilling operation. The amplitude of the continuous-type AE signal could be used to monitor the wear of a cutting tool in turning operation, as reported in literature [93-94]. Heinemann *et al.* [95] reported that the thrust force exhibits very weak correlations with the progression of tool wear. They also reported that torque and AE signals are much more suitable for tool condition monitoring in drilling.

2.3 Signal analysis techniques

Various signal analysis techniques have been used in context of drill wear monitoring. It is very important what kind of signal analysis technique is used. In principle signal analysis tries to identify the meaningful part of the signal that gives an indication of wear and to remove the noise i.e. part of the signal that do not contain or show wear related trend. Signal analysis technique is necessary, as the high dimension of the measurement vector needs to be transformed to low dimension vector by implementation of such features so as to reduce the data string. The used signal analysis method should be quick to perform, because during drilling the wear progress very rapidly towards the end of tool life

2.3.1 Time domain signal

Time series modeling of force and vibration signals are popular methods primarily to calculate model coefficient, which subsequently are treated as feature for sensor fusion in TCM. Auto-regressive, time domain sample and moving average modeling methods are basically the method, which is mostly used in time series modeling. Grzesik and Brol [96] correlated mean and standard deviation of acoustic emission and force signal with flank wear in turning operation. They used both kurtosis and skewness to reveal the presence of surface defect resulting from a poor machining operation. Houshmand [97] reported that the variation over time of spectral components was due to non-stationary of the time domain signal and was characterized by a stationary autoregressive process in turning operation. Moriwaki and Hino [98] fused the extracted feature of AE signal (mean, variance, and moment) for automatic detection of cutting tool wear and life in turning operation.

Most researchers [99-102] used root mean square value of time series signal as a simplified and less computational to change high dimension vector to low dimension vector thus reducing the sample size in online monitoring of tool wear in turning as well as in drilling operation. Wilkinson and Reuben [103] analyzed signal through application of selective time windowing, i.e. block averaging to reduce the data size in milling. Masory [104] used the signal increments to eliminate or to reduce the influence of variable cutting conditions. The above technique is based on a least-squares approximation of a time series using a basis of orthogonal polynomials. Some works [105-106] reported the time-series models of the sensor signals and the model coefficients are best features indicative of tool wear in turning.

2.3.2 Frequency domain signal

Fast Fourier Transform (FFT) and spectral analysis are the most commonly applied frequency domain signal processing techniques in engineering. However FFT has many weaknesses. The first one is that the frequency resolution of the entire frequency spectrum depends on the sampling frequency and the number of data points. The second weakness is representation of the entire spectrum, with the addition of harmonic signals, by assuming that the data window is repeated indefinitely. A third weakness is the existence of considerable noise in the transformation due to the large degree of freedom of the system. Therefore FFT analysis has to be repeated many times and their result must be averaged in order to get a smooth output. Basically the idea looking at the frequency content of a measured signal is based on the concept that some frequency wear influences the signal more than that at some other.

McPhee *et al.* [107] in their work, the drill was examined after periodical interval of hole using optical and scanning electron microscopy, to determine the extent of coating wear and to study wear mechanisms in a work. They used FFT of thrust force and torque data and reported that frequency domain analysis distinguish between jamming and failure of cutting tool. They also reported that the frequency-domain analysis could be used to identify the failure of a drill. They also reported that the frequency-domain analysis provides further evidence, which verifies that coating a tool affects the actual cutting process. Dimla *et al.* [108] collected the dynamic and static force as well as vibration signal and passed through FFT to calculate power spectra density in drilling. They used multi sensor TCM technique based on fusion of independent and different sensor signal to check the inter-relationship. Wardany *et al.* [109] used cepstrum in frequency domain, which is insensitive to the location of sensor and cutting condition to monitor the tool wear in drilling.

Rangwala and Dornfeld [110] suggested that it is possible to find regions in the spectrum, which are sensitive to tool wear and independent from changes of cutting conditions at the same time. Brigham [111] used single fourier coefficients which does not make sense due to leakage effects. He suggested that, in order to keep the number of features small (to avoid an over fitting of neural networks at the wear model level) and to reduce leakage effects on the one hand and to consider a shift of relevant spectral bands on the other hand, it is necessary to make a compromise concerning the width and the number of these bands. Monostori [112] presented an alternative solution by using the frequency of the highest peak in the spectrum (or a part of the spectrum) together with the power in a spectral band around this peak. The most common frequency domain characteristic in drilling is the spectral energy around the first natural frequency of the tool-work piece system as reported in literature [113-115]. Chelladurai *et al.* [116] used frequency domain of vibration as well as strain signals as input to ANN and reported that ANN is good enough to classify the flank wear at different levels in turning operation.

2.4 Tool condition prediction system

Today machining processes are usually automatic and unmanned. However various types of problem of fault in the process necessitate manual intervention. Tool wear leading to breakage is one of the factors that prohibit fully automatic production. If tool wear monitoring is used, in practice it needs to be automatic i.e. system used for tool wear monitoring needs to be able to predict the condition of the tool automatically, which means some sorts of artificial intelligence is involved.

2.4.1 Analytical and statistical approach

Armarego and Cheng [117] developed a thin shear zone analysis for flat rake face drills. The analysis was, based on oblique cutting models, accounts for the variations in drill geometry. Elhachimi *et al.* [118] gives an analytical approach of thrust and torque in drilling in terms of the geometry of the tool, thermal and mechanical properties of the work material and the cutting conditions in order to detect the progression of drill wear. Bouzid Sa_1 [119] concluded that the wear at the failure varies with the cutting speed in turning operation. He proposed an equation to describe the three stages of the wear process. Bhattacharya and Ham [120] developed a theoretical model for estimating the tool flank wear in a turning operation. Armarego and Cheng [121] described a method for reduction in thrust force and torque due to drill lip correction and point relieving. They reported that the cutting analysis for the drill lips of modified drills has been qualitatively and quantitatively sound.

Gupta *et al.* [122] developed a dynamic drilling model that incorporates the effect of the alignment errors associated with the location of the drill in the spindle. In their study they included drill linear offset, the axial tilt angle, the drill orientation angle, and the locating angle of the cutting lips in the alignment errors. Gong *et al.* [123] made the concepts of dynamic chip thickness and dynamic chip area using models of chip thickness variations due to drill deflections and drill-grinding errors. Zhang *et al.* [124] approached an analytic method, which provided an expression of thrust and torque in drilling in terms of the geometrical parameters of the drill, the cutting conditions, the vibration parameters and shear flow stress.

Williams [125] studied on the process parameter affecting the drill wear and found an empirical relationship with wear with feed rate, spindle speed and drill diameter. Stephenson and Agapiou [126] reported a model based on a parametric description of drill point geometry and empirical cutting force equations for calculation the main cutting edge contributions to the torque, thrust force generated when drilling cast iron with carbide drills. This model is applicable to arbitrary drill point geometries and predicts torque due to drill point asymmetry. Lee *et al.* [127] used abductive network modeling for drilling process for predicting the tool life, tool wear and surface roughness. The network had number of polynomial functional nodes. Optimal network architecture is prepared based on a predicted square error criterion. Liu *et al.* [128] used the algorithm for the synthesis of polynomial networks for predicting (ASPNS) the corner wear in drilling operation. Chryssolouris and Domroese [129] used regression model for estimating the wear and wear rates by using inverse least square techniques.

Regression analysis of the cutting forces [130-131] and data dependent system modeling [131] in turning provided good correlation between force component with progressive tool wear. Khajavi and Komanduri [132] used statistical technique i.e. power spectra density (PSD) of sensor signals in correlating with drill wear and reported that good correlation of sensor signal with drill wear found in frequency domain. Here it was shown that the power of sensor signal at all frequency increases proportionally with increase of tool wear. Khajavi and Komanduri [133] reported that in the frequency domain, the noise of the estimate of power at any two frequencies either for one sensor or two sensors is uncorrelated; however correlation can be seen between two different sensors at same frequency in drilling operation. Ertunc and Oysu [134] used cutting force signals as input to Hidden Markov Model (HMM) for prediction of drill flank wear. Xiaoli and Tso [135] used current signals as a parameter to model drill flank wear by using regression model.

2.4.2 Neural networks, fuzzy logic and hybrid network

Lin and Ting [136] used a back propagation neural network (BPNN) for predicting drill wear with sample and batch mode, and observed a faster convergence of error in the case of the sample mode. They also observed that for a neural network with two hidden layers with same number of nodes, convergence is achieved faster than that with one hidden layer, and they reported that at higher learning rate, error is reduced. Ertunc and Loparo [137] used the decisions fusion center algorithm (DFCA) for monitoring online tool wear condition in drilling process, and a number of numerical methods for predicting the condition of drill. Das *et al.* [138] used the cutting force signal in a three-layer back propagation network to monitor the wear of insert in turning operation. They used three different models for three different inputs and found that if the input is more, then it will be more effective compared to other models to estimate the tool wear. Xioli and Zhejun [139] used fuzzy clustering method for monitoring the wear state of bore in boring operation. They used membership grade of wear state of bore as a control variable for its replacement.

Karri and Kiatcharoenpol [140] used optimization by layer bay layer (OLL) algorithm for drill life prediction in terms of hole. They had used four input parameter like drill diameter, spindle speed, feed rate and cutting time and output is number of holes to failure. In their work, flank wear of average 0.3 mm was used as the criterion for tool life. They reported that root mean square (RMS) error decreases when number of hidden neuron increases. They had tested same results using back propagation neural network (BPNN) and found that OLL has better prediction capacity than BPNN. Tsao [141] used the radial basis function network (RBFN) and adaptive based radial basis function network (ARBFN) to predict the flank wear of different coated drill. Liu and Anantharaman [142] used nine features representing drill condition as input to multi layer perceptron and found 100 percent accuracy for correct classifications of drill wear. Dutta *et al.* [143] studied the efficacy of back propagation neural network with delta bar delta learning rule (MBPNND) in milling operation and reported better performance achieved with compared to BPNN, modified back propagation neural network (MBPNN) and fuzzy back propagation neural network (FBPNN) in terms of number of iterations and prediction accuracy. They reported that BPNN is the slowest and FBPNN provides a faster training for achieving the target level. Dimla *et al.* [144] studied that a single layer perceptron (SLP) could satisfactorily classify worn and sharp tool data from a turning process by partitioning the input data into two subspaces using a hyper plane. Furthermore, this study has also shown an SLP as not being ideally suited for TCM since it cannot cope with the non-linearity of metal cutting process.

However, if one is concerned in the state of the cutting tool only (worn or sharp defined by some criteria), then it suffices, as its classification performance is comparable to that of hybrid neural networks.

Dimla *et al.* [145] again investigated the generalization capability of typical three layered back-propagation neural networks with different number of hidden neuron, and success rate of classification were made in turning process. Szecsi [146] used back propagation neural network with 12 input parameters to predict three different cutting forces in turning operation. He used a modified learning technique in order to avoid oscillation of average error. Obikawa and Shinozuka [147] used unsupervised and self-organizing neural network with Adaptive Resonance Theory (ART2) for monitoring of flank wear in high speed machining operation. Wong and Hamouda [148] used reinforced retraining (RR) scheme instead of steepest descent method to find out the global minimum instead of strucking at local minima in back propagation network. They had used machinability data of turning operation to test their algorithm and found it suitable. Few researchers used [149-151] ANN based method for detection of wear and breakage of cutting tool in different machining operation.

Harpham *et al.* [152] used RBF network for mapping the input-output parameter using genetic algorithm for determining the optimal set of data input and number of radial basis center. Hashmi *et al.* [153] proposed a fuzzy model for correlating the drilling speed with hardness of work material. They have used triangular membership function with fuzzy rule base in there analysis. Baradie [154] used fuzzy rule based control algorithm to study the life of tool in turning operation. He purposed fuzzy rule base control algorithm in order to find and optimize the cutting speed as a function of material hardness. Lo [155] described the tool state in turning operation using artificial neuro- fuzzy inference system (ANFIS) architecture, and concluded that higher accuracy could be achieved in the case of triangular and bell shape membership function. Guillot and Quafi [156] initially experimented with three different multi layer perceptron (MLP) network types both having same number of input and output nodes but different number of hidden nodes (20, 10 and 5 nodes respectively). They concluded that the best result convergences with least number of hidden neuron in hidden layer.

Elanayar and Shin [157] investigated three different basis function in RBF network to aid in tool wear (flank and crater wear) identification process in turning operation. Yao and Fang [158] in their work with different number of neuron in hidden layer and different transfer functions reached the conclusion that contradicts with the result in the literature [157]. Self-

organizing network have been utilized among the researchers, Govekar and Grabec [159], Kamarthi *et al.* [160], Govekar *et al.* [161]. All of them used the technique based on competitive learning and constructed from fully connected arrays of neurons requiring no output data for training. Chien and Tsai [162] used BPNN for the prediction of tool wear and determining the optimum cutting condition in a turning operation. They also used a genetic algorithm in the optimizing model, as well as Taguchi method to find the optimum parameter for both the model. Kuo and Cohen [163] applied a modified fuzzy neural network for detecting the defective sensor signal using membership function at the input node and fuzzy rule base.

With regard to selecting the data sets for training and testing of the neural network, many published works are available [164-167]. Li *et al.* [168] proposed hybrid learning for monitoring of drill wear using a combination of fuzzy system and neural network. Balazinski *et al.* [169] used three artificial intelligence (AI) methods: feed forward back propagation neural network, fuzzy decisions support system and an artificial neural network based fuzzy inference system to monitor the flank wear in turning operation. Chungchoo and Saini [170] used fuzzy neural network model for online tool wear estimation in CNC turning. In literatures [171-172] authors concluded that single hidden layer of feed forward neural network could classify the pattern well. Brophy *et al.* [173] used BPNN model to detect the condition of the drill state, either normal or abnormal for short term and long term experiment and reported that short run predict better than long run. Petersen [174] reported that degree of variation of material properties of the blanks used is much less compared to that of other input parameters such as measured force.

Yao and Fang [175] reported that the chip characteristics significantly change with the growth of the tool wear as cutting temperature and mechanics of machining are affected and thus chip characteristics may be used as input to decision system in turning operation. Kohonen [176] developed the self-organising map (SOM), for data analysis. The SOM has been implemented successfully in numerous applications, in fields such as process analysis, machine perception, control and communication. Yao *et al.* [177] used a fuzzy neural network to describe the relation between the monitoring features (which were derived from wavelet-based AE signals) and the tool wear condition. Scheffer *et al.* [178] reported that the best method to monitor tool wear during hard turning would be by means of force-based monitoring with an Artificial Intelligence (AI) model. They proposed a novel formulation of the proposed AI model, which could accurately monitor the crater and flank wear during hard turning operation.

Choudhury and Bartarya [179] work focused on the two of the techniques, namely design of experiments and the neural network for predicting tool wear. In their work flank wear, surface finish and cutting zone temperature were taken as response (output) variables and cutting speed, feed and depth of cut were taken as input parameters measured during turning operation. They predicted for all the three response variables with the help of empirical relation between different responses and input variables using design of experiments (DOE) and also through neural network (NN) program. Yumak and Ertunc [180] used two decision making mechanisms by using statistical parameters of cutting forces collected during drilling process based on fuzzy logic and the neuro-fuzzy system (ANFIS) for tool wear monitoring. They reported that fuzzy system results are reliable on all tool data but ANFIS results reliable only if the system trained by the same tool group of data with testing data. Ezugwu *et al.* [181] reported that multi layer perceptron with two hidden layers with Levenberg- Marquardt training algorithm found to be the optimum network for correlating between cutting and process parameters in high speed machining of Inconel 718 alloy. Sun *et al.* [182] reported that support vector machine as a decision making system could make good assessment for selection of training sample for achieving better generalization. Liu and Anantharaman [183] reported that modified neural network with adaptive activation function converge much faster than convention neural network in drilling. Dimla [184] reported that MLP performed better classification of tool state compared to single layer perceptron in a turning operation.

Chryssolouris and Guillot [185] reported that the models built from neural networks were in general superior to conventional modeling techniques such as polynomial fits using multiple regression or GNDH. Lippmann [186] reported that neural networks offer unexpected possibilities for continuous modeling. When properly trained, they are able to accurately represent process states within the range in which they have been trained despite the presence of complex interrelated phenomena occurring during processing. According to Simpson [187], neural networks are highly advantageous in situations where nonlinear mappings must be automatically acquired from the training data. Benardos and Vosniakos [188] reported that artificial intelligence models take into consideration the particulars of equipment used and real machining phenomenon but the theoretical method is based on conventional and idealization are responsible for errors generation in predicting surface roughness in a turning operation.

Palanisamy *et al.* [189] reported that ANN model much more robust and accurate in estimating the values of tool wear with compared to regression model in a milling operation.

Quiza *et al.* [190] reported that neural network could predict accurate tool wear compared to statistical model in a hard machining operation. Ozel and Karpat [191] reported that the neural network models provided better prediction capabilities because of the ability to model more complex non-linearities and interactions compared to linear and exponential regression models can offer. Sanjay *et al.* [192] used back propagation algorithm as well as regression model for the prediction of drill wear using drill diameter, cutting speed, feed rate, machining time, thrust force and torque. They reported that BPNN gives better correlation with drill wear compared to regression model.

2.5 Motivation and objectives of the present work

Literature review reveals that many of the proposed intelligent techniques such as artificial neural network were shown to be much simpler and indeed more accurate compared to traditional non-linear predictors for tool condition monitoring. The uncertainties in estimating statistical parameters were also overcome through the use of several neural and fuzzy solutions. Most notable advantages of intelligent techniques are learning from experience, scalability, adaptability and the ability to extract rules without the need for detailed or precise mathematical modeling. ANNs have several advantages over traditional statistical techniques. First, ANNs do not require the knowledge of functional relationship between independent variable and dependent variable to estimate the model and unlike traditional statistical techniques, ANNs learn from example. Second, ANNs are useful when statistical techniques are unable to fully recognize the complexity of data. Third, unlike statistical techniques ANNs detect non-linearities and interactions automatically and can estimate multiple outputs at a time. Artificial neural network algorithms are regarded as multivariate nonlinear analytical tools capable of recognizing patterns from noisy complex data and estimating their nonlinear relationships. Their major advantages include superior learning, noise suppression, and parallel data processing capabilities, which cannot achieve through any statistical technique. Statistical techniques are only capable when limited numbers of process variables and performances measure are considered.

It has been observed from the literature review that, TCM has been a very important area of research and many works have been reported in literatures for TCM in machining using different techniques. Most of these works have been reported in turning, a few are also reported in drilling. As reported in literature, because of complexity in mechanism it is difficult to have empirical or mathematical models for predicting wear in drilling. Some researchers have tried to develop drill wear prediction systems using ANN, however a complete comparative performances analysis of different TCM strategies using different

ANN models could be of great importance in the direction of development of an automated drill wear monitoring systems. Keeping these points in mind, the present work aims at studying the performances of different drill wear prediction systems developed using different TCM strategies and different ANN architectures. The specific objectives of the present work have been laid down as:

(1) Development of multi sensor based TCM strategies for drill wear prediction based on

(i) Thrust force and torque signals

(ii) Vibration signals

(iii) Chip thickness characteristics

(iv) Surface roughness characteristic of drilled hole

(2) Comparative assessment of the performances of different drill wear prediction systems developed using different TCM strategies and using the following ANN architectures

(i) Back propagation neural network (BPNN)

(ii) Fuzzy back propagation neural network (FBPNN)

(iii) Self organizing feature map (SOFM) network

(iv) Fuzzy self organizing feature map (FSOFM) network

CHAPTER 3

SOFT COMPUTING TECHNIQUES FOR MULTI SENSOR BASED DRILL WEAR MONITORING

This chapter describes in brief multi sensor based TCM using ANN and the principles of four different types of ANN architectures namely BPNN, Fuzzy BPNN, RBFN, and Fuzzy RBFN which have been used in the present work.

3.1 Multi sensor based tool condition monitoring (TCM)

In the present work of drill wear monitoring, relevant data (thrust force, torque, feed vibration and radial vibration) are collected using sensors such as dynamometers and accelerometers and are stored in a digital computer for further analysis. The continuous data thus collected are analyzed in time domain as well as frequency domain to extract the significant features having correlation with tool wear. In addition to the sensor data, important cutting parameters such as spindle speed, feed rate, drill diameter, chip thickness and surface roughness of the hole are also stored intermittently corresponding to a measured drill wear. Therefore, the basic procedure to be followed combines data acquisition, signal analysis and development of a prediction system for drill wear monitoring. A schematic diagram for such a procedure is given in figure 3.1. The on-line indirect TCM is preferably designed with multiple sensors due to the fact that process information which are sometimes over looked by single sensors are also captured. Input parameters such as cutting conditions, chip quality and analyzed sensor data are than correlated with output parameter of the drilling operation such as flank wear through decision systems such as ANN, Fuzzy logic, Hybrid network in order to evaluate correlation performance. Among different types of expert system, ANN is reported to be effective and is being extensively used in the tool condition monitoring. Among the various scheme of ANN, multi layer perceptron with back propagation learning algorithm and fuzzy back propagation learning algorithm is most popular and effective for prediction of tool wear while it may as well as be used for pattern classification though unsupervised ANN like radial basis network and fuzzy radial basis network.

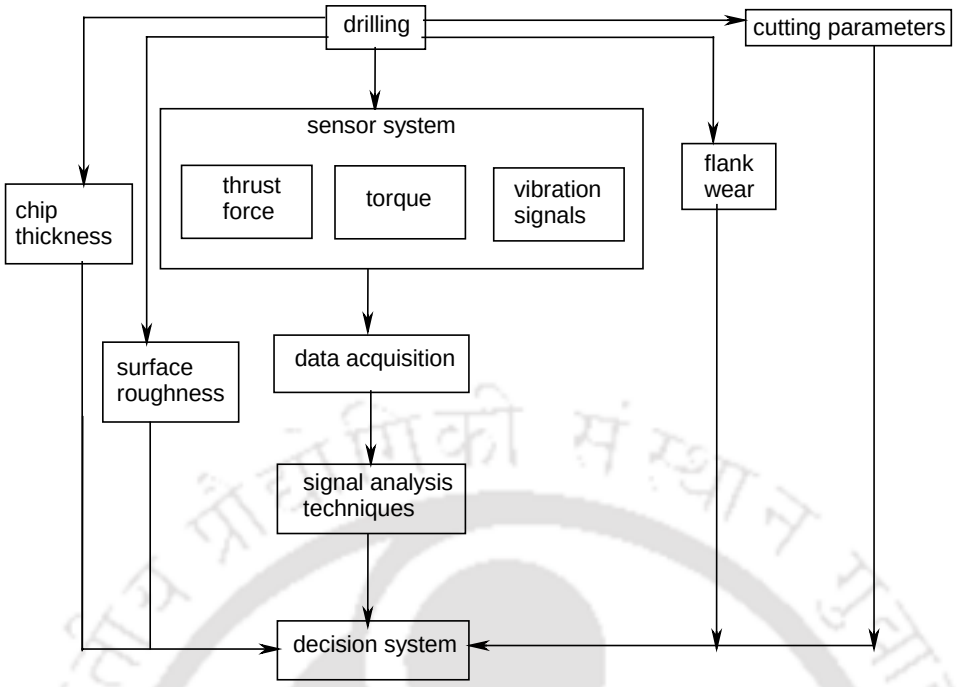

Figure 3.1 Schematic diagram for tool condition monitoring

3.2 Artificial neural network

ANN approaches to machine intelligence is centered upon the study of brain and its emerging properties. ANN is an information-processing system that consists of a large number of simple nonlinear processing modules, connected by elements that have information storage and programming functions. The information-processing properties of neural networks depend mainly on two factors namely the network topology (the scheme used to connect elements or nodes together), and the algorithm (the rules) employed to specify the values of the weights connecting the nodes. While the ultimate configuration and parameter values are problem-specific, it is possible to classify neural networks, on the basis of how information is stored or retrieved, in four broad categories

(i) Neural networks behaving as learning machines with a teacher

(ii) Neural networks behaving as learning machines without a teacher

(iii) Neural networks behaving as associative memories

(iv) Neural networks that contain analog as well as digital devices and result in hybrid-machine implementations that integrate complex continuous dynamic processing and logical functions.

ANN systems do not possess a well-defined termination condition or goal. Several neurons in ANN model have no predefined meaning; they evolve and specialize during learning

process. There are three main components in ANN, i.e. network topology and learning algorithm and generalization capability.

3.2.1 Topology and structure of neural network

A typical feed forward neural network is shown in figure 3.2, which consists of one input layer, hidden layer (s) and one output layer. Number of nodes in the input layer represents the number of input features responsible for the output and the number of output nodes represents the output features to be predicted. The network receives the data from input layer and passes this information to the network for processing. Hidden layer receives the information from the input layer and quietly does all the information processing and finally output layer receives processed information from the network, and sends the results out to an external receptor. In the figures the input features are shown as the cutting parameters and sensor signals in drilling process and the output is the drill wear.

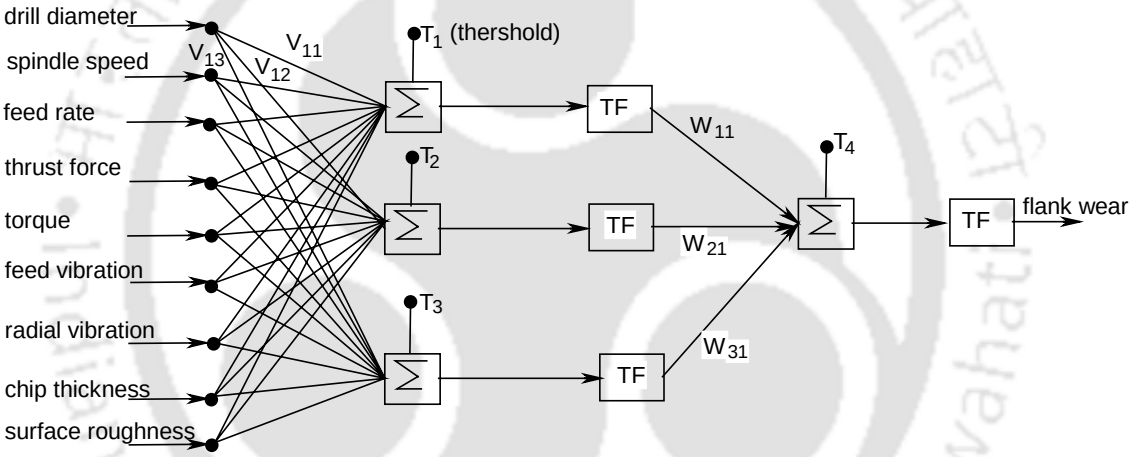

Figure 3.2 Anatomy of feed forward neural network

(i) Input output nodes: The input to the j^{th} nodes are represented as *an input vector* I, with component $I_i (i = 1....n)$, where n is the number of nodes in that layer. The node activates these inputs, to give the output b_j, which can then form the part of the input to the other nodes as shown in figure 3.3.

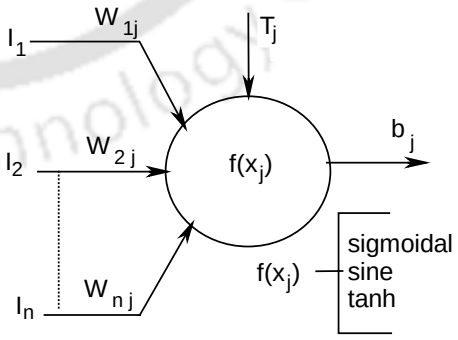

Figure 3.3 Anatomy of node

(ii) Weight factor: The input signals are modified by interconnection weights, known as weight factors W_{ji}, which represents the interconnection of i^{th} node of one layer to j^{th} node of the next layer. Weight factor can

either inhibitory or excitatory effect. If the weight factors W_{ji} adjusted in such a way that $W_{ji}I_i$ is positive, then excitement at the node initiated. If $W_{ji}I_i$ is negative, it inhibits the nodes. Weight factors should be small in magnitude.

(iii) Internal thresholds: The internal threshold for the j^{th} node, denoted by T_j, controls activation of that node. The node calculates all its $W_{ji}I_i$, sums the terms together, and calculates the total activation, x_j by putting the internal threshold value. If T_j is large and positive, the node has a high internal threshold, which inhibits the firing, conversely if T_j is zero or negative the node has low internal threshold which excites the node firing. The activation function is given in equation (3.1)

$$Total\ activation = x_j = \sum_{i=1}^{i=n}(W_{ij}I_i) - T_j \qquad (3.1)$$

(iii)Transfer function: The final factor governing a node's output is the transfer function. Once the node calculates total activation function, it passes this result to a transfer function $f()$. Thus the complete node calculation is shown in eq^n (3.1). Figure 3.4 shows the different type of transfer functions used for a network model, and they are

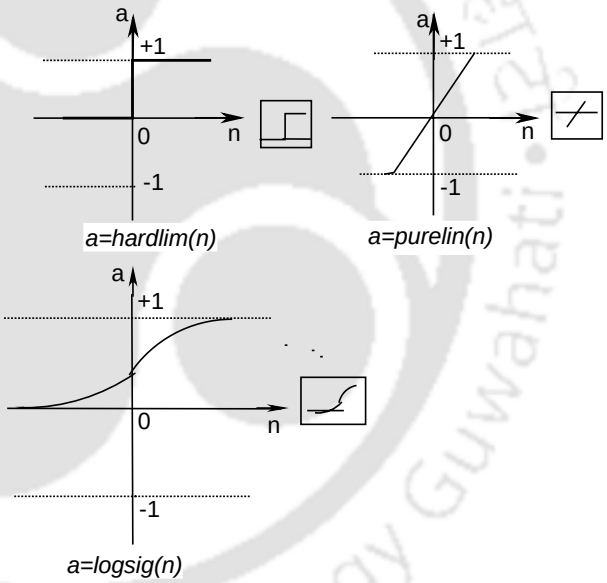

Figure 3.4 Type of transfer function

(a) ***Linear function*****:** $f(x) = \alpha x$, where α is a real valued constant that regulate the magnification of input.

(b) ***Non linear ramp function*****:** The linear function is bounded to the range $[-\gamma, +\gamma]$ such that $\gamma(-\gamma)$ is processing element's maximum (minimum) output value.

(c) ***Step threshold function*****:** The threshold function only responds to the sign of the input, $f(x) = +\gamma$ if $x > 0$ and $f(x) = -\delta$ otherwise, with γ and δ being positive scalar, and ranges in between 0 and 1.

(d) ***Sigmoid threshold function***: Sigmoid function is a bounded, monotonic, non-decreasing, S-shaped function that provides a graded nonlinear response. Example includes

the logistic sigmoid function $S(x) = \frac{1}{1+e^{-x}}$ with saturation level of 0 to 1 and the hyperbolic tangent function $S(x) = \tanh(x)$ with saturation levels of -1 to +1.

(iv) Normalization

If input and output variables are not of the same order of magnitude, some variables may appear to have more significance than they actually do. To avoid such problem, the data sets are normalized in the specified range (generally 0 to 1).

3.2.2 Multiple layer

A network can have several layers. Each layer has a weight matrix *W*, an internal threshold vector *T*, and an output vector *b* (refer figure 3.3). The outputs of each intermediate layer are the inputs to the following layer. A layer that produces the network output is called an *output layer*. Similarly layer connected with input signal is known as *input layer* and rest all other layers are called *hidden layers*. The layers of a multiple layer network are quite powerful and play different roles. For instance, a network of two layers, where the first layer is sigmoid and the second layer is linear, can be trained to approximate any function.

3.2.3 Learning

Learning or training is the process in which, weights factor are adjusted until the output pattern (response) calculated from the given input reflects the desired relationship. There are many different approaches of learning technique available, broadly they are classified as *supervised* and *un-supervised* learning.

Supervised learning incorporates an external teacher and /or global information and includes such technique as error correction learning, reinforcement learning and stochastic learning. Every input pattern that is used to train the network is associated with an output pattern, which is the target or desired pattern. A teacher is assumed to be present during the learning process, when a comparison is made between the network's computed output and the correct expected output, to determine the error. The error can then be used to change the network parameter, which results in an improvement in performance of network are known as *error correction learning*. *Reinforcement learning* is a technique by which the weights are reinforced for properly performed actions and punished for inappropriate one where performance of output layer is captured in a single scalar error value. Stochastic learning works by making a random change in the weight matrix and then determining the properties of the network called resultant energy. If change has made this energy value lower then it was accepted, otherwise change is accepted according to the pre-chosen probability

distribution. These random acceptances of change that temporarily degrade the performance of the system allows it to escape from a local energy minima in its search for optimal system state. Type of supervised learning, which includes perceptron, adaptive linear neural element (ADALINE), many ADALINE (MADALINE), back-propagation, Boltzman machine, has their own importance in pattern classification.

Unsupervised learning is a process that does not incorporate an external teacher and relies only upon the local information and internal control strategies. In unsupervised learning, a teacher though available does not present the expected answer but only indicates if the computed output is correct or incorrect. The information provided helps the network in its learning process. A reward is given for correct answer computed and a penalty for wrong answer. Example includes adaptive resonance theory (ART1 and ART2), Hopfield network, Bidirectional associative memory (BAM), learning vector quantization (LVQ) and counter propagation.

3.2.4 Generalization

One of the important aspects in developing the neural network is determining the network performance after the completion of training process. Checking the performance of trained network involves two main criteria. One how well the network *recall* the predicted response (output vectors) from the data sets used to train the network known as network training, other is how well the network predicts responses from the data sets that were not used in training known as network testing.

3.2.5 Types of ANN

Out of various artificial neural networks, most promising network used in the present work are back propagation neural network (BPNN), fuzzy back propagation neural network (FBPNN), radial basis function network (RBFN), and fuzzy radial basis function network (FRBFN). ANN is particularly well suited for certain applications especially trainable pattern association. The notion that ANN can solve all problems in automated reasoning or even all mapping problems is probably unrealistic.

Advantages of ANN

(i) massively parallel (ii) fault tolerant because of parallelism (iii) designed to be adaptive (iv) little need for extensive characterization of problem

Disadvantages of ANN

(i) No clear rule and design guidelines for arbitrary application (ii) no general way to assess the internal operation of network (iii) difficult in training the pattern (no thumb rule for

training) (iv) difficult in predicting future network performance (no thumb rule for generalization)

3.2.6 Back-propagation neural network

The multi layer perceptron network with supervised learning paradigm which minimizes the error by weight adoption using back propagation of error is known as BPNN. Back propagation is used to calculate the gradient of the error of the network with respect to the network's modifiable weights. This gradient is almost always then used in a simple stochastic gradient descent algorithm to find weights that minimize the error. Back propagation usually allows quick convergence on satisfactory local minima for error in the kind of networks to which it is suited. It is important to note that back propagation networks are necessarily multiple layer (usually with one input, one hidden, and one output layer). In order for the hidden layer to serve any useful function, multiple layer networks must have non-linear activation functions for the multiple layers.

Back propagation neural network is a three-layered feed forward architecture. The three layers are input layer, hidden layer and output layer. Functioning of back propagation proceeds in three stages, namely learning or training, testing or inferences and validation.

Figure 3.2 shows the *l*-*m*-*n* (*l* input neurons, *m* hidden neurons, and *n* output neurons) architecture of a back propagation neural network model. Input layer receives information from the external sources and passes this information to the network for processing. Hidden layer receives information from the input layer, and does all the information processing, and output layer receives processed information from the network, and sends the results out to an external receptor. The input signals are modified by interconnection weight, known as weight factor w_{ji}, which represents the interconnection of i^{th} node of the first layer to j^{th} node of the second layer. The sum of modified signals (total activation) is then modified by a sigmoid transfer function. Similarly, outputs signal of hidden layer are modified by interconnection weight (w_{kj}) of k^{th} node of output layer to j^{th} node of hidden layer. The sum of the modified signal is then modified by sigmoid transfer function and output is collected at the output layer.

Let $I_p = (I_{p1}, I_{p2}, ...I_{pl}), p = 1, 2....N$ be the p^{th} pattern among N input patterns and $d_p = (d_{p1}, d_{p2}, ...d_{pl}), p = 1, 2....N$ be the p^{th} pattern among N output patterns and W_{ji} and W_{kj} are connection weights between i^{th} input neuron to j^{th} hidden neuron, and j^{th} hidden neuron to k^{th} output neuron, respectively. The steps involved in BPNN is shown in flow chart of figure 3.5 and are as follows [167, 193].

Step1- Initialization

Start with a reasonable network configuration (i.e. number of layers, number of nodes in each layer) and set all connection weights with small random numbers from uniform distribution.

Step 2- Presentation of training sample

First normalize the data set to be used for training, testing and validating. Present the network with an epoch of training example ($I_{pi}(n), d_{pi}(n)$).The data sets are normalized in the range of 0.1 to 0.9 using equation (3.2) as follows.

$$y = 0.1 + 0.8\left(\frac{x - x_{\min}}{x_{\max} - x_{\min}}\right) \tag{3.2}$$

where,

x = Actual value,

$x_{\max}$ = Maximum value of x,

$x_{\min}$ = Minimum value of x,

y = Normalized value corresponding to x.

For each training pair, assume there are l inputs given by I_l and n output given by O_n

Step 3- Forward Pass

(i) For the training data present all set of inputs and outputs. By using linear activation function, Output from a neuron in the input layer is given by,

$$O_{pi} = I_{pi}, i = 1, 2.....l \tag{3.3}$$

(ii) Output from a neuron in the hidden layer is,

$$O_{pj} = f(NET_{pj}) = f\left(\sum_{i=1}^{l} W_{ji} O_{pi}\right), j = 1, 2.....m \tag{3.4}$$

(iii) Output from a neuron in the output layer is,

$$O_{pk} = f(NET_{pk}) = f\left(\sum_{j=1}^{m} W_{kj} O_{pj}\right), k = 1, 2.....n \tag{3.5}$$

$f(x)$ = sigmoid transfer function = $1/(1+e^{-x})$

Output error $e_{pk}(n) = d_{pk}(n) - O_{pk}(n)$ (3.6)

Mean square error $E_p = \sum_{i=1}^{n} \frac{1}{2}(D_{pi} - O_{pi})^2$ (3.7)

Step 4- Backward pass

The error surface is given by the function of layer weight W_{ji} , W_{kj} and input data I_{pi}.

$$E = f(W, I) \tag{3.8}$$

For minimization of error it is differentiated, using chain rule as

$$\frac{\partial E}{\partial W_{kj}} = \frac{\partial E}{\partial O_k} \times \frac{\partial O_k}{\partial I_k} \times \frac{\partial I_k}{\partial W_{kj}} \tag{3.9}$$

(i) Local gradient is given by

$$\begin{aligned} d_{pk} &= (T_{pk} - O_{pk}) \times O_{pk} \times (1 - O_{pk}) \\ d^*_{pj} &= -e_{pk} \times O_{pj} \times (1 - O_{pj}) \end{aligned} \tag{3.10}$$

Where d and d^* are local gradients between hidden-output and input-hidden layer.

(ii) Change of weight factors between two layers is given by

$$\begin{aligned} \Delta W_{kj} &= \eta \times O_{pj} \times d_{pk} \\ \Delta W_{ji} &= \eta \times I_{pi} \times d^*_{pj} \end{aligned} \tag{3.11}$$

Learning rate (η) coefficient determines the size of weight adjustment made at each iteration and hence influences the rate of convergences. Poor choice of the coefficient can result in a failure in convergences. We should keep the learning rate coefficient constant through out all iteration for best result. There is another possible way to expedite the convergences and thus to speed up the training process by adding a momentum (α) in gradient expression. The addition of such term helps to smooth out the descent path by preventing extreme changes in the gradient due to local anomalies. Change in weight factors is given by

$$\begin{aligned} \Delta W_{kj}(n) &= \eta \times O_{pk} \times d_{pk} + \alpha \times \Delta W_{kj}(n-1) \\ \Delta W_{ji} &= \eta \times I_{pl} \times d^*_{pj} + \alpha \times \Delta W_{ji}(n-1) \end{aligned} \tag{3.12}$$

(iii) Modified weight factors are given by

$$\begin{aligned} W_{kj}(n+1) &= W_{kj}(n) + \Delta W_{kj} \\ W_{ji}(n+1) &= W_{ji}(n) + \Delta W_{ji} \end{aligned} \tag{3.13}$$

Step 5- Iteration

Iterate by repeating from step 2 until the error norm reduces to an acceptable level set by the user at the output or maximum number of iteration is reached.

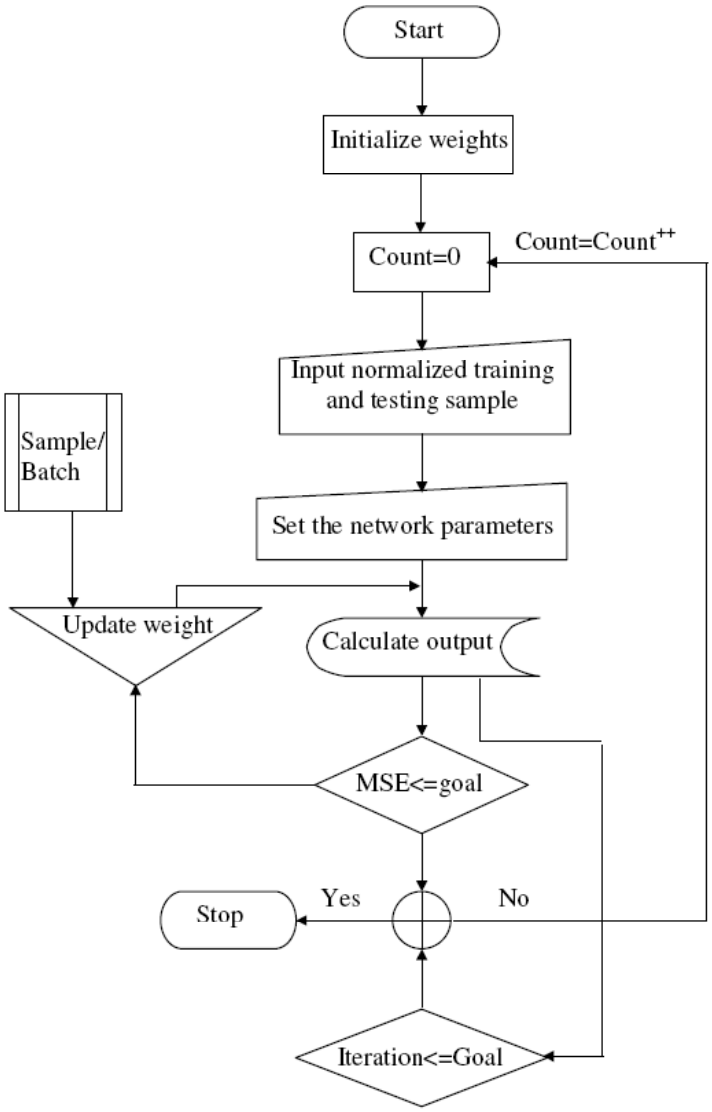

Figure 3.5 Flow chart of BPNN

3.2.7 Fuzzy back propagation neural network

In fuzzy back propagation neural network, fuzzy input is mapped with crisp output. The fuzzy neuron makes use of left and right (*LR* type) fuzzy number [193]. A triangular type membership function has been used for simplification of architecture and reduction in computational load.

(i) LR type of fuzzy number

LR type fuzzy number having two function values called left and right (*L* and *R*) which maps with real number within [0,1] and are the decreasing shape function if

$$\begin{aligned} &L(0)=1, \\ &L(x)<0, \forall x<1, \\ &L(1)=0, L(\infty)=0 \end{aligned} \tag{3.14}$$

A fuzzy number *M* is of type *LR* if there exists reference functions *L* (for left), *R* (for right and scalar, $\alpha_1 > 0, \beta_1 > 0$ with

$$\mu_m = \begin{Bmatrix} L(\frac{m-x}{\alpha_1}), x \le m \\ R(\frac{x-m}{\beta_1}), x \ge m \end{Bmatrix} \tag{3.15}$$

Here *m* is called the mean value of *M*, is a real number, and α_1 and β_1 are called left and right spread, respectively. μ_m is the membership function of fuzzy number *M*. So an *LR* type fuzzy number *M* can be expressed as $(m, \alpha_1, \beta_1)_{LR}$. If α_1, β_1 are both zero, the *LR* type function indicates a crisp value.

(ii) Operation on LR type fuzzy number

Let M and N be two LR type fuzzy number given by $M = (m, \alpha_1, \beta_1)$ and $N = (n, \gamma, \delta)$, the basic operation are [194]

Addition $(m, \alpha_1, \beta_1)_{LR} \oplus (n, \gamma, \delta)_{LR} = (m+n, \alpha_1 + \gamma, \beta_1 + \delta)_{LR}$

Subtraction $(m, \alpha_1, \beta_1)_{LR} - (n, \gamma, \delta)_{LR} = (m-n, \alpha_1 + \delta, \beta_1 + \gamma)_{LR}$

Multiplication

$(m, \alpha_1, \beta_1)_{LR} \otimes (n, \gamma, \delta)_{LR} = (mn, m\gamma + n\alpha_1 - \gamma\alpha_1, m\delta + n\beta_1 + \beta_1\delta)_{LR}$ *if* $m \ge 0, n \ge 0$

$(m, \alpha_1, \beta_1)_{LR} \otimes (n, \gamma, \delta)_{LR} = (mn, m\gamma - n\beta_1 + \gamma\beta_1, m\delta - n\alpha_1 - \delta\alpha_1)_{LR}$ *if* $m \ge 0, n < 0$

$(m, \alpha_1, \beta_1)_{LR} \otimes (n, \gamma, \delta)_{LR} = (mn, n\alpha_1 - m\delta + \alpha_1\delta, n\beta_1 - m\gamma - \beta_1\gamma)_{LR}$ *if* $m < 0, n \ge 0$

$(m, \alpha_1, \beta_1)_{LR} \otimes (n, \gamma, \delta)_{LR} = (mn, -m\delta - n\beta_1 - \delta\beta_1, -m\gamma - n\alpha_1 + \alpha_1\gamma)_{LR}$ *if* $m < 0, n < 0$

Scalar multiplication

$\lambda \otimes (m, \alpha_1, \beta_1)_{LR} = (\lambda m, \lambda\alpha_1, \lambda\beta_1), \forall \lambda \ge 0, \lambda \in R$

$\lambda \otimes (m, \alpha_1, \beta_1)_{LR} = (\lambda m, -\lambda\alpha_1, -\lambda\beta_1), \forall \lambda < 0, \lambda \in R$

(iii) Types of membership function

There are various types of membership functions exist to define the degree of belongingness. This could be triangular, trapezoidal, tan sigmoid curve defined by some mathematical equation. Quite often membership function is defined by a continuous function. Figure 3.6 shows some of membership function used in fuzzy sets theory.

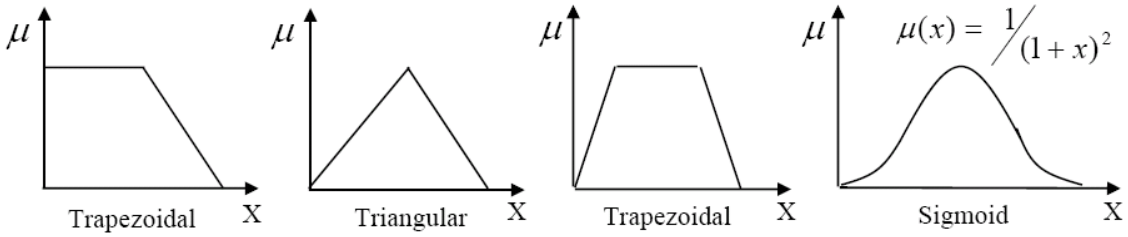

Figure 3.6 Types of membership function

(iii) Fuzzy neuron

The fuzzy neuron is the basic element of a fuzzy back propagation neural network model. Given the input vector $I = (I_1, ...I_l)$ and weight vector $W = (W_1, ...W_l)$, the fuzzy neuron computes the crisp output *O*, given by

$$O = f(NET) = f\left(CE\left(\sum_{i=1}^{l} W_i I_i\right)\right) \tag{3.16}$$

Where $I_0 = (1, 0, 0)$ is the bias. Here, fuzzy weight summation is

$$net = \sum_{i=1}^{l} W_i I_i \tag{3.17}$$

The function *CE* is the centroid operation of the triangular fuzzy number, and can be treated as defuzzification operation, which maps fuzzy weight summation value to a crisp value. Thus, if $net = (net_m, net_{\alpha_1}, net_{\beta_1})$ is the fuzzy weight summation then function *CE* is given by

$$CE = net_m + 1/3(net_{\beta_1} - net_{\alpha_1}) \tag{3.18}$$

The function *f* is the sigmoid function, which performs nonlinear mapping between input and output is and defined as

$$f(NET) = \frac{1}{1 + \exp(-NET)} \tag{3.19}$$

In the fuzzy neuron, both input vector *I*, and weight vector *W* are represented by a triangular *LR* type fuzzy number. Thus for $I = (I_1, ...I_l)$ the input component vector I_i is represented by *LR* type fuzzy number $(I_{mi}, I_{\alpha_i i}, I_{\beta_i i})$. Similarly for $W = (W_1, ...W_l)$, the weight vector component W_i is represented as $(W_{mi}, W_{\alpha_1 i}, W_{\beta_1 i})$.

(iv) Fuzzy back propagation neural network architecture

Fuzzy back propagation neural network is a three-layered feed forward architecture. The three layers are input layer, hidden layer and output layer. Functioning of fuzzy back propagation proceeds in three stages, namely learning or training, testing and validating as described in section 3.2.3. Figure 3.7 shows the *l*-*m*-*n* (*l* input neurons, *m* hidden neurons and *n* output neurons) architecture of a fuzzy back propagation neural network model. Let

$I_p = (I_{p1}, I_{p2}, ...I_{pl}), p = 1, 2....N$ be the p^{th} pattern among N input patterns. O_{pi}, O_{pj} and O_{pk} are the i^{th}, j^{th} *and* k^{th} crisp defuzzification output of neuron from input, hidden and output layers, respectively. W_{ji} and W_{kj} are LR type fuzzy connection weights between i^{th} input neuron to j^{th} hidden neuron, and j^{th} hidden neuron to k^{th} output neuron, respectively. Steps involved in FBPNN are as follows [193].

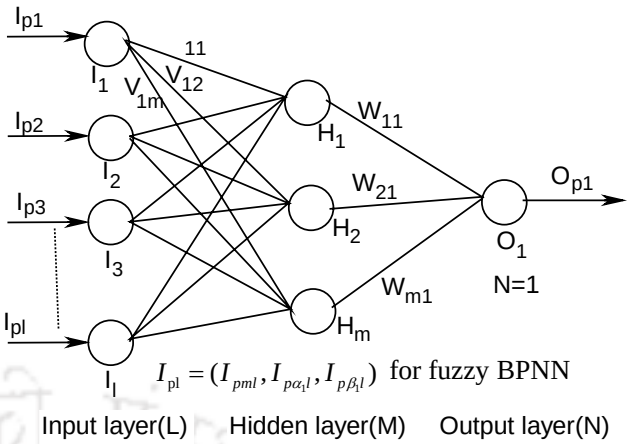

Figure 3.7 Architecture of fuzzy BPNN

Step 1 -forward pass

Output from a neuron in the input layer is,

$$O_{pi} = I_{pi}, i = 1, 2.....l \tag{3.20}$$

Output from a neuron in the hidden layer is,

$$O_{pj} = f(NET_{pj}) = f\left(CE\left(\sum_{i=1}^{l} W_{ji} O_{pi}\right)\right), j = 1, 2.....m \tag{3.21}$$

Output from a neuron in the output layer is,

$$O_{pk} = f(NET_{pk}) = f\left(CE\left(\sum_{j=1}^{m} W_{kj} O_{pj}\right)\right), k = 1, 2.....n \tag{3.22}$$

Step 2- Backward pass

Error can be minimized by differentiating mean square error (MSE) with fuzzy weight, is given by

$$\frac{\partial E}{\partial W} = \left(\frac{\partial E}{\partial W_m}, \frac{\partial E}{\partial W_{\alpha_1}}, \frac{\partial E}{\partial W_{\beta_1}}\right) \tag{3.23}$$

$$\begin{aligned} d_m &= \frac{\partial E}{\partial W_{mkj}} = -(T_{pk} - O_{pk}) O_{pk} (1 - O_{pk}) O_{pj} \\ d_\alpha &= \frac{\partial E}{\partial W_{\alpha_1 kj}} = -(T_{pk} - O_{pk}) O_{pk} (1 - O_{pk}) (-\frac{1}{3}) O_{pj} \\ d_\beta &= \frac{\partial E}{\partial W_{\beta_1 kj}} = -(T_{pk} - O_{pk}) O_{pk} (1 - O_{pk}) (\frac{1}{3}) O_{pj} \end{aligned} \tag{3.24}$$

Layers weights are updated using local gradient d similar to equation 3.13.

Step 3- Iteration

Iterate by repeating from step 1 until the error norm reduces to an acceptable level set by the user at the output or maximum number of iteration are reached.

3.2.8 Radial basis function network

Basically radial basis function network (RBFN) is composed of large number of simple and highly interconnected artificial neurons and can be organized into several layers, i.e. input layer, hidden layer, and output layer as shown in figure 3.8.

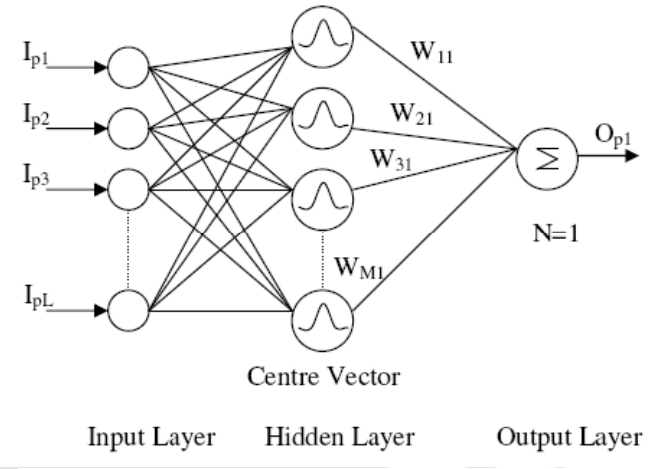

Figure 3.8 Architecture of radial basis network

(i) Algorithm of RBFN

Following steps shows the basic algorithm of radial basis network [166-167, 176] with a flow chart as shown in figure 3.9.

Input layer:

A normalized input pattern enters the input layer and is subjected to direct transfer function and output from input layer is same as input pattern. Number of nodes in the input layer is equal to the dimension of input vector L.

Output from input layer with element $I_{i(i=1\,to\,L)}$ is I_i.

Hidden layer:

The hidden layer does all the important process and these nodes satisfy a unique property being radially symmetry. Being *radially symmetry* it must have the following.

a. A *center vector* v_j in the input space, made up of cluster center with element $v_{ji(j=1\,to\,M)}$. '$M \le P$' where M is the number of center vectors and P is number of training patterns. The vector typically is stored as weight factors from input layer to hidden layer.

b. A *Distance measure* to determine how far an input pattern with element I_i is from cluster center v_{ji}. Euclidean distance norm is given by

$$\text{Euclidean distance } ed_j = \|I - v_j\| = \sqrt{\sum_{i=1}^{L}(I_i - v_{ji})^2} \qquad (3.25)$$

c. A *Transfer function*, which transfers Euclidean distance to give output for each node. Different type of transfer function available are

Linear function $f(x) = x$

Cubic approximation $f(x) = x^3$

Thin-plate-spline function $f(x) = x^2 \ln x$

Gaussian function $f(x) = e\left(\frac{-x^2}{\sigma^2}\right)$

Multi quadratic function $f(x) = \sqrt{x^2 + \sigma^2}$

Inverse multi quadratic function $f(x) = \left(\frac{1}{\sqrt{x^2 + \sigma^2}}\right)$

In our case Gaussian function has been used is given by

$$output_j = \exp(ed_j^{\,2} \div \sigma^2) \tag{3.26}$$

where σ controls the width of the RBF center referred to as spread parameter determined from [195]

$$\sigma = \max(ed) / \sqrt{M} \tag{3.27}$$

where $\max(ed)$ is maximum Euclidean distance between selected centers and M is the number of centers.

Output layer:

There are weight factor $w_{kj(k=1\,to\,N,\,j=1\,to\,M)}$ between kth nodes of output layer and jth nodes of hidden layer.' N 'is the dimension of output vector. Output from output layer transferred through a sigmoid transfer function.

Output from the output layer is given by

$$output_k = f(\sum_{j=1}^{M} w_{kj} \times output_j) \tag{3.28}$$

(ii) Learning by self-organized center

1. It is a self-organizing feature map network also known as 'SOFM' in which initial center vectors (v_j) are chosen randomly. The only restriction is that these initial values must be different.
2. The training samples are read and Euclidean distance is calculated for the initial center vector as per equation (3.25)
3. The corresponding center vector is modified closest to the training sample as

$$v_j^{new} = v_j^{old} + \eta \times (I_{pi} - v_j^{old}) \tag{3.29}$$

$P = training\ sample$

$j = number\ of\ cener\ vector$

$i = input\ node$

$\eta = learning\ rate\ i.e\ 0 < \eta < 1$

4. This process is continued for fixed number of iteration until no noticeable change is observed for the center vector v_j. This is known as k-means clustering algorithm [176], a special case of competitive (winners takes all) learning process.
5. Spread parameter is calculated as per equation (3.27)
6. The weights of output layer are initialized to small random values, and output from output layer is calculated as per equation (3.28)
7. MSE of training sample is calculated and if the MSE training does not reach the goal specified then the weights are updated based on gradient descent method. The weights are updated based on batch mode.
8. The process is carried out for a definite number of iteration.

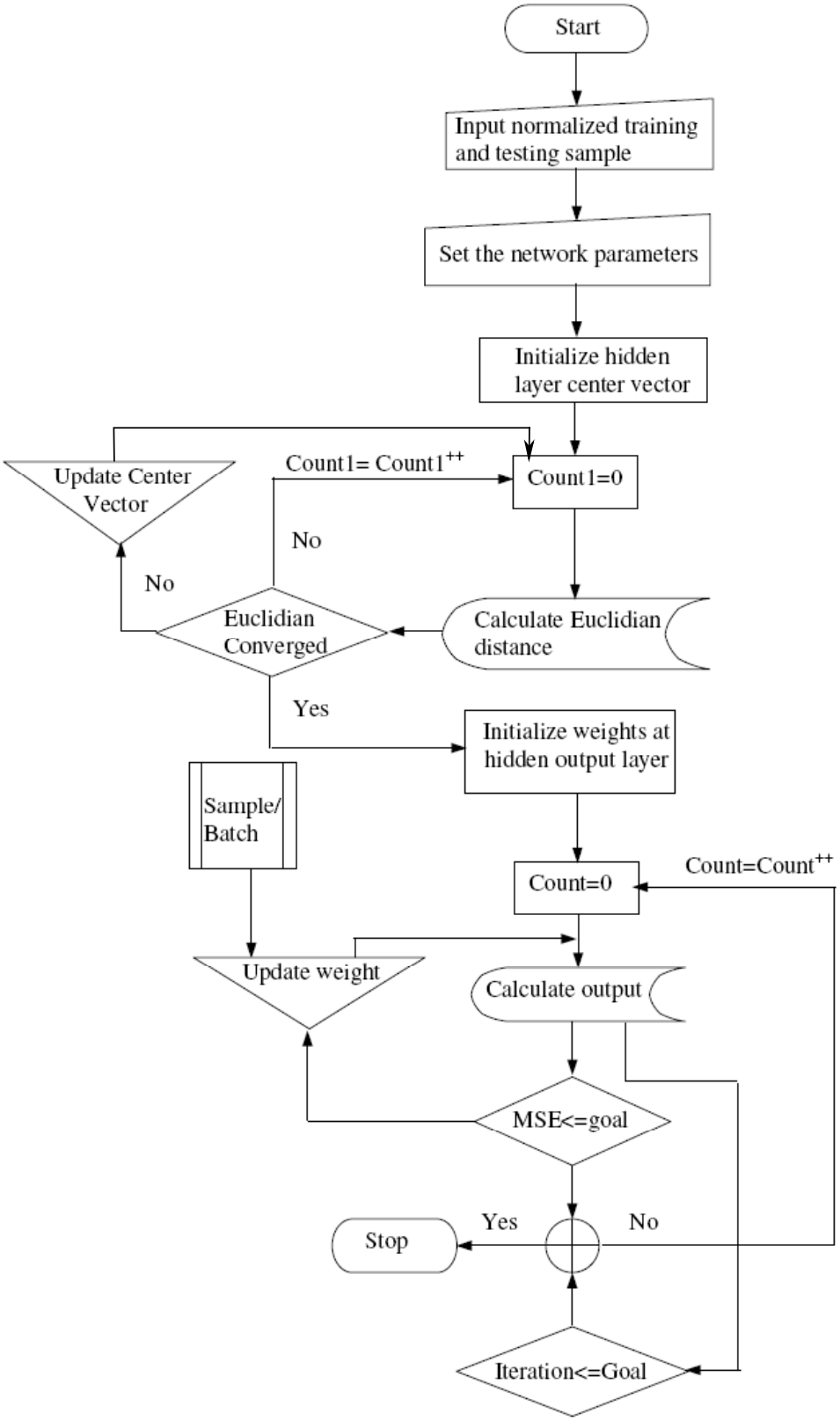

Figure 3.9 Flow chart of radial basis function network

3.2.9 Fuzzy radial basis function network

Step1-Initialization: First normalize the data set to be used for training, testing and validating. Present the network with an epoch of normalized training example $(I_{pi}(n), d_{pi}(n))$. Data set are normalized as per equation 3.2. Start with a reasonable network configuration (i.e. number of layers, number of nodes in each layer) and set all the connection weights and center vector with small random numbers from uniform distribution.

Step2-Degree of membership function

Calculate the degree of membership of input $I_{pi}(i=1....l)$ by using membership function value. Both input vector I, and weight vector W are represented by a triangular LR type fuzzy number. Thus for $I=(I_1,.....I_l)$ the input component vector I_i is represented by LR type fuzzy number $(I_{mi}, I_{\alpha_1 i}, I_{\beta_1 i})$. Similarly for $v_{ji}=(v_1.....v_l)$ for $(i=1.....l)$ the fuzzy center vector component v_{ji} is represented as $(v_{\alpha_1 i}, v_{\beta_1 i}, v_{\delta i})$ and for $W_{kj}=(W_1.....W_m)$ for $(j=1.....m)$ the weight vector component W_{kj} is represented as fuzzy weight $(W_{\alpha_1 j}, W_{\beta_1 j}, W_{\delta j})$.

Step3- Euclidean distance

A distance measure to determine how far an input pattern with element I_i is from cluster of fuzzy center v_{ji}. We have used Euclidean distance norm for this purpose. Given the input vector $I=(I_1,.....I_l)$ and center vector $v_{ji}=(v_1.....v_l)$, the fuzzy neuron computes the crisp output of Euclidian distance, given by

$$ed_j = \left\| I - v_j \right\| = CE\sqrt{\sum_{i=1}^{L}(I_i - v_{ji})^2} \tag{3.30}$$

Here fuzzy vector subtraction is following the same rule of fuzzy number theory and fuzzy weight summation is given by

$$net_j = \sum_{i=1}^{L}(I_i - v_{ji})^2 \tag{3.31}$$

The function CE is the centroid operation of the triangular fuzzy number, and can be treated as defuzzification operation, which maps fuzzy weight summation value to a crisp value. Thus, if $net=(net_m, net_{\alpha_1}, net_{\beta_1})$ is the fuzzy weight summation then function CE is given by

$$CE = net_m + 1/3(net_{\beta_1} - net_{\alpha_1}) \tag{3.32}$$

Step4- Updating center vectors

The corresponding fuzzy center vector was modified closest to the training sample as

$$\begin{aligned} v_j^{new} &= v_j^{old} + \eta \times (I_{pi} - v_j^{old}) \\ P &= training\ sample \\ j &= number of\ center\ vector \\ i &= input\ node \\ \eta &= learning\ rate\ i.e\ 0 < \eta < 1 \end{aligned} \tag{3.33}$$

This process was continued for fixed number of iteration until no noticeable change was for the center vector v_j .

Step5- Output calculation

A *transfer function*, which transfers Euclidean distance to give output for each node. In the present work Gaussian function has been used for this purpose. Output from a neuron in the hidden layer is

$$O_j = \exp(ed_j^{\,2} \div \sigma^2),\ j = 1.....m \tag{3.34}$$

where σ is the spread parameter determined from $\sigma = \max(ed)/\sqrt{M}$

Output from a neuron in the output layer is,

$$O_k = f(NET_k) = f\left(CE\left(\sum_{j=1}^{m} W_{kj} O_j\right)\right), k = 1, 2.....n \tag{3.35}$$

The function *f* is the sigmoid function, which performs nonlinear mapping between hidden and output is defined as

$$f(NET) = \frac{1}{1 + \exp(-NET)} \tag{3.36}$$

Step6- MSE calculation

Mean square error of each pattern is calculated by

$$\text{Output error } e_{pk}(n) = d_{pk}(n) - O_{pk}(n) \tag{3.37}$$

$$\text{Mean square error } E_p = \sum_{i=1}^{n} \frac{1}{2}(D_{pi} - O_{pi})^2 \tag{3.38}$$

Step 7- Backward pass

In the backward pass, local gradient, change in weight factor and modified weight can be calculated similar to equation 3.13.

3.2.10 Learning in ANN

Methodology described in the present work is BPNN, FBPNN, RBFN and FRBFN. In all cases of different ANNs, learning proceeds in one of the two basic ways i.e. sample and batch mode of learning. In sample mode, weight updating is performed based on presentation of individual training example. In batch mode, weight updating is performed based on presentation of all training example that constitute an epoch. Batch mode type of supervised learning has been used in the present case. During training, the predicted output is compared with the desired output, and the mean square error is calculated. If the mean square error is more than a prescribed limiting value, it is back propagated from output to input, and weights are further modified till the error or number of iteration are within a prescribed limit. Mean square error, E_p for pattern *p* is given in equation 3.7.

Weight change at any time *t*, is given by

$$\Delta W(n) = -\eta E_p(n) + \alpha \times \Delta W(n-1) \tag{3.39}$$

where, η is learning rate, and α momentum parameter.

3.2.11 Testing and validation of ANN

Entire experimental data set is randomly partitioned into training set and testing set. The training set is further partitioned into estimation subset and validation subset. The motivation here is to validate the model on a data set different from the one used for parameter estimation. The error on the validation set is monitored during the training process. The validation error will normally decrease during the initial phase of training, as does the training set error. However, when the network begins to over fit the data, the error on the validation set will typically begin to rise. In order to guard against this possibility, generalization performance of selected model is measured on the test set which is different from the validation set. When the validation error starts increasing for a specified number of iterations, the training is stopped and the weights at the minimum value of the validating error are returned. With the trained network, unseen data sets (test set) are verified and percentage of variation of output (flank wear) of actual test data thus evaluated.

3.2.12 Heuristic optimization of ANN parameters

The performance of ANN with respect to minimum error level or number of iteration required for convergence of results is dependent on learning rate (η) and momentum parameter (α), number of hidden layers and number of nodes in hidden layers. In the present case optimum values of learning rate and momentum parameter, number of hidden

layers and number of nodes in hidden layers has been obtained heuristically by trying large number of architectures as follows

- For a fixed variation of η and α (in the range 0.1 to 0.9) large number of ANN architectures are tried with different hidden layers (between 1 and 2) as well as number of neuron in hidden layers (1-40) and the optimum number of hidden neurons are based on minimum prediction error.
- Keeping the number of hidden neuron fixed different values of η and α are tried to get the optimum combination of η and α. This combination of η and α are tried again for ANN architectures near the optimum to get the best one.

CHAPTER 4

EXPERIMENTAL PROCEDURE

This chapter describes the experimental set up used, the details of the equipment and sensors used in conducting experiments, measurement of drill flank wear and acquisition of sensor signals.

4.1 Experimental Set up

Large numbers of drilling operations have been conducted at different cutting conditions (combination of speed, feed rate and drill diameter). Different sensors such as force sensor, torque sensor, vibration sensor are attached and sensor signals have been acquired using data acquisition system during drilling. Intermittently, the flank wear of the drills are also measured to know the condition of the drill corresponding to each cutting condition. Figure 4.1 shows the photograph of the experimental setup and the details of each component of the system have been described in the following.

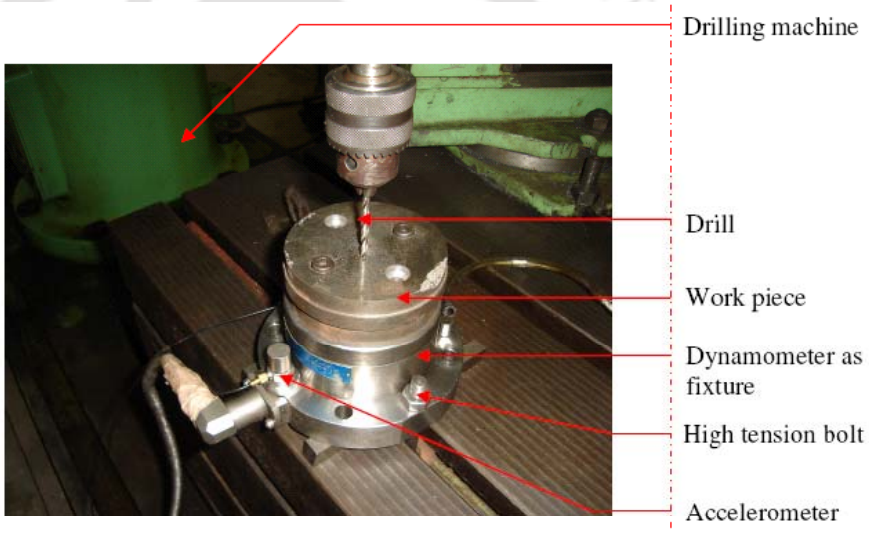

Figure 4.1 Photograph of experimental set-up

(i) Work piece: Wear rate of drill depends upon the relative hardness of the work-piece material and drill material for a given cutting condition. In order to represent a wide range of hardness of work-piece material in the present work three types of work piece materials viz. Copper (soft), Mild Steel and Cast Iron (hard) have been chosen. Drilling operations are carried out for a 25mm through hole on work pieces made of, copper, and cast iron mild steel. Table 4.1(a) shows the chemical compositions of materials for different work pieces measured by the help of digital scanning electron microscope (Model LEO 1430VP) used in the present experiment and table 4.1(b) shows the corresponding mechanical properties.

Table 4.1 Chemical composition and mechanical properties of the work piece materials

(a) Chemical composition (wt %)

Work piece	Carbon	Manganese	Silicon	Sulfur	Phosphorous	Copper	Iron
Mild steel	0.07	1.1	0.5	0.035	0.025		Rest
Cast iron	3.3	0.5	1.9	0.1	0.15		Rest
Copper		2.5	1.5			Rest	

(b) Mechanical properties

Work piece	Density (Kg/m^3)	Brinell hardness number (BHN)
Mild steel	7850	110
Cast iron	7000	185
Copper	8940	75

(ii) Drill: Since the present study intend to monitor wear on drill, therefore High Speed Steel (HSS) uncoated drills (Make: Addison Co. India) drills have been chosen to have a substantial wear in drilling in Copper, Mild Steel and Cast iron. HSS drills with different diameters have been used for drilling in various work pieces at different cutting conditions. Table 4.2(a) shows the drill geometry as supplied by manufacturer and these were checked before conducting experiments using toolmaker microscope and vernier caliper. Table 4.2(b) shows the chemical composition of the material of the drill measured by help of digital scanning electron microscope (Model LEO 1430VP) used in the present work.

Table 4.2 HSS drill geometry and chemical composition

(a) Geometry of HSS drill (long series)

Tool diameter (mm)	Flute length (mm)	Total length (mm)	Point angle (degree)	Helix angle (degree)
5	87	132	118	30
7.5	102	156	118	30
9	115	175	118	30
10	121	184	118	30
11	128	195	118	30
12	134	205	118	30

Flute	2 flutes
Flute type	parabolic
Shank type	straight cylindrical
Coating, if any	No

(b) Chemical Composition of HSS drill materials (wt %)

Tungston	Cromium	Vanadium	Cobalt	Molybdenum	Carbon	Iron	Hardness
18	4.3	1.6	5	0.8	0.8	Rest	235 BHN

(iii) Drilling machine: A radial drilling machine (Make: Batliboi Limited, BR618 model) has been used for conducting the drilling operations. The spindle speeds for model range from 50 to 1600 rpm in 16 steps and feed rate range from 0.13 to 1.4 mm/rev in 8 steps. Figure 4.2 shows the photograph of the radial drilling machine used for the present work.

Figure 4.2 Photograph of radial drilling machine

(iv) Dynamometer: A four channel (Model: Kistler 9272) has been used to record thrust force and torque signals during drilling operation. The sensitivity for the thrust force and torque for the dynamometer are -3.8 pC/N and -1.6 pC/N-cm respectively. Figure 4.3 shows the photograph of the dynamometer used in the present work. The dynamometer has been attached at the bottom side of the work piece as shown in figure 4.1.

Figure 4.3 Dynamometer (Kistler, types 9272)

(v) Charge amplifier: The torque and thrust force signals from the dynamometer are passed through two amplifiers (Model: Kistler 5015) having sensitivities of 1000 N/V and 10 Nm/V corresponding to thrust force and torque respectively. Figure 4.4 shows the photograph of the amplifier used in the present work.

Figure 4.4 Amplifier

(vi) Data acquisition system: All the data from the amplifiers are stored in a personal computer (PC) through a data acquisition card (Model: Advantech PCL-818HG)

which has the facilities of A/D conversion, D/A conversion, digital input, digital output. Analog signal collected over a period of time is passed through a 16 channel A/D converter in 16 bit digital time-discrete value with 100 kHz sampling rate. Software selectable analog input within the ranges of ± 5 volts has been used in the present analysis and low level programme is written in C in order to collect data during drilling.

(vii) Accelerometer probe: In the present work, two piezo-electric accelerometers (Model: Bruel & Kjaer, 4396) have been used to capture vibration signals. One accelerometer has been attached to the top surface of the work piece to extract feed vibration and other to the side surface of the work piece to extract radial vibration. A low noise coaxial cable has been used. Figure 4.5 shows the photograph of the accelerometer used in the present work.

Figure 4.5 Accelerometer (model, 4396)

(viii) Vibration analyzer: Signals from accelerometer were passed through vibration analyzer (Model: Bruel & Kjaer, 3560 D) in the frequency range 7Hz-25.6kHz and is stored in the PC through a Bruel & Kjaer pulse software. Figure 4.6 shows the photograph of the vibration analyzer used in the present experiment.

Figure 4.6 Vibration analyzer (model, 3560 D)

(ix) Microscope: Flank wear which determines the condition of the drill has been measured intermittently corresponding to all cutting condition with the help of reflected light optical microscope (Model: Carl Zeiss Axiotech, 25×25 mm travel range, height of 440 mm with a 30° viewing angle). A charge couple display (CCD) color camera (Model: WAT-201A, 280K Pixels, 350 TV Lines resolution, -10° ~ +45°C operating temperature) is attached to capture the image and KS 300 software has been interfaced with microscope for characterizing the surface under investigation. A variety of magnified lenses available in the microscope and in the present work, lens of magnification $20\times$ has been used to focus an illuminated area of $1.7\times1.7\,mm^2$. Figure 4.7 shows the photograph of the microscope used in the present work.

(xi) Portable Surface Roughness Tester: In the present work, centerline average (CLA) values of surface roughness of drilled holes has been measured by a surface roughness tester (Model: Mahr, GmbH). After drilling to a specified depth, roughness values at three different points (120^0 to each other at the periphery of the hole) have been measured and are averaged out. Figure 4.8 shows the photograph of surface roughness tester used in the present work and it has the following specifications

Figure 4.7 Optical microscope

Specification

R_a is average roughness (0.2 μm to 5.3 μm)

Max. Stylus Force (15.0mN)

Traverse Speed (5.08mm per second)

Operating Temperature (-10 ^0C to 45 ^0C)

Figure 4.8 Surface roughness tester

4.2 Measurement of flank wear

Flank wear on the drill has been measured intermittently corresponding to each cutting condition by taking out the drill and focusing the flank faces of the cutting edges under the optical microscope. The drill is placed with the help of a fixture so that the cutting edges are focused for the wear measurement. This is repeated so as to cover the entire length of the cutting edges and wear is measured at number of points on the cutting edges (points 1, 2, 3 and 4 as shown in figure 4.9). The maximum depth of flank wear among these points is taken as the wear on the drill.

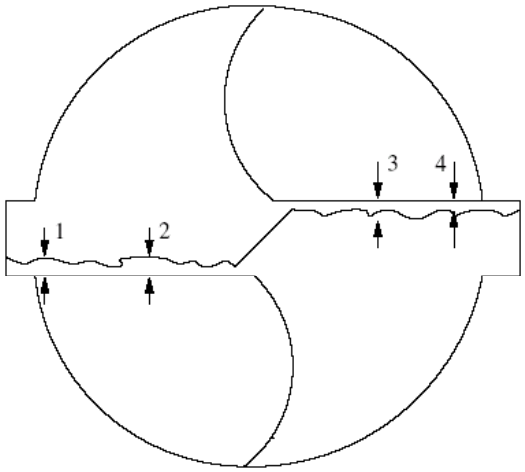

Figure 4.9 Flank wear measurement

4.3 Acquisition of sensor signals

Data in regard to thrust force, torque and vibration signals are analyzed both in time domain as well as in frequency domain to determine which gives better correlation with flank wear on drill. All the sensor signals along with other process parameters have been

stored corresponding to each cutting condition and the measured flank wear at that cutting condition. In many cases, chip thickness and surface roughness have also been collected intermittently along with tool wear for incorporating their features in the present study. These data are used to train an ANN for future prediction of drill wear. Figure 4.10 shows the schematic diagram for the drill wear prediction system used in the present work.

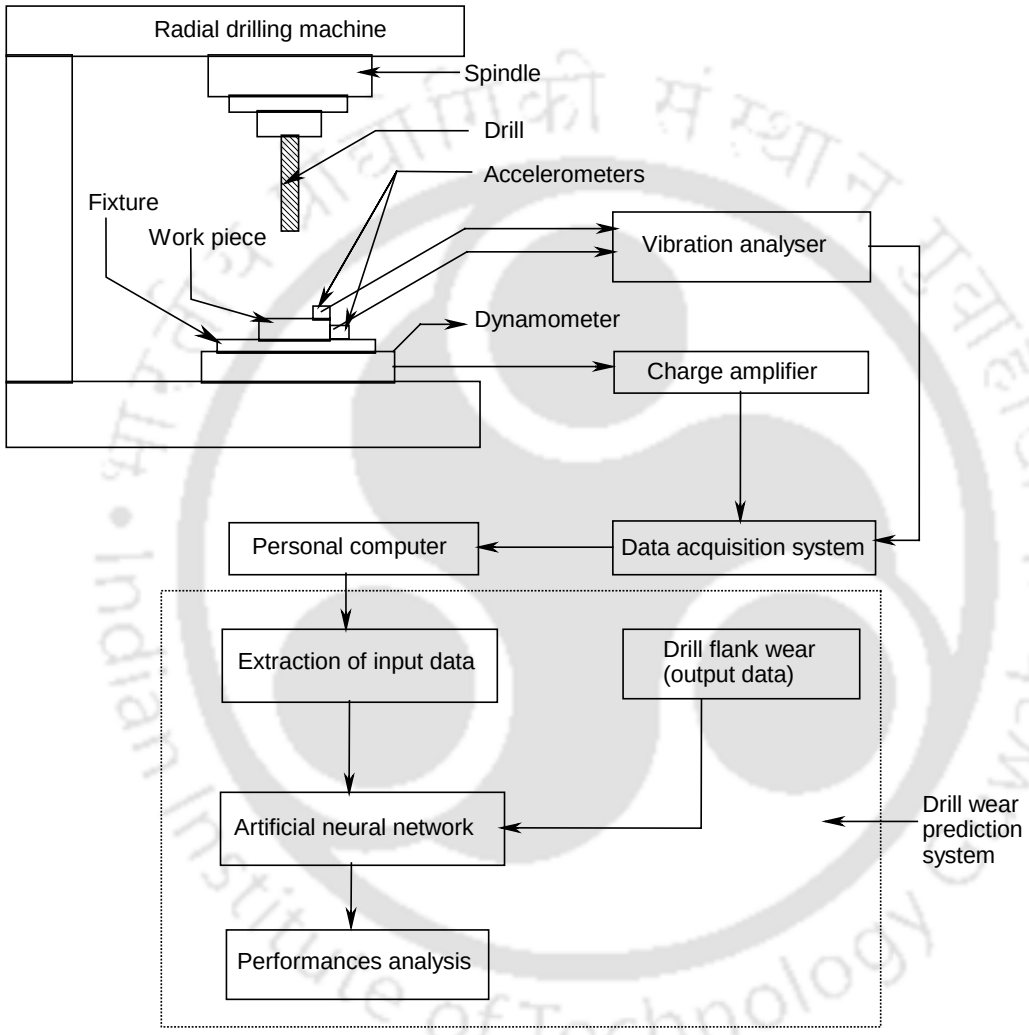

Figure 4.10 Schematic diagram of drill wear prediction system

CHAPTER 5

EXPERIMENTAL RESULTS AND DISCUSSION

This chapter describes the experimental observation during drilling on different work pieces materials viz. copper, cast iron and mild steel by HSS drill at different cutting conditions. Variation of important process parameters as well as sensor signals with the extent of wear has been presented in this chapter.

5.1 Experiments conducted and experimental condition

In the present work, experiments using HSS drill have been conducted on different work piece materials under different cutting conditions as listed in table 5.1. As far as possible the process parameters like spindle speed, feed rate and drill diameter have been chosen within the recommended range [11]. Experimental strategies in the present work evolved in the following manner.

- In the first set of experiments done on copper, only two sensor signals viz. thrust force and torque has been acquired.
- In the second stage of experiments done on cast iron, accelerations in radial and feed direction are also recorded in addition to thrust force and torque to look for a better combination of sensor signals.
- In the final stage of the experiments, mild steel has been taken as work-piece material and thrust force, torque, feed vibration and radial vibration, along with chip thickness has been measured. In this experiments surface roughness of drilled holes were also measured in order to study its effectiveness as an indicative parameter for drill wear.

Table 5.1 Stages of experiments

	Work-piece	Ranges of spindle speed (rpm)	Ranges of feed rate (mm/rev)	Ranges of drill diameter (mm)	Sensor signals acquired	Others
Experiment I	Copper	315,400, 500, 630,800, 1000	0.13,0.18, 0.25, 0.36,0.5, 0.71	5,7.5,10	Thrust force, Torque	Nil
Experiment II	Cast iron	250,315, 400, 500	0.13,0.18, 0.25, 0.36	9,10,11, 12	Thrust force, Torque, Feed vibration, Radial vibration	Nil
Experiment III	Mild steel	315,500, 630, 1000	0.13,0.18, 0.25, 0.36	9,10,11, 12	Thrust force, Torque, Feed vibration, Radial vibration	Chip thickness, surface roughness

5.2 Analysis of sensor signals

All the sensor signals acquired in the present work are in time domain. In order to study the relative performances of these signals in co-relating with drill wear, sensor signals are converted to frequency domain using Fast Fourier Transform (FFT). Co-relationship of both time domain and frequency domain signals with drill flank wear is done with the help of a polynomial regression equation. For a fixed regression model, co-relationship of wear with both time and frequency domain signals are shown in table 5.2 in terms of regression coefficient. A polynomial regression model has been chosen owing to non-linearity existing during the operation

Table 5.2 Regression coefficients

		R^2 (Regression coefficient) of sensor signals with wear			
	Polynomial order	Thrust force	Torque	Feed vibration	Radial vibration
Time domain	3rd order	0.98313	0.9721	0.96851	0.99698
	5th order	0.98883	0.9812	0.97477	0.99747
	7th order	0.99363	0.9903	0.99738	0.99854
	9th order	0.99372	0.9927	0.99921	0.99885
Frequency domain	3rd order	0.9447	0.9547	0.95306	0.98958
	5th order	0.95423	0.9631	0.96035	0.99368
	7th order	0.96925	0.9784	0.99396	0.99459
	9th order	0.97004	0.9814	0.99414	0.99749

It could be observed from the table that regression coefficient corresponding to time domain signals as well as frequency domain signals have strong correlation with flank wear even through the time domain signals correlated marginally better compared to frequency domain signals in the present case. Through the observation shown in table 5.2 is for drilling mild steel work piece a similar trend has also been observed while drilling cast iron and copper work pieces. It is also observed that among the sensor signals radial vibration correlates with drill wear better compared to thrust force, torque and feed vibration. In the present work time domain representation of the sensor signals has been used.

5.3 Experimental observations

Experiments were conducted at different stages for drilling pre-defined depth of through-holes in different work-pieces. Sensors were attached to the work-piece to collect signals during drilling as described in chapter 4 (figure 4.1). In the present work no coolant has been used.

5.3.1 Drilling holes in copper work pieces

In the first stage of experiments, 49 holes have been drilled using HSS drill on a copper work-piece at different cutting conditions. Thrust force and torque have been recorded through the dynamometer. In the present work, time domain sensor signals were recorded and root mean square (RMS) values of thrust force and torque have been stored corresponding to each cutting condition. Flank wear has also been measured using optical microscope corresponding to each cutting condition. Table 5.3 shows thrust force, torque and drill flank wear corresponding to different cutting conditions.

Table 5.3 Experimental data of experiments I

Serial number	Drill diameter (mm)	Spindle speed (rpm)	Feed rate (mm/rev)	RMS values of thrust force (N)	RMS values of torque (N-m)	Drill flank wear (μ m)
1	10	500	0.13	1925	19.253	110
2	7.5	500	0.13	510	7.1	60
3	5	500	0.13	245	2.5	30
4	10	500	0.18	3860	25.1	195
5	7.5	500	0.18	595	4.41	80
6	5	500	0.18	275	2.75	60
7	10	500	0.25	3740	27.44	210
8	7.5	500	0.25	539	5.39	105
9	5	500	0.25	386	2.9	95
10	10	400	0.13	2518	23.52	185
11	7.5	400	0.13	853	11.27	85
12	5	400	0.13	267	3.1	50
13	10	400	0.18	3921	26.78	200
14	7.5	400	0.18	646	12.64	100
15	5	400	0.18	451	3.96	85
16	10	400	0.25	4010	29.25	260
17	7.5	400	0.25	1051	16.54	100
18	5	400	0.25	505	1.96	70
19	10	630	0.13	1258	10.11	120
20	7.5	630	0.13	488	5.86	90
21	5	630	0.13	186	2.94	80
22	10	630	0.18	1470	13.23	125
23	7.5	630	0.18	524	3.95	100
24	5	630	0.18	187	2.64	70
25	10	630	0.25	3077	15.68	180
26	7.5	630	0.25	441	4.41	100
27	5	630	0.25	285	2.15	25
28	10	800	0.36	2234	22.34	160
29	7.5	800	0.36	1666	8.66	130
30	10	800	0.5	2548	24.1	190
31	7.5	800	0.5	1440	13.3	130
32	5	800	0.5	1087	11.27	90
33	10	315	0.36	3303	25.33	200
34	7.5	315	0.36	1866	12.74	160
35	5	315	0.36	592	7.72	100
36	10	315	0.5	3413	29.54	205

Table 5.3 (contd.)

37	7.5	315	0.5	1688	15.19	140
38	5	315	0.5	1210	13.39	80
39	10	315	0.71	3920	36.22	240
40	7.5	315	0.71	1828	17.15	120
41	5	315	0.71	1282	16.66	100
42	10	1000	0.36	1460	12.25	140
43	7.5	1000	0.36	554	5.39	95
44	5	1000	0.36	421	4.21	60
45	10	1000	0.5	1960	18.13	130
46	7.5	1000	0.5	784	7.35	100
47	5	1000	0.5	651	6.17	70
48	10	1000	0.71	2009	20.58	170
49	7.5	1000	0.71	970	8.05	120

5.3.1.1 Dependencies of thrust force and torque on drill diameter and spindle speed

Figure 5.1 shows the variation of thrust force with drill diameter for different spindle speeds for a constant feed rate of 0.5 mm/rev and figure 5.2 shows the variation of torque with drill diameter for different spindle speeds for a constant feed rate of 0.5 mm/rev. In both the figures it could be observed that thrust force and torque increase with the increase in drill diameter and decrease with increase in spindle speeds. These observations agree well with already established results [2,42].

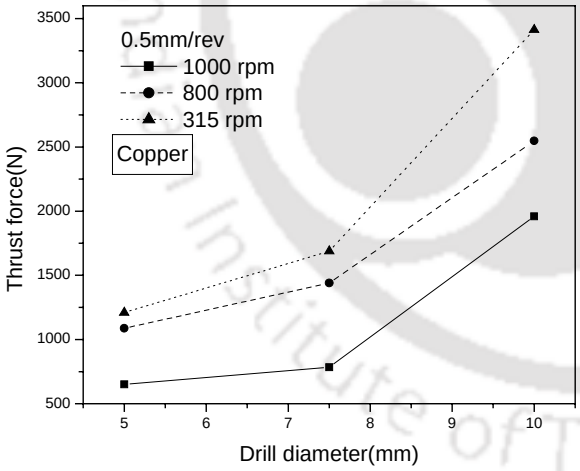

Figure 5.1 Effect of drill diameter and spindle speeds on thrust force

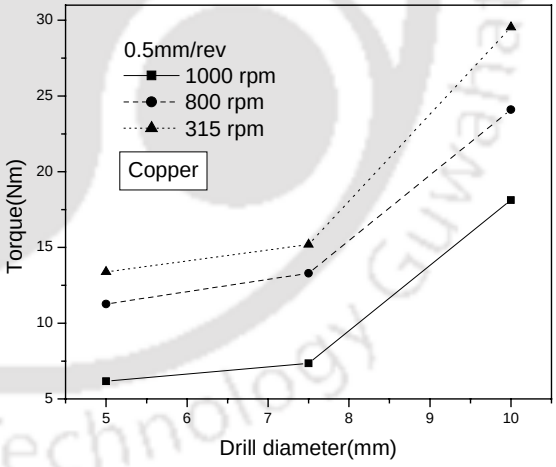

Figure 5.2 Effect of drill diameter and spindle speeds on torque

5.3.1.2 Dependencies of thrust force and torque on feed rate

Figure 5.3 shows the variation of thrust force with feed rate for different drill diameters for a constant spindle speed of 1000 rpm and figure 5.4 shows the variation of torque with feed rate for different drill diameters for a constant spindle speed of 1000 rpm. In both the figures it could be observed that thrust force and torque increase with the increase in feed rate. These observations agree well with already established results [2,42].

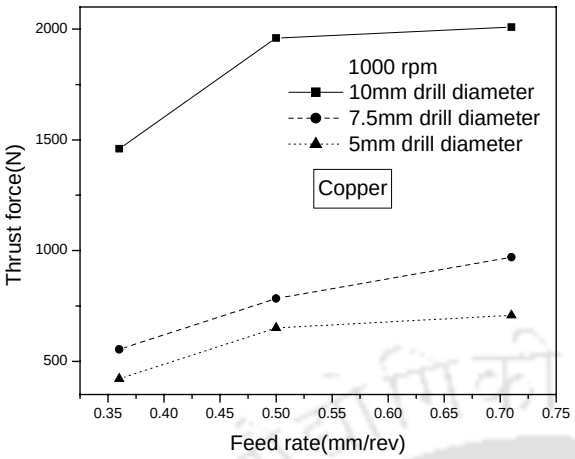

Figure 5.3 Effect of feed rate on thrust force

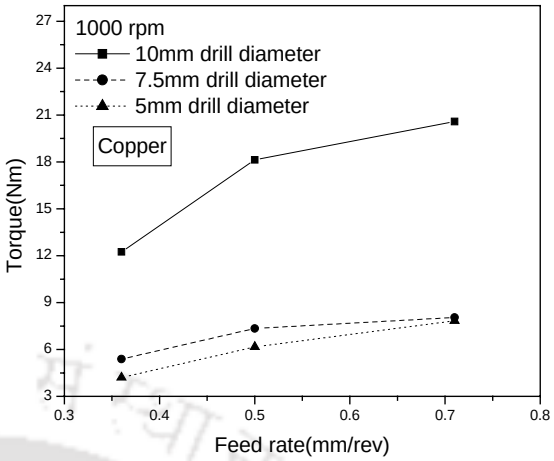

Figure 5.4 Effect of feed rate on torque

5.3.1.3 Progress of flank wear

Figure 5.5 shows the progressive nature of flank wear while drilling successive holes with a 10 mm diameter HSS drill on copper work piece at a spindle speed of 400 rpm and feed rate of 0.13 mm/rev. It could be observed that slope of the curve increases rapidly beyond 150 seconds showing the beginning of unsteady region of wear. Figures 5.6 show the photograph of the focused wear land under optical microscope where growth of wear after 50 second and 150 second are shown in figures 5.6(a) and 5.6(b) respectively.

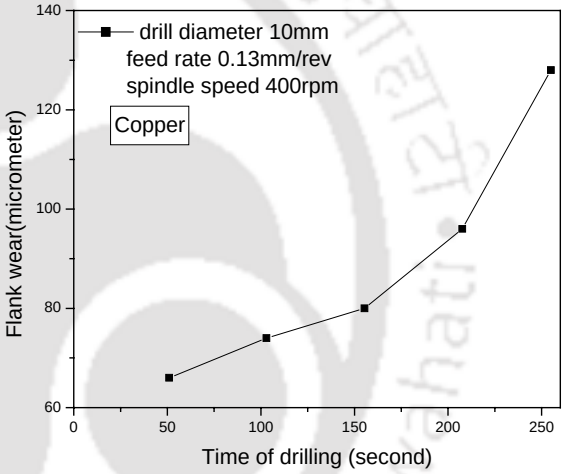

Figure 5.5 Progressive nature of flank wear

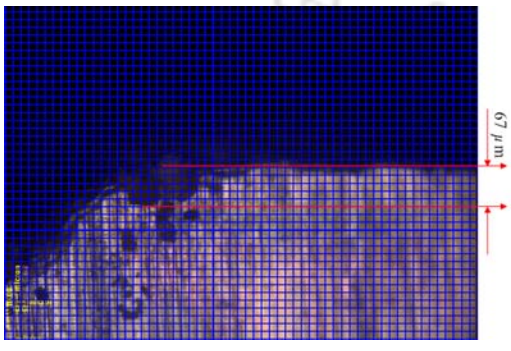

Figure 5.6 (a) Wear on drill at 50 second

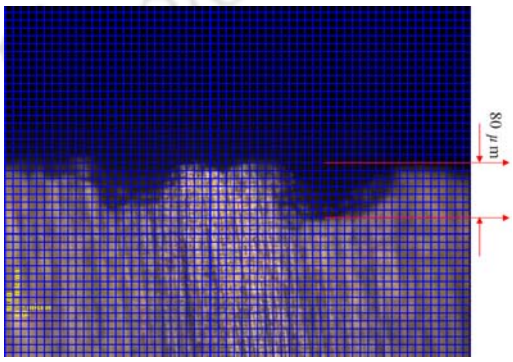

Figure 5.6 (b) Wear on drill at 150 second

5.3.1.4 Influence of wear on thrust force and torque

Figure 5.7 shows variations of thrust force with progressive drill wear for a 10 mm diameter drill at 400 rpm spindle speed and 0.13 mm/rev feed rate. It could be observed that thrust force increases with increase in drill wear and at different ranges of flank wear slopes are different. Figure 5.8 shows the variation of torque with progressive drill wear for a 10 mm diameter drill at 400 rpm spindle speed and 0.13 mm/rev feed rate. Here also torque increases with increase in flank wear. The increase in thrust force and torque with increased wear may be due to the increase in friction between the drill and the work piece.

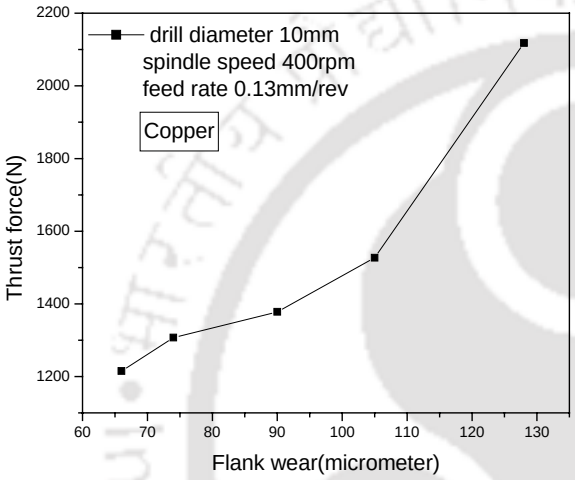

Figure 5.7 Effect of flank wear on thrust force

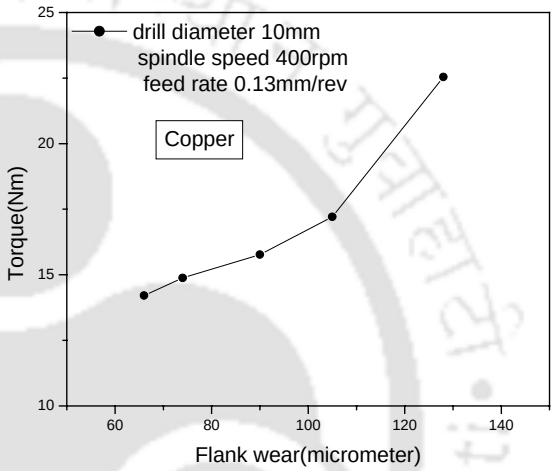

Figure 5.8 Effect of flank wear on torque

5.3.1.5 Summary

Holes have been drilled in a copper work piece by HSS drill at different cutting conditions and thrust force and torque signals have been acquired. Drill wear has been measured intermittently. Dependencies of sensor signals on cutting parameters like spindle speed, feed rate and drill diameter have been studied and they agree with already established results. More importantly, dependencies of sensor signals on the wear of the drill has been studied and it has been observed that both thrust force and torque show an increasing trend with the increase in extent of flank wear. Therefore thrust force and torque signals may be possible candidates to be used for indirect drill wear monitoring.

5.3.2 Drilling holes in cast iron work pieces

In drilling holes in copper by HSS drill, the rate of wear was much less and hence it took long time (or large number of holes to be drilled) to have appreciable wear on the drill. In order to have appreciable wear on the drill in a relatively shorter time, cast iron has been chosen as the work piece material. At this stage it was also thought to acquire more sensor signals with an expectation that better indication of drill wear could be achieved. A total of 64 different drilling operations have been performed at different cutting conditions. Thrust force and torque have been recorded through the dynamometer and additionally vibration signals have also been recorded using accelerometers. Figures 5.9(a-b) show typical cutting force signals in time domain as obtained through the data acquisition system during drilling a hole. Figures 5.10(a-b) show typical accelerometers signals in time domain as obtained through the data acquisition system for one revolution. In the present work, time domain sensor signals were recorded and root mean square (RMS) values of thrust force, torque and accelerations have been stored corresponding to each cutting condition. Flank wear has also been measured using optical microscope corresponding to each cutting condition and table 5.4 shows thrust force, torque, accelerations and drill flank wear corresponding to different cutting conditions.

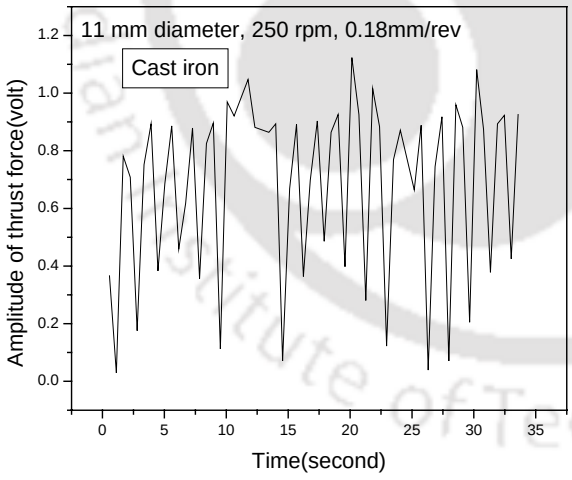

Figure 5.9 (a) Variation of thrust force with time

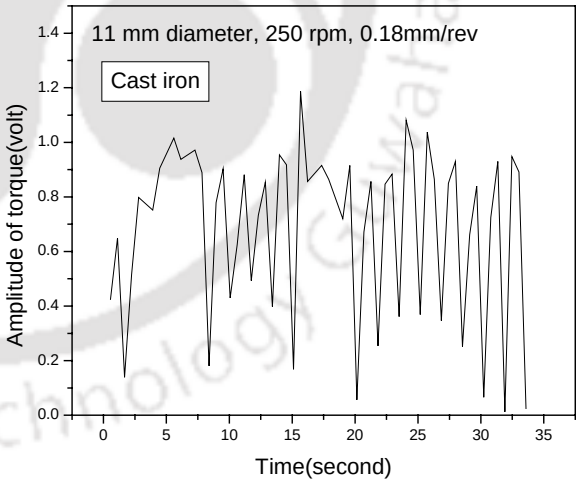

Figure 5.9 (b) Variation of torque with time

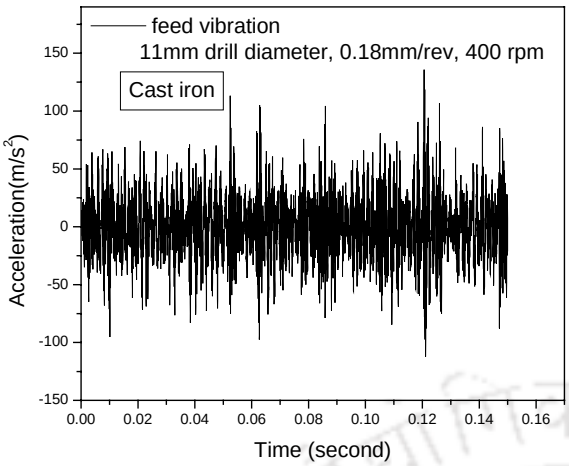

Figure 5.10(a) Variation of feed vibration with time

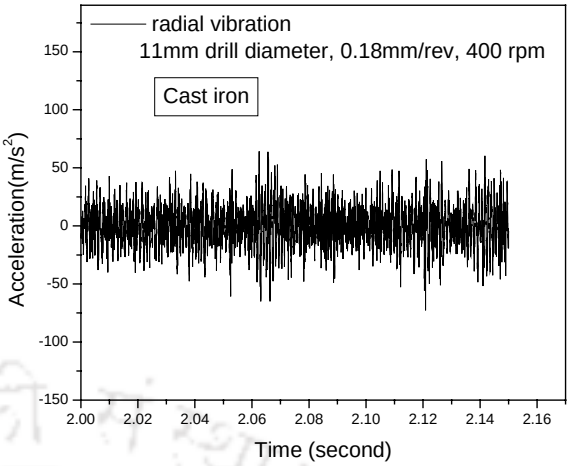

Figure 5.10(b) Variation of radial vibration with time

Table 5.4 Experimental data of experiments II

Serial No	Dill diameter (mm)	Spindle speed (rpm)	Feed rate (mm/rev)	RMS values of thrust Force (N)	RMS values of torque (Nm)	RMS values of feed vibration (m/s^2)	RMS values of radial vibration (m/s^2)	Drill flank wear (μ m)
1	9	500	0.13	1088.1	10.67	37.36	39.28	100
2	9	400	0.13	1150.9	11.22	31.24	33.22	120
3	9	315	0.13	1185.2	11.43	24.52	25.12	150
4	9	250	0.13	1212.4	11.47	20.06	21.16	160
5	9	500	0.18	1435.1	14.66	35.48	36.75	130
6	9	400	0.18	1486.4	15.01	29.32	30.48	150
7	9	315	0.18	1707.8	16.97	21.24	22.26	160
8	9	250	0.18	1752.6	17.23	18.85	19.52	180
9	9	500	0.25	1588.3	16.04	33.72	35.52	60
10	9	400	0.25	1642.8	16.36	27.21	27.86	100
11	9	315	0.25	2025.8	20.06	19.14	21.32	110
12	9	250	0.25	2077.1	20.35	17.21	18.10	130
13	9	500	0.36	1669.8	17.12	30.93	31.11	90
14	9	400	0.36	1721.3	17.64	24.18	25.14	110
15	9	315	0.36	2778	27.82	17.63	18.40	120
16	9	250	0.36	2816.7	28.22	15.46	16.21	140
17	10	500	0.13	1188.3	11.06	43.21	45.30	70
18	10	400	0.13	1215.6	11.18	39.54	41.26	80
19	10	315	0.13	1627.3	15.8	33.27	35.52	110
20	10	250	0.13	1677.3	16.01	27.30	28.69	120
21	10	500	0.18	1504.8	15.11	41.12	42.24	120

Table 5.4 (contd.)

22	10	400	0.18	1547.7	15.71	36.28	37.72	150
23	10	315	0.18	1827.6	18.27	30.41	31.10	160
24	10	250	0.18	1869.7	18.64	22.51	24.24	180
25	10	500	0.25	1668.9	16.85	39.54	40.44	110
26	10	400	0.25	1715.2	17.08	35.44	36.42	140
27	10	315	0.25	2786.7	27.84	28.26	29.67	160
28	10	250	0.25	2824.2	28.11	20.52	22.60	170
29	10	500	0.36	1754.8	17.69	37.24	38.65	80
30	10	400	0.36	1782.6	17.95	31.22	33.46	120
31	10	315	0.36	3284.2	32.95	25.37	26.30	150
32	10	250	0.36	3323.1	33.08	18.63	20.23	140
33	11	500	0.13	1254.9	12.54	47.26	49.32	100
34	11	400	0.13	1318.6	13.04	43.22	44.62	110
35	11	315	0.13	1342.9	13.61	36.03	37.41	130
36	11	250	0.13	1394.6	13.88	31.24	33.14	170
37	11	500	0.18	1556.8	18.32	45.92	47.24	130
38	11	400	0.18	2067	20.71	40.29	42.10	140
39	11	315	0.18	2097	21.03	34.27	35.80	160
40	11	250	0.18	2156.8	21.72	28.67	29.88	170
41	11	500	0.25	1724.3	23.41	44.66	45.54	140
42	11	400	0.25	2538.9	25.42	38.23	39.28	150
43	11	315	0.25	2753.8	27.68	31.58	33.41	160
44	11	250	0.25	2885.6	28.04	27.49	28.62	180
45	11	500	0.36	1869.4	24.65	41.25	43.21	90
46	11	400	0.36	2752.7	27.66	35.45	37.68	120
47	11	315	0.36	2860.1	28.55	28.66	29.67	150
48	11	250	0.36	3001.4	29.14	25.33	27.26	170
49	12	500	0.13	1277.8	13.28	61.51	62.36	140
50	12	400	0.13	1464.3	14.39	56.58	58.12	160
51	12	315	0.13	1524.6	15.28	48.26	49.24	170
52	12	250	0.13	1578.2	15.62	41.72	43.76	200
53	12	500	0.18	1624.3	18.51	57.11	59.49	110
54	12	400	0.18	2114.6	18.64	55.46	57.43	130
55	12	315	0.18	2121.8	21.17	44.69	45.56	140
56	12	250	0.18	2163.4	21.41	38.25	39.58	170
57	12	500	0.25	1856.3	23.51	54.62	56.24	100
58	12	400	0.25	2558.6	23.58	51.12	53.22	170

Table 5.4 (contd.)

59	12	315	0.25	2612.6	26.21	41.52	43.37	210
60	12	250	0.25	2672.6	26.52	35.68	37.2	240
61	12	500	0.36	2005.4	24.78	50.26	52.27	100
62	12	400	0.36	2924.3	24.92	48.88	49.62	150
63	12	315	0.36	3270	32.99	38.26	40.11	170
64	12	250	0.36	3311.2	33.11	33.28	35.26	190

5.3.2.1 Dependencies of thrust force and torque on feed rate and spindle speed

Figures 5.11 shows the variation of thrust force with feed rate for different spindle speeds at a constant drill diameter of 11 mm. Figures 5.12 shows the variation of torque with feed rate for different spindle speeds at a constant drill diameter of 11 mm. In both the figures it could be observed that thrust force and torque increase with the increase in feed rate and decrease with increase in spindle speeds. These observations agree well with already established results [2,42].

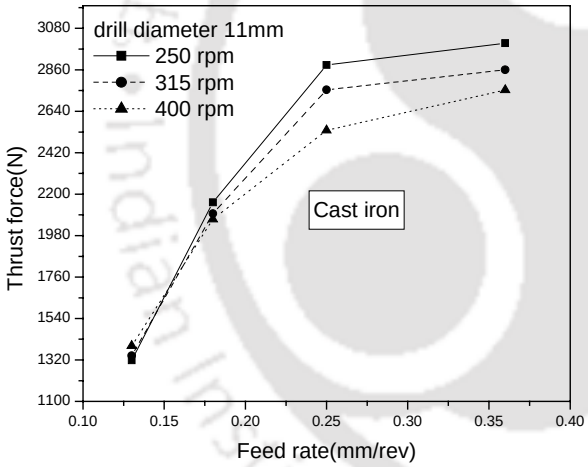

Figure 5.11 Effect of feed rate and spindle speed on thrust force

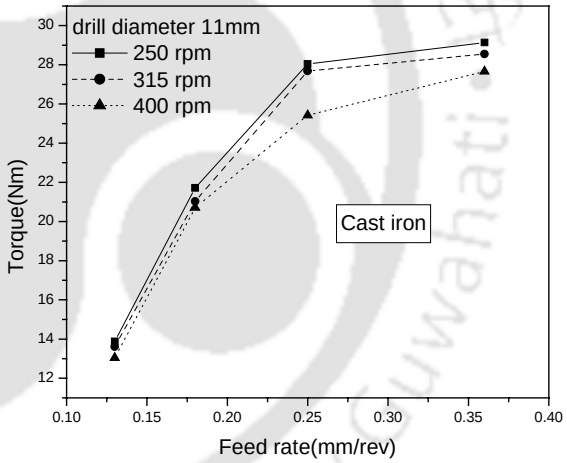

Figure 5.12 Effect of feed rate and spindle speed on torque

5.3.2.2 Dependencies of thrust force and torque on drill diameter

Figure 5.13 shows the variation of the thrust force with drill diameter for different feed rates at constant spindle speed of 500 rpm. Figure 5.14 shows the variation of torque with drill diameter for different feed rates at constant spindle speed of 500 rpm. In both the figures it could be observed that thrust force and torque increase with the increase in drill diameter. These observations agree well with already established results [2,42].

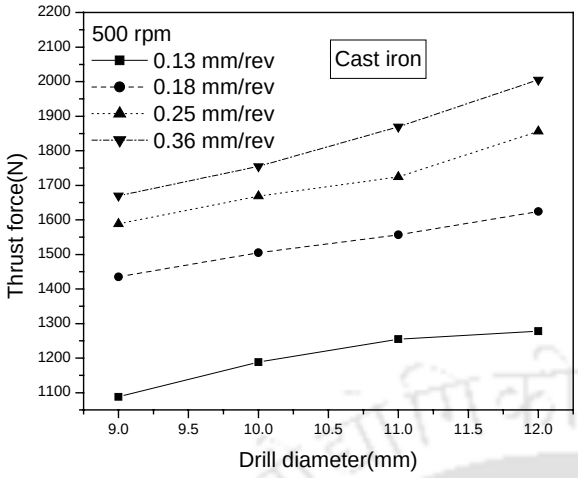

Figure 5.13 Effect of drill diameter on thrust force

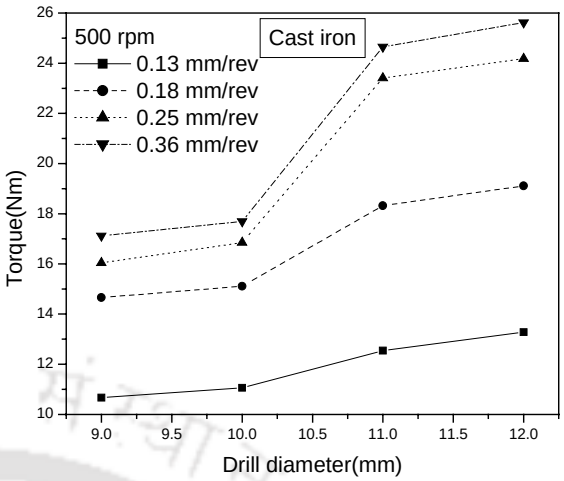

Figure 5.14 Effect of drill diameter on torque

5.3.2.3 Dependencies of vibration signals on feed rate and spindle speed

Figure 5.15 shows the variation of feed vibration with feed rate at different spindle speeds at constant 9 mm diameter drill. It could be observed that amplitude of feed vibration decreases with increase in feed rate and increases with increase in spindle speed. These results agree well with already established results [34].

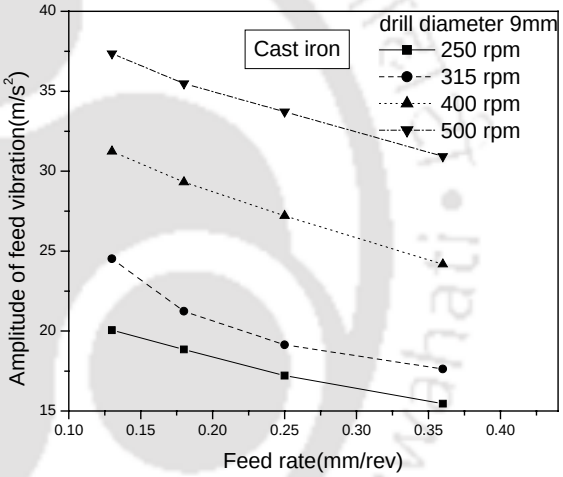

Figure 5.15 Effect of feed rate and spindle speed on feed vibration

5.3.2.4 Dependencies of vibration signals on drill diameter

Figure 5.16 shows variation of feed vibration amplitude with drill diameter for different feed rates at a constant spindle speed of 500 rpm. It could be observed that amplitude of feed vibration increases with increase in drill diameter, and this is due to the fact that increase in drill diameter increases the mass of drill hence increase the amplitude of feed vibration [80].

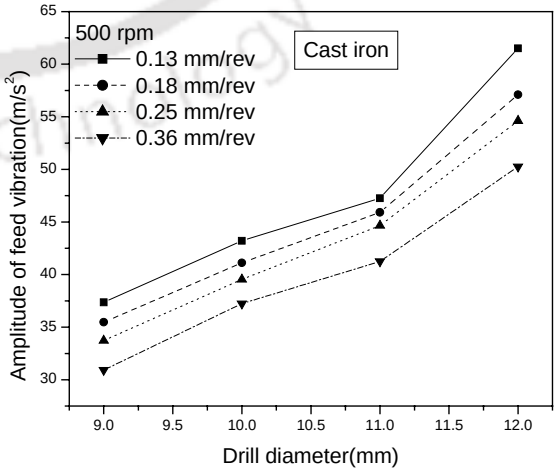

Figure 5.16 Effect of drill diameter on feed vibration

5.3.2.5 Comparison of feed vibration with radial vibration

Figure 5.17 shows the variations of the both the components of vibration signals with drill diameter at constant spindle speed of 500 rpm and constant feed rate of 0.13 mm/rev. It could be observed that the amplitude of feed vibration is less than that of radial vibration because of the restriction along cutting edges.

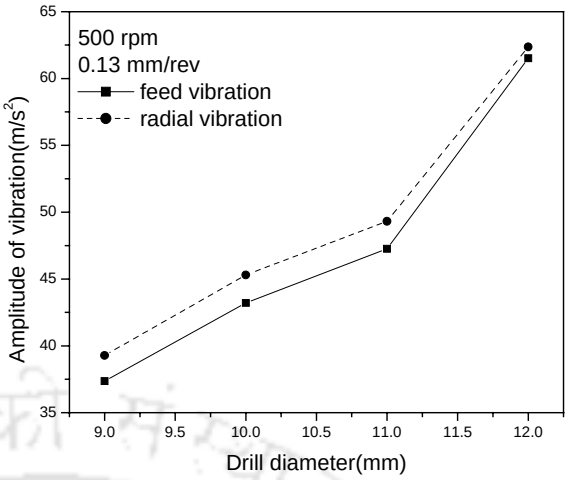

Figure 5.17 Comparison of feed vibration with radial vibration

5.3.2.6 Progress of flank wear

Figure 5.18 shows the progressive nature of flank wear while drilling successive holes with a 11 mm diameter HSS drill on cast iron work piece at a spindle speed of 500 rpm and feed rate of 0.13 mm/rev. It could be observed that slope of the curve increases rapidly beyond 90 second showing the beginning of unsteady region of wear. Figures 5.19 show the photograph of the focused wear land under optical microscope where growth of wear after twenty three second and seventy second are shown in figures 5.19(a) and 5.19(b) respectively.

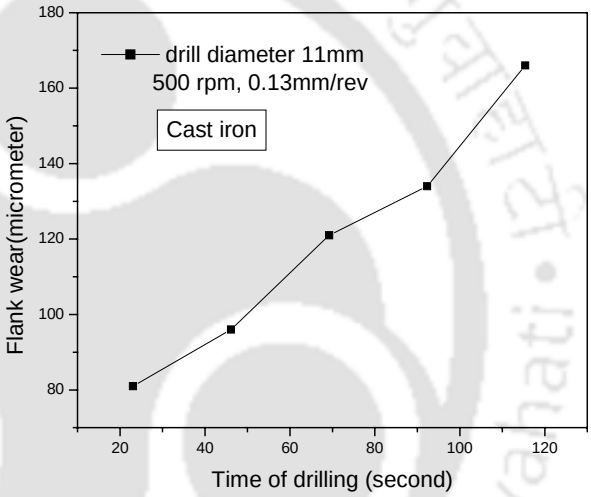

Figure 5.18 Progressive nature of flank wear

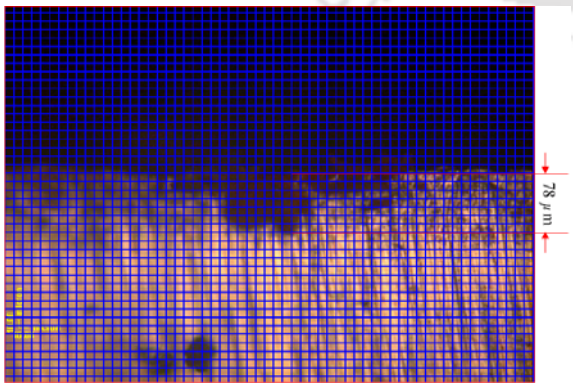

Figure 5.19(a) Wear on drill at 23 second

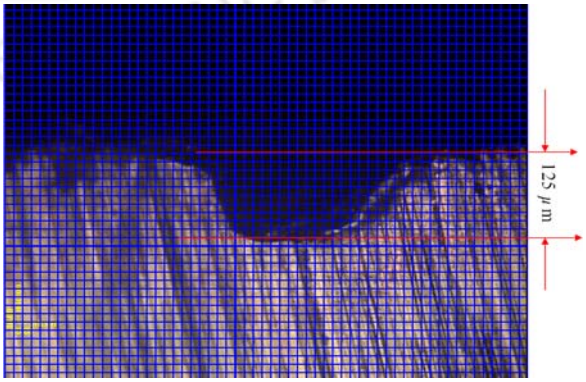

Figure 5.19(b) Wear on drill at 70 second

5.3.2.7 Influence of wear on thrust force and torque

Figure 5.20 shows variations of thrust force with progressive drill wear for a 9 mm diameter drill for different feed rates at constant spindle speed of 500 rpm. It could be observed that thrust force increases with increase in drill wear and at different ranges of flank wear slopes are different. Figure 5.21 shows the variation of torque with progressive drill wear for a 9 mm diameter drill for different feed rates at constant spindle speed of 500 rpm. Here also torque increases with increase in flank wear. The increase in thrust force and torque with increased wear may be due to the increase in friction between the drill and the work piece.

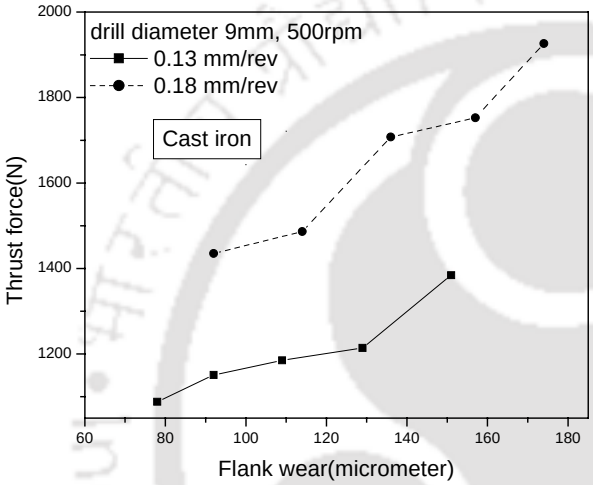

Figure 5.20 Effect of wear on thrust force

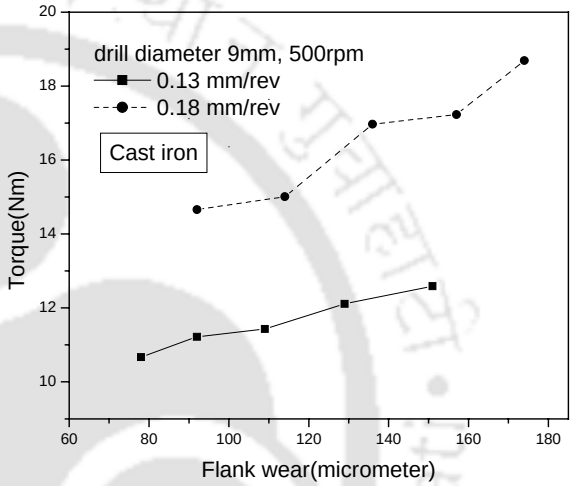

Figure 5.21 Effect of wear on torque

5.3.2.8 Influence of wear on vibration signals

Figure 5.22 shows the variation of feed vibration with time in drilling consecutive holes on a cast iron work piece at a constant drill diameter of 9mm, feed rate 0.18mm/rev and spindle speed of 500 rpm. It could be observed from figure 5.22 that initially the amplitude of vibration increase with the wear and then decreases. This is due to the fact that due to initial wear, vibration amplitude increases but as the drilling progresses, the reduction in mass of the work piece dominates and the amplitude decreases [80]. Figure 5.23 shows the variation of progressive drill wear with feed vibration for 9 mm diameter drill for different feed rates

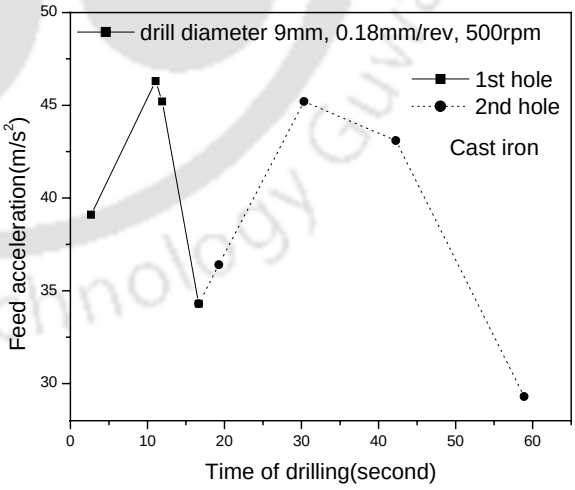

Figure 5.22 Effect of wear on vibration

at constant spindle speeds of 500 rpm. Figure 5.24 shows the variation of progressive drill wear with radial vibration for 9 mm diameter drill for different feed rates at constant spindle speeds of 500 rpm. It could be observed that feed vibration and radial vibration decreases with increase in drill wear. It is due to fact that increase in drill wear reduces the mass of drill as well as work piece and hence reduces the amplitude of feed vibration.

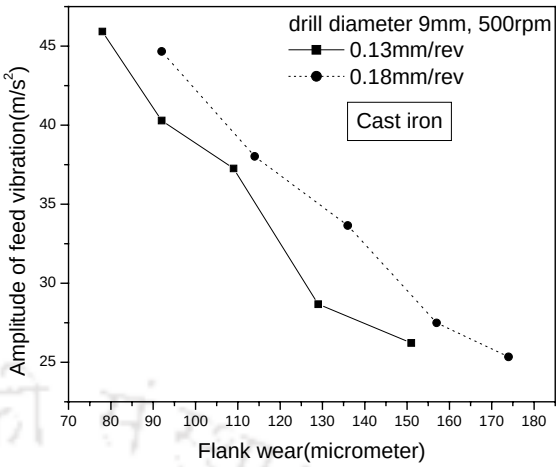

Figure 5.23 Effect of wear on feed vibration

5.3.2.9 Effect of feed rate on drill wear

Figure 5.25 shows variation of progressive drill wear with number of hole for a constant 11mm drill diameter and 500 rpm spindle speed at two different feed rates. It could be observed from the figure 5.25 that increase in feed rate increase drill wear. This may be due to the fact that increase in feed rate increases frictional force and hence increases the drill wear [173].

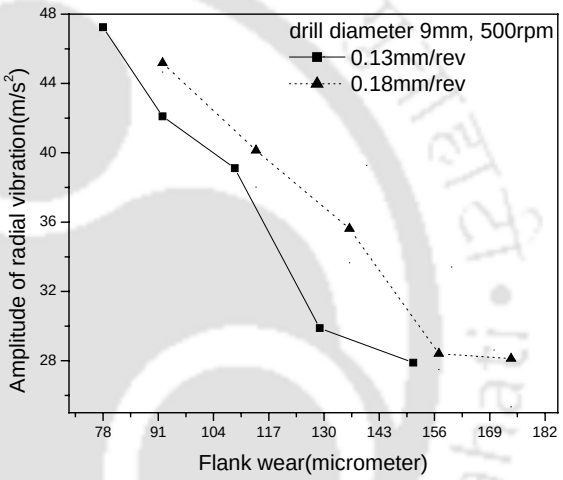

Figure 5.24 Effect of wear on radial vibration

5.3.2.10 Effect of drill diameter on drill wear

Figure 5.26 shows variation of progressive drill wear with number of hole at 0.18mm/rev feed rate and 500 rpm spindle speed for two different drills diameter. It could be observed from figure 5.26 that increase in drill diameter increases the drill flank wear. This may be due to the fact that increase in drill diameter increases frictional force and hence increases the drill wear.

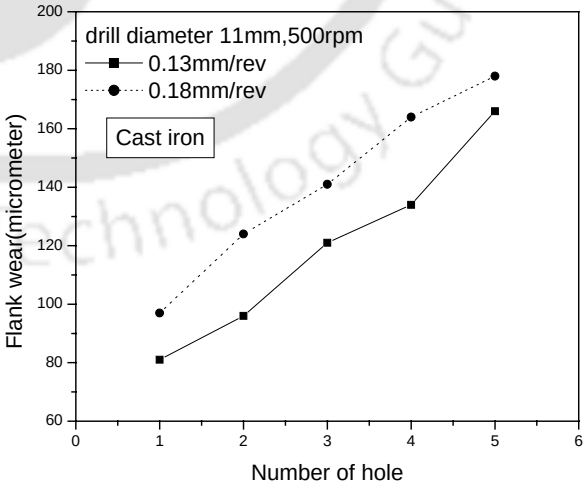

Figure 5.25 Effect of feed rate on drill wear

5.3.2.11 Effect of spindle speed on drill wear

Figure 5.27 shows variation of progressive drill wear with number of hole at 0.13mm/rev feed rate, for a 11 mm drill diameter for two different spindle speed. It could be observed from figure 5.27, that spindle speeds have negligible effect on the drill flank wear. It may be due to fact that increase in spindle speed reduces the time of cutting and hence reduces the wear on drill but amount of reduction is least influenced in the range of spindle speed.

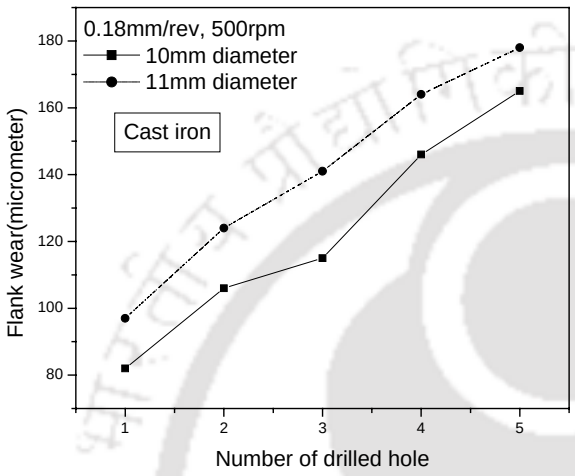

Figure 5.26 Effect of drill diameter on drill wear

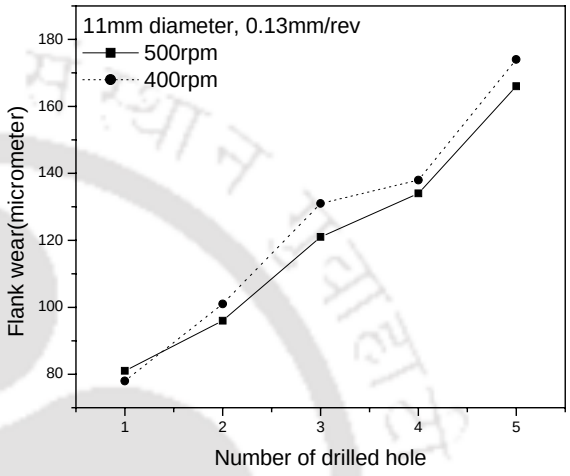

Figure 5.27 Effect of spindle speed on drill wear

5.3.2.12 Summary

It could be observed from the above experiments that cutting parameters (spindle speed, feed rate and drill diameter) have significant influence on the sensor signals and drill wear and the extent of wear influences the sensor signals such as thrust force, torque and vibrations.

5.3.3 Drilling holes in mild steel work pieces

In the last set of experiments, mild steel has been considered as work piece material for drilling holes using HSS drill. It has been reported in literature [175] that chip quality is influenced by the condition of the tool (or the extent of wear on drill in the present case). Therefore it was decided to observe the chip thickness along with other sensor signals with an objective of getting better indication of drill wear. It is also known that surface roughness of drilled holes get affected by the drill wear and hence surface roughness of drilled holes was also thought of as one of the indicative parameter for drill wear. Therefore, in these experiments, in addition to thrust force, torque and vibration signals, chip thickness and surface roughness were also recorded during drilling operation. A total of 64 different drilling operations have been performed at different cutting conditions. Thrust force and torque have been recorded through the dynamometer and additionally vibration signals have also been recorded using accelerometers. Figures 5.28(a-b) show typical cutting force signals in time domain as obtained through the data acquisition system during drilling a hole. Figures 5.29(a-b) show typical accelerometers signals in time domain as obtained through the data acquisition system for one revolution. In

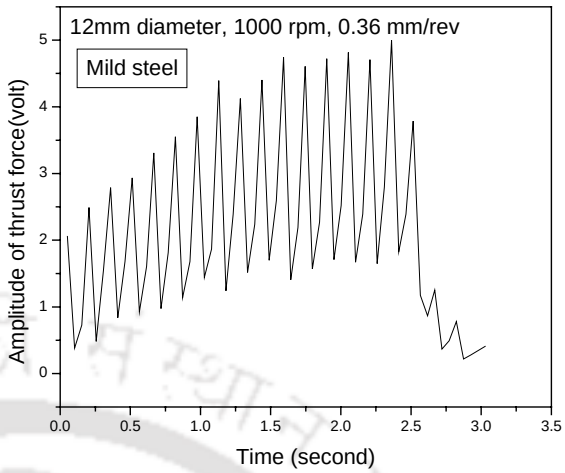

Figure 5.28(a) Variation of thrust force with time

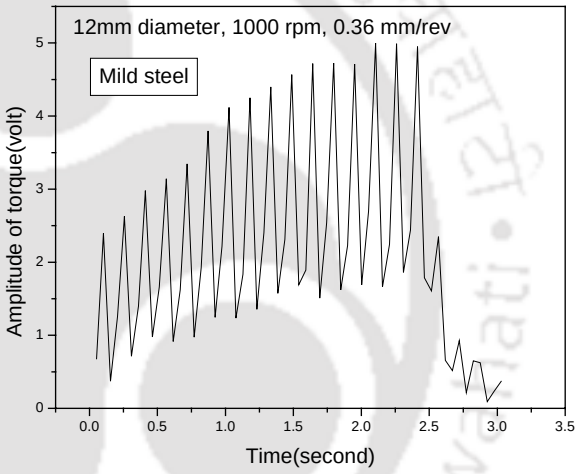

Figure 5.28(b) Variation of torque with time

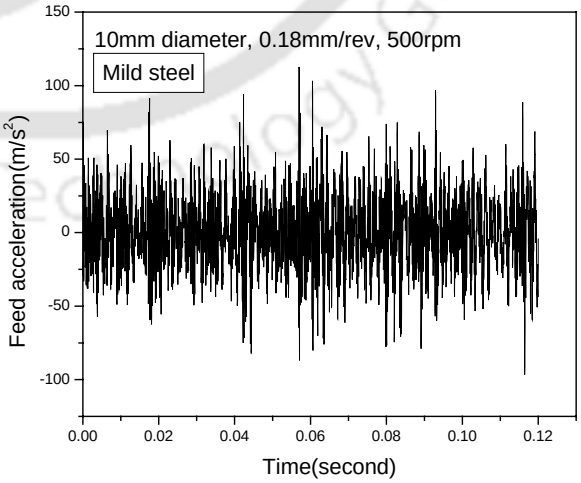

Figure 5.29(a) Variation of feed vibration with time

the present work, time domain sensor signals were recorded and root mean square (RMS) values of thrust force, torque and accelerations have been stored along with chip thickness and surface roughness of the drilled holes corresponding to each cutting condition. Flank wear has also been measured using optical microscope corresponding to each cutting condition and table 5.5 shows thrust force, torque, accelerations, chip thickness, surface roughness and drill flank wear corresponding to different cutting conditions.

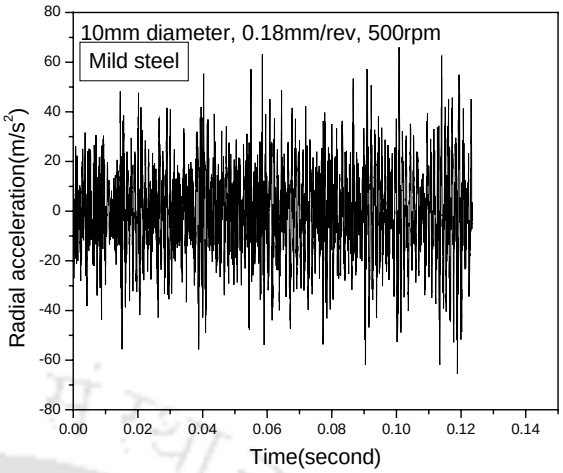

Figure 5.29(b) Variation of radial vibration with time

Table 5.5 Experimental data of experiment III

Serial No	Drill diameter (mm)	Spindle speed (RPM)	Feed rate (mm/rev)	RMS values of thrust force (N)	RMS values of torque (N-m)	RMS values of vibration (m/s^2)		Chip thickness (mm)	Average surface roughness (μm)	Drill Flank wear (μm)
						Feed	Radial			
1	9	1000	0.13	922.9	9.04	24.22	24.86	0.40	0.76	50.00
2	9	1000	0.18	1349	13.39	14.81	15.11	0.45	1.64	90.00
3	9	1000	0.25	1762.4	17.24	11.46	12.03	0.82	2.45	125.00
4	9	1000	0.36	3833.2	38.89	9.27	10.20	1.10	3.80	160.00
5	9	630	0.13	1096.9	10.52	18.67	18.96	0.47	0.77	80.00
6	9	630	0.18	1411.2	14.6	11.28	11.42	0.52	1.71	130.00
7	9	630	0.25	1814.6	17.88	8.84	9.31	0.88	2.51	155.00
8	9	630	0.36	3867.5	39.54	7.72	8.11	1.10	3.82	190.00
9	9	500	0.13	1187.9	12.12	10.42	11.06	0.50	0.81	110.00
10	9	500	0.18	1483.7	15.46	9.67	10.10	0.64	1.76	165.00
11	9	500	0.25	1887.4	19.11	5.55	5.88	0.95	2.59	190.00
12	9	500	0.36	3924.6	40.23	4.20	4.63	1.15	3.89	220.00
13	9	315	0.13	1221.5	12.54	8.76	9.45	0.60	0.84	150.00
14	9	315	0.18	1532.7	16.24	6.58	6.94	0.70	1.81	195.00
15	9	315	0.25	1926.3	20.06	4.71	5.12	1.00	2.62	220.00
16	9	315	0.36	4006.8	41.11	3.42	3.68	1.10	3.95	255.00
17	10	1000	0.13	1265.8	13.09	29.67	30.80	0.60	0.84	80.00
18	10	1000	0.18	1758.6	17.88	25.07	26.20	0.66	1.75	115.00

Table 5.5(contd.)

19	10	1000	0.25	2232.7	22.62	18.80	19.64	0.88	2.61	150.00
20	10	1000	0.36	4254.2	43.14	14.21	15.12	1.15	3.96	190.00
21	10	630	0.13	1366.8	13.66	21.14	21.86	0.65	0.83	110.00
22	10	630	0.18	1884.6	18.88	19.42	20.77	0.70	1.72	170.00
23	10	630	0.25	2334.1	23.76	14.28	15.67	0.90	2.63	190.00
24	10	630	0.36	4325.6	44.12	10.24	10.68	1.20	3.95	230.00
25	10	500	0.13	1425.1	14.56	15.67	16.66	0.72	0.85	140.00
26	10	500	0.18	1950.8	19.37	11.26	12.04	0.80	1.74	205.00
27	10	500	0.25	2468.9	25.64	7.78	8.46	0.95	2.60	240.00
28	10	500	0.36	4464.1	45.2	5.78	6.32	1.22	3.97	265.00
29	10	315	0.13	1511.1	15.96	11.14	11.96	0.77	0.88	165.00
30	10	315	0.18	2012.4	20.31	9.52	10.20	0.83	1.76	240.00
31	10	315	0.25	2584.3	26.23	5.96	6.66	1.00	2.63	265.00
32	10	315	0.36	4568.9	45.8	4.65	5.50	1.20	3.95	300.00
33	11	1000	0.13	1312.5	13.1	33.24	34.36	0.80	1.08	110.00
34	11	1000	0.18	1826.7	19.11	29.42	29.83	0.85	1.86	150.00
35	11	1000	0.25	2735.9	27.12	25.47	26.05	0.90	2.77	190.00
36	11	1000	0.36	4426.8	44.36	19.24	19.66	1.18	4.11	230.00
37	11	630	0.13	1465.2	14.24	24.82	25.47	0.85	1.05	130.00
38	11	630	0.18	1960.8	19.34	20.34	21.12	0.96	1.85	190.00
39	11	630	0.25	2864.9	32.56	17.26	17.88	1.10	2.75	230.00
40	11	630	0.36	4659.8	45.45	13.66	14.24	1.20	4.07	255.00
41	11	500	0.13	1612.5	16.68	20.56	21.18	0.90	1.08	170.00
42	11	500	0.18	2132.5	21.54	16.66	17.32	1.00	1.87	235.00
43	11	500	0.25	3214.6	33.21	12.29	12.76	1.05	2.79	275.00
44	11	500	0.36	4863.7	49.17	9.64	10.50	1.25	4.13	300.00
45	11	315	0.13	1779.8	18.35	16.27	17.08	0.90	1.10	185.00
46	11	315	0.18	2229.9	22.57	13.33	13.77	1.10	1.91	260.00
47	11	315	0.25	3422.1	35.64	8.56	9.14	1.15	2.77	285.00
48	11	315	0.36	4784.3	47.17	7.74	8.86	1.20	4.12	315.00
49	12	1000	0.13	1569.4	16.46	35.61	36.42	1.00	1.24	120.00
50	12	1000	0.18	2114.8	21.11	30.54	31.14	1.10	1.97	165.00
51	12	1000	0.25	3124.9	31.52	26.85	27.65	1.17	2.88	210.00
52	12	1000	0.36	4668.3	47.06	21.62	22.38	1.20	4.19	250.00
53	12	630	0.13	1666.6	17.02	28.47	29.24	0.90	1.23	150.00
54	12	630	0.18	2331.2	23.67	23.59	24.10	0.95	2.01	205.00

Table 5.5(contd.)

55	12	630	0.25	3268.4	32.66	19.92	20.88	1.15	2.87	245.00
56	12	630	0.36	4886.9	49.27	16.27	16.91	1.25	4.16	270.00
57	12	500	0.13	1841.5	18.66	24.88	25.83	1.05	1.25	180.00
58	12	500	0.18	2489.7	25.26	19.76	20.44	1.05	2.00	250.00
59	12	500	0.25	3434.1	35.14	17.49	18.50	1.30	2.90	290.00
60	12	500	0.36	4712.6	46.69	15.52	16.37	1.35	4.19	310.00
61	12	315	0.13	1996.3	20.11	19.11	19.53	1.10	1.21	200.00
62	12	315	0.18	2662.1	27.08	15.42	16.67	1.25	2.03	270.00
63	12	315	0.25	3611.2	36.87	11.26	11.97	1.35	2.89	300.00
64	12	315	0.36	4946.8	48.89	9.67	10.33	1.35	4.22	325.00

5.3.3.1 Dependencies of thrust force and torque on feed rate and spindle speed

Figure 5.30 shows the variation of thrust force with feed rate for different spindle speeds at a constant drill diameter of 9 mm. Figure 5.31 shows the variation of torque with feed rate for different spindle speeds at a constant drill diameter of 9 mm. In both the figures it could be observed that thrust force and torque increase with the increase in feed rate and decrease with increase in spindle speeds. These observations agree well with already established results [2,42].

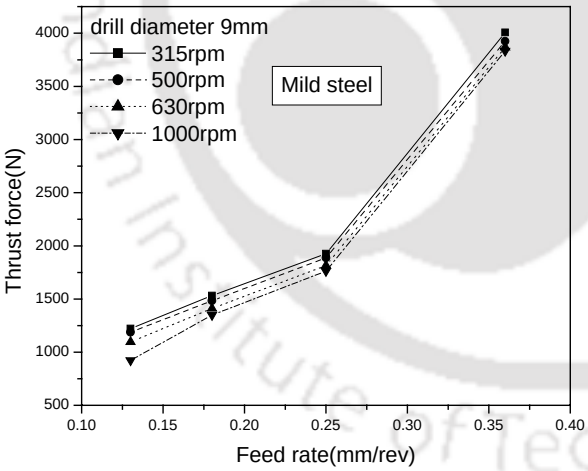

Figure 5.30 Effect of feed rate and spindle speed on thrust force

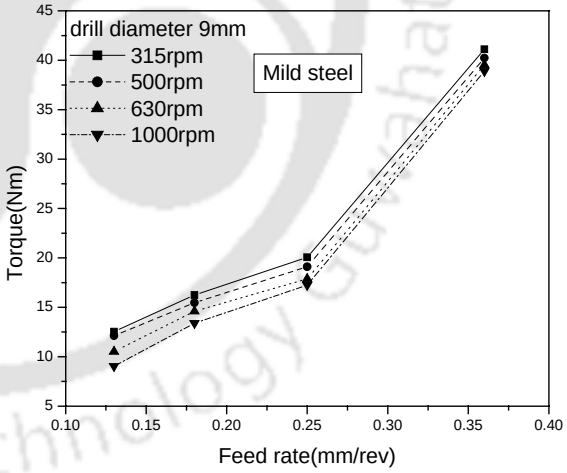

Figure 5.31 Effect of feed rate and spindle speed on torque

5.3.3.2 Dependencies of thrust force and torque on drill diameter

Figure 5.32 shows the variation of the thrust force with drill diameter for different feed rates at constant spindle speed of 630 rpm. Figure 5.33 shows the variation of torque with drill diameter for different feed rates at constant spindle speed of 630 rpm. In both the figures it could be observed that thrust force and torque increase with the increase in drill diameter. These observations agree well with already established results [2,42].

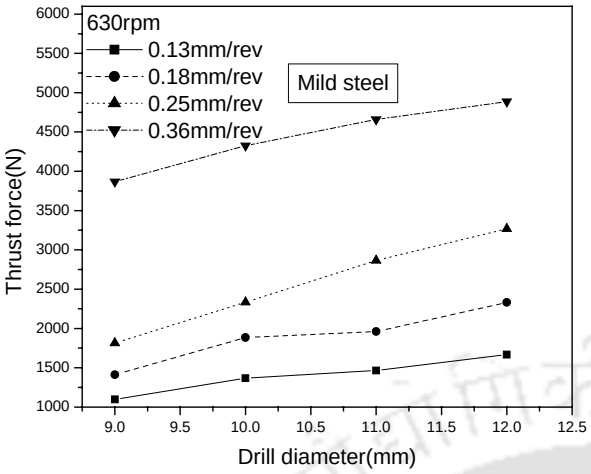

Figure 5.32 Effect of drill diameter on thrust force

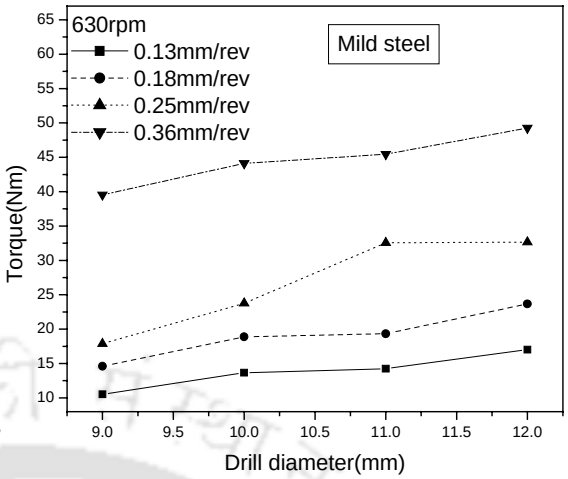

Figure 5.33 Effect of drill diameter on torque

5.3.3.3 Dependencies of vibration signals on feed rate and spindle speed

Figure 5.34 shows variation of feed vibration with feed rate for different spindle speeds for a 9 mm diameter drill. It could be observed that the amplitude of feed vibration decreases with increase in feed rate and increases with increase in spindle speed. This result agrees well with already established result [34].

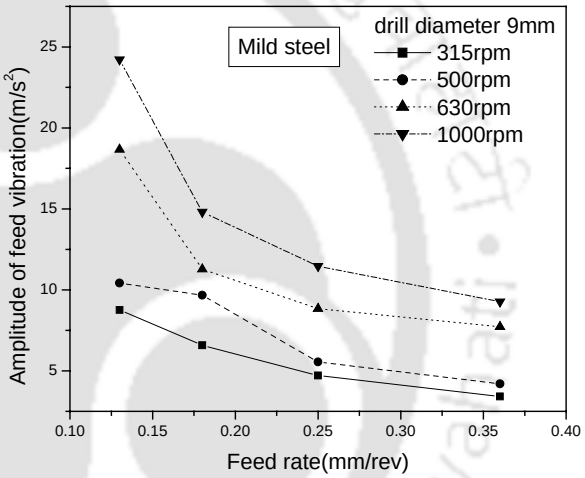

Figure 5.34 Effect of feed rate and spindle speed on feed vibration

5.3.3.4 Dependencies of vibration signals on drill diameter

Figure 5.35 shows variation of feed vibration amplitude with drill diameter for different feed rates at a constant spindle speed of 630 rpm. It could be observed that amplitude of feed vibration increases with increase in drill diameter, and this is due to the fact that increase in drill diameter increases the mass of drill hence increase the amplitude of feed vibration [80].

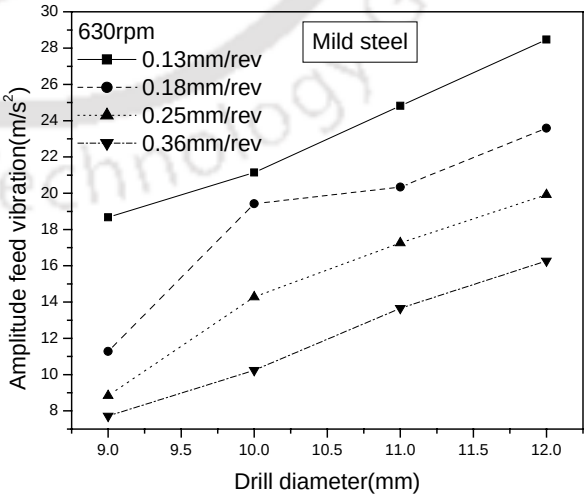

Figure 5.35 Effect of drill diameter on feed vibration

5.3.3.5 Comparison of feed vibration with radial vibration

Figure 5.36 shows the variation of the both the components of vibration signals with drill diameter at constant spindle speed of 630 rpm and constant feed rate of 0.13 mm/rev. It could be observed that the amplitude of feed vibration is less than that of radial vibration because of the restriction along cutting edges.

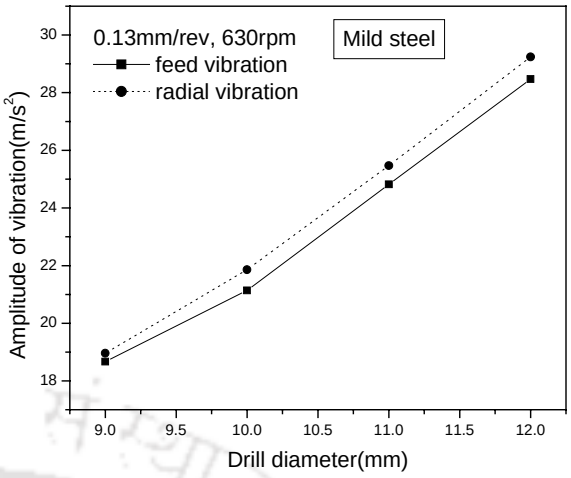

Figure 5.36 Comparison of feed vibration with radial vibration

5.3.3.6 Dependencies of surface roughness on spindle speed and feed rate

Figure 5.37 shows the variation of surface roughness of the hole with spindle speed and feed rate at constant drill diameter of 9mm. It could be observed that spindle speed have negligible effect on surface roughness of drilled hole surface. However increase in feed rate leads to increased surface roughness. This result well agrees with established result [2,34].

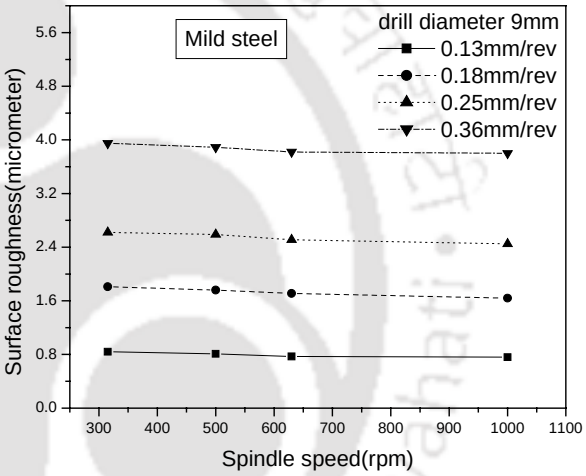

Figure 5.37 Effect of spindle speed and feed rate on surface roughness

5.3.3.7 Dependencies of surface roughness on drill diameter

Figure 5.38 shows the variation of surface roughness with drill diameter for different feed rates at a constant spindle speed of 1000 rpm. It could be observed that surface roughness increases with increase in drill diameter. It may be due to fact that increase in drill diameter increase the cutting forces hence increase the surface roughness.

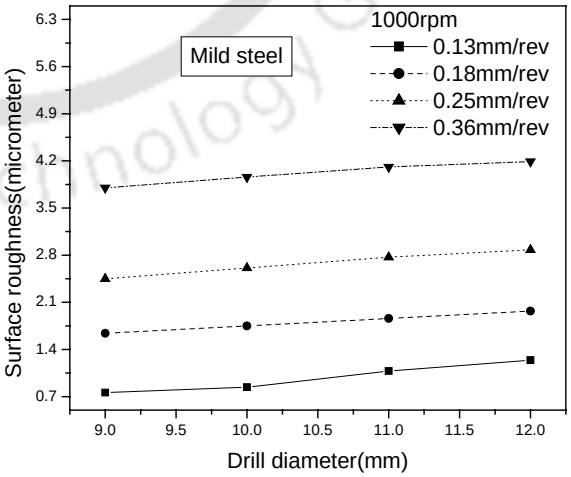

Figure 5.38 Effect of drill diameter on surface roughness

5.3.3.8 Dependencies of chip thickness on drill diameter and feed rate

The qualities of chips indicate the machining temperature and mechanism of chip formation, which are related to state of tool [175] under given cutting condition. Figure 5.39 shows variation of chip thickness with drill diameter for different feed rates at a constant spindle speed of 1000 rpm. It could be observed that chip thickness increases with increase in feed rate [196, 197]. It is due to the fact that increase in the feed rate increases un-deformed chip thickness. It is also observed that chip thickness is least sensitive to drill diameter in the ranges of drill diameters considered.

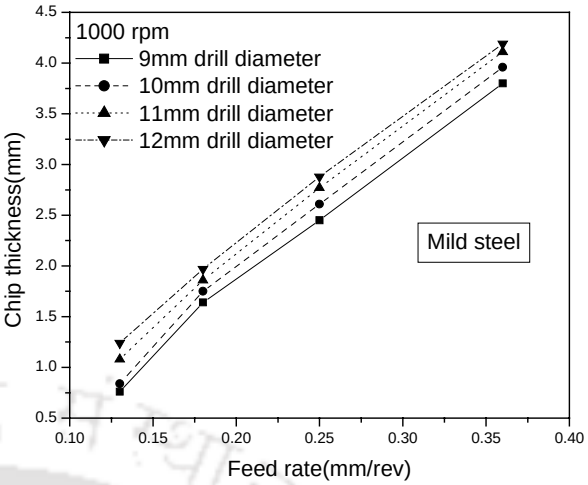

Figure 5.39 Effect of feed rate on chip thickness

5.3.3.9 Dependencies of chip thickness on spindle speed

Figure 5.40 shows the variation of chip thickness with spindle speed at four different feed rates for 9mm diameter drills. Figure shows that spindle speed has negligible effect on chip thickness. This agrees well with established result [197].

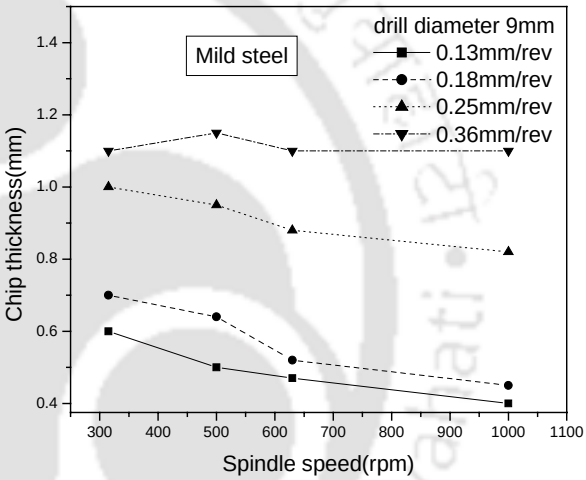

Figure 5.40 Effect of spindle speed on chip thickness

5.3.3.10 Progress of flank wear

Figure 5.41 shows the progressive nature of flank wear while drilling successive holes with a 9 mm diameter HSS drill on mild steel work piece at a spindle speed of 630 rpm and feed rate of 0.18 mm/rev. Figures 5.42 show the photograph of the focused wear land under optical microscope where growth of wear after twenty three second and seventy second are shown in figures 5.42(a) and 5.42(b) respectively.

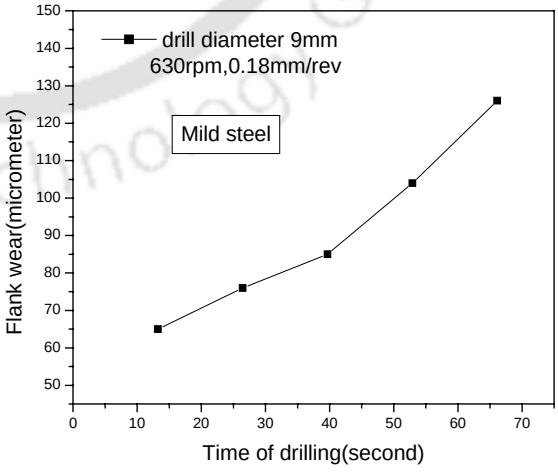

Figure 5.41 Progressive nature of flank wear

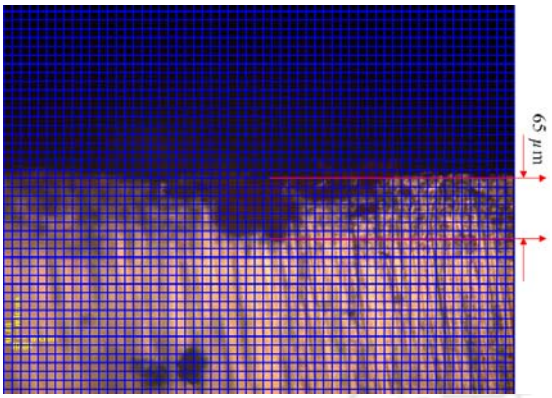

Figure 5.42 (a) Wear on drill at 13.22 second

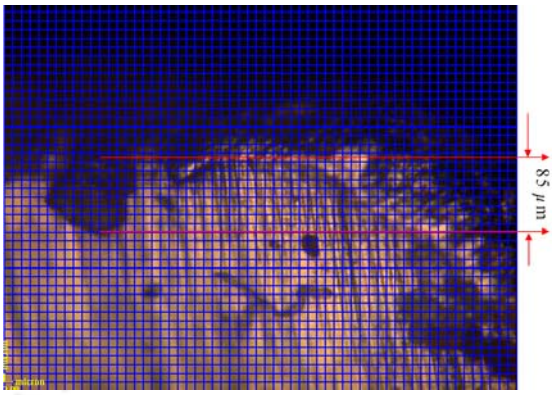

Figure 5.42 (b) Wear on drill at 40 second

5.3.3.11 Influence of wear on thrust force and torque

Figure 5.43 shows variations of thrust force with progressive drill wear for a 9 mm diameter drill for different feed rates at constant spindle speed of 630 rpm. It could be observed that thrust force increases with increase in drill wear and at different ranges of flank wear slopes are different. Figure 5.44 shows the variation of torque with progressive drill wear for a 9 mm diameter drill for different feed rates at constant spindle speed of 630 rpm. Here also torque increases with increase in flank wear. The increase in thrust force and torque with increased wear is due to the increase in friction between the drill and the work piece.

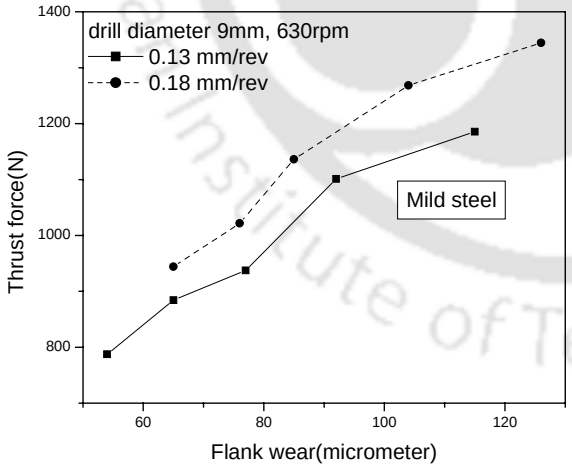

Figure 5.43 Effect of flank wear on thrust force

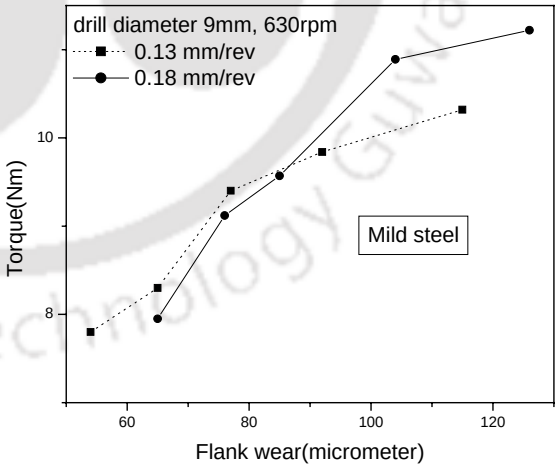

Figure 5.44 Effect of flank wear on torque

5.3.3.12 Influence of wear on vibration signals

Figure 5.45 shows the variation of progressive drill wear with feed vibration for 9 mm diameter drill for different feed rates at constant spindle speeds of 630 rpm. It could be

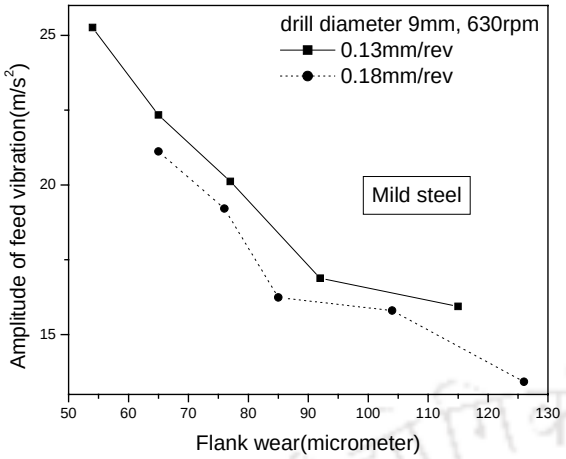

Figure 5.45 Effect of wear on feed vibration

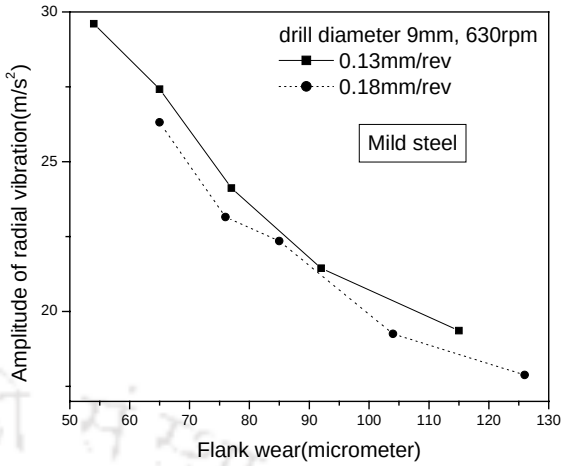

Figure 5.46 Effect of wear on radial vibration

observed that increase in drill wear indicates a lower value of feed vibration Figure 5.46 shows the variation of progressive drill wear with radial vibration for 9 mm diameter drill for different feed rates at constant spindle speeds of 630 rpm. It could be observed that increase in drill wear indicates a lower value of radial vibration. It is due to fact that increases drill wear reduces the mass of drill as well as mass of the work piece and hence reduces the amplitude of feed and radial vibration [80].

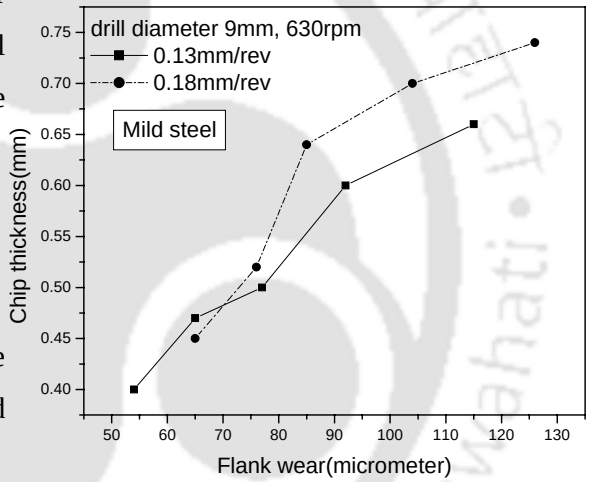

Figure 5.47 Effect of wear on chip thickness

5.3.3.13 Influence of wear on chip thickness

Figure 5.47 shows the variation of chip thickness with drill wear for a 9mm diameter drills at 630 rpm for different feed rates. It could be observed that more is the drill wear, higher is the chip thickness resulting from the drilling operation. This may be due to the fact that more is the drill wear more is the un-deformed chip thickness hence more is the chip thickness.

5.3.3.14 Influence of wear on surface roughness

Figure 5.48 shows the variations of surface roughness with flank wear for a 9mm diameter drill at 630 rpm spindle speed for different feed rates. This shows that an increase in surface roughness value indicates an increase in flank wear. This may be due the fact that increase in flank wear increases the frictional forces and hence surface roughness increases [2,34].

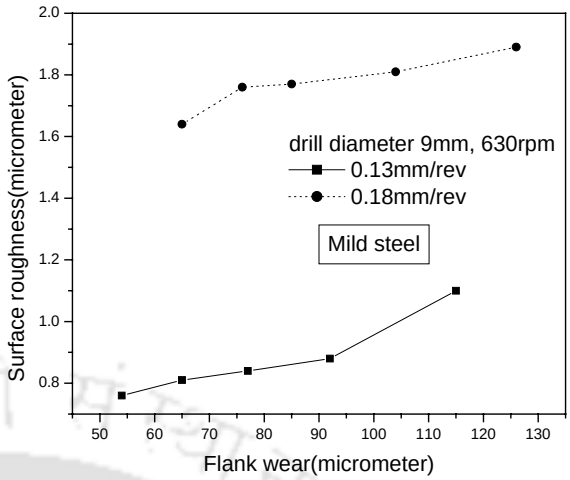

Figure 5.48 Effect of wear on surface roughness

5.3.3.15 Effect of drill diameter on wear

Figure 5.49 shows variation of progressive drill wear with number of hole at 0.18mm/rev feed rate and 630 rpm spindle speed for two different drills diameter. It could be observed that increase in drill diameter increases the drill flank wear. This may be due to the fact that increase in drill diameter increases frictional force and hence increases the drill wear.

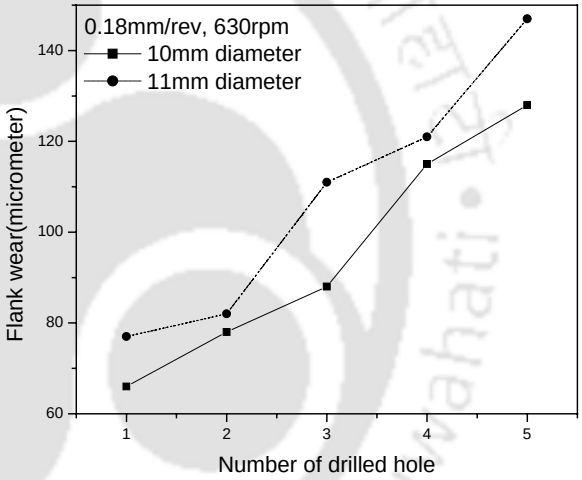

Figure 5.49 Effect of drill diameter on wear

5.3.3.16 Effect of spindle speed and feed rate on wear

Figure 5.50 shows variation of progressive drill wear with number of hole at constant spindle speed of 630 rpm and a constant drill diameter of 11 mm. It could be observed from figure 5.50, that spindle speeds have negligible effect on the drill flank wear. It may be

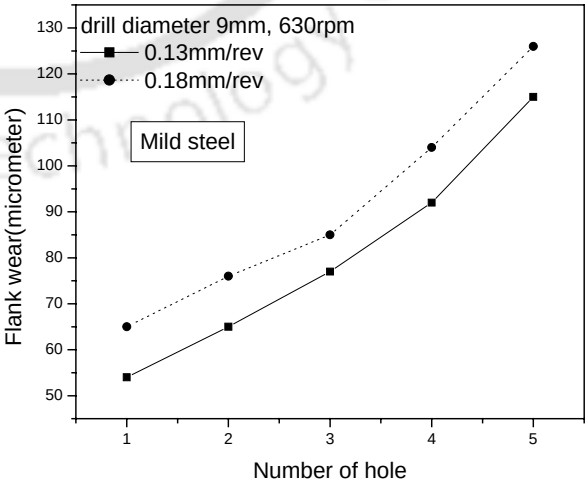

Figure 5.50 Effect of feed rate on wear

due to fact that increase in spindle speed reduces the time of cutting and hence reduces the wear on drill but amount of reduction is least influenced in the range of spindle speed. Figure 5.51 shows variation of progressive drill wear with number of hole at constant spindle speed of 630 rpm and a constant drill diameter of 9 mm. It could be observed from figure 5.51 that flank wear increases with increase in feed rate. This may be due to the fact that increase in feed rate increases frictional force and hence increases the drill wear [173].

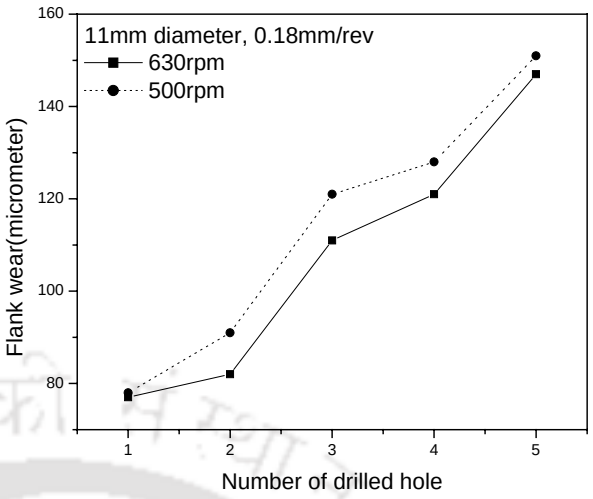

Figure 5.51 Effect of spindle speed on wear

5.3.3.17 Summary of observation in drilling a mild steel work-piece

It could be observed from the above experiment that cutting parameters (spindle speed, feed rate and drill diameter) have effect on the condition of drill (flank wear). Sensor signals (thrust force, torque, vibrations) being influenced by cutting parameters and also the condition of drill is influenced by sensor signals. Similarly it could also be observed that chip thickness and surface roughness of drilled holes are also affected by the extent of drill wear. Hence chip thickness as well as surface roughness could be utilized along with sensor signals for indirect method of drill wear prediction.

CHAPTER 6

DRILL WEAR PREDICTION USING ARTIFICIAL NEURAL NETWORK

This chapter presents the performances of BPNN and SOFM as tools to be used for prediction of drill wear. Selection of appropriate ANN architecture and input parameters is very important from the point of view of the success of the ANN for future prediction. Computer codes have been developed in C for BPNN and SOFM network for development of drill wear prediction systems in the present work. Various TCM strategies have been tried in order to study their efficacies for drill wear prediction.

6.1 Fusion of sensor signals in wear prediction

Data generated from the experiments conducted have been used to train ANN for future prediction of drill wear. Different possible combinations of inputs to the ANN have been tried following some specific TCM strategies. In the present case, the output of the ANN has been drill wear and the inputs to the ANN have been decided from the process parameters, sensors signals collected during drilling, chip thickness and surface roughness of the drilled holes. Table 6.1(a) shows eleven different strategies tried in the present work to train ANN for developing a drill wear prediction system. Among large number of possible combinations of inputs to the ANN, these eleven strategies have been chosen with an aim to study the effect of inclusion of more sensors signals on the performances of the ANN. In table 6.1, even through surface roughness of the drilled holes does not qualify to be a parameter which could be recorded online, the aim of including the same as one of the input parameter is to study how it affects the performances of ANN for drill wear prediction. All other parameters could be recorded online and hence could lead to feasible strategies for online drill wear monitoring. As shown in table 6.1(b), four different types of ANN architectures have been used for developing drill wear prediction system in conjunction with different strategies.

Table 6.1(a) Strategies for TCM

	Input to ANN									Output of ANN
Strategy	Speed	Feed	Diameter	Thrust force	Torque	Feed vibration	Radial Vibration	Chip thickness	Surface roughness	Flank wear
I	+	+	+	+	+					+
II	+	+	+			+	+			+
III	+	+	+	+	+	+				+
IV	+	+	+		+	+	+			+
V	+	+	+	+	+	+	+			+
VI	+	+	+	+	+			+		+
VII	+	+	+			+	+	+		+
VIII	+	+	+	+	+	+		+		+
IX	+	+	+		+	+	+	+		+
X	+	+	+	+	+	+	+	+		+
XI	+	+	+	+	+	+	+	+	+	+

Table 6.1 (b) TCM strategies used for different work pieces

Work pieces	Methodology		Strategies
Copper	BPNN		I
	RBFN	SOFM	I
Cast iron	BPNN		I, III, V
	RBFN	SOFM	
Mild steel	BPNN		I, II, III, IV, V, VI, VII, VIII, IX, X, XI
	RBFN	SOFM	
	FBPNN		
	FSOFM		

6.2 Wear prediction in drilling hole in copper work piece by HSS drill

TCM strategy-I as given in table 6.1(a) has been used for developing the drill wear prediction system. In this case, only two sensor signals (thrust force and torque) have been recorded. Two types of neural networks have been considered for drill wear prediction viz. back propagation neural network (BPNN) and radial basis function network (RBFN).

6.2.1 Wear prediction by BPNN

Batch mode type supervised learning has been used in the present case. In deciding the best ANN architecture, large number of ANN architectures have been tried with different combination of number of hidden layer, number of neurons in the hidden layers, learning rate (η) and momentum coefficient (α) and in each case mean square error (MSE) in training and testing have been recorded along with corresponding number of iterations.

Table 6.2 shows only a few samples of the actual number of runs. It could be observed from the table that in the present case the 5-3-1 network with $\eta = 0.5$ and $\alpha = 0.6$ happens to be the best in terms of percentage of testing error. Figure 6.1 shows the variation of MSE in training and testing for the best network with number of iteration. Comparison of actual values of flank wear with the values predicted by the network has been shown in figure 6.2. It could be observed from the figure that the predicted flank wear values are within $\pm 25\%$ of actual values.

Table 6.2 Network architectures for BPNN in drilling copper work piece

Architecture L-M-N	η	α	Iteration	MSE training	Maximum % testing error	TCM Strategy
5-3-1	0.7	0.8	1119	0.11	29.849	
5-3-1	0.8	0.9	4903	0.11	40.836	
5-3-1	**0.5**	**0.6**	**4141**	**0.00984**	**25.082**	
5-3-1	0.6	0.4	4639	0.00937	26.325	
5-3-1	0.3	0.3	16034	0.00857	32.648	
5-4-1	0.7	0.8	234	0.0079	40.629	
5-4-1	0.8	0.9	1251	0.0075	49.853	
5-4-1	0.5	0.6	448	0..075	32.337	
5-4-1	0.6	0.4	220	0.00799	32.337	**I**
5-4-1	0.3	0.3	875	0.006	29.124	
5-4-1	0.1	0.1	4551	0.004588	30.777	
5-4-1	0.1	0.3	3341	0.004826	30.533	
5-4-1	0.1	0.5	2089	0.005341	29.77	
5-4-1	0.1	0.7	993	0.006413	27.974	
5-4-1	0.3	0.1	791	0.006581	26.791	
5-4-1	0.3	0.5	328	0.00787	27.134	
5-4-1	0.3	0.7	169	0.008681	28.367	

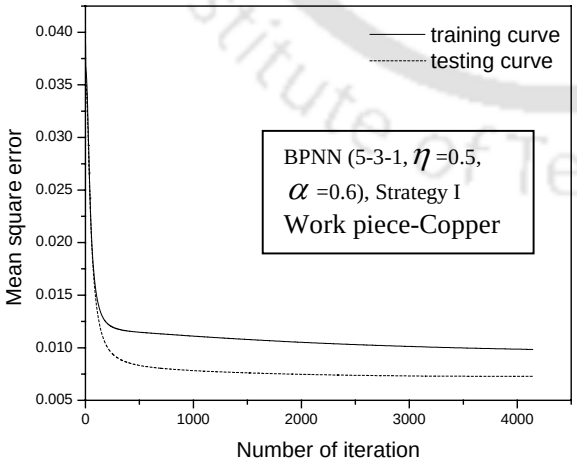

Figure 6.1 Variation of MSE with iteration

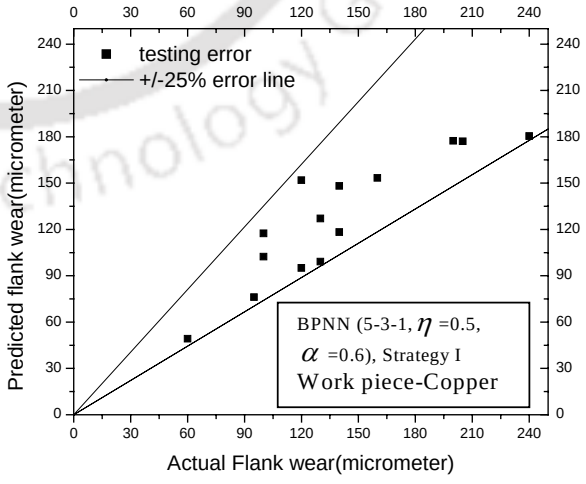

Figure 6.2 Comparison of predicted values of flank wear with actual values

6.2.2 Wear prediction by RBFN using self organizing feature map (SOFM)

SOFM is advantageous in regards to the non-requirement of initial training samples for its center vectors at hidden layer. Best network architecture (i.e. number of hidden layer, number of center vectors in the hidden layers, learning rate and momentum coefficient) has been obtained by trial and error based on mean square error in training, testing, and the number of iterations. Large numbers of runs were given for selecting the best architecture and few of these are shown in table 6.3. The best network architecture obtained by heuristically optimizing the network parameters arrived at in the present model is 5-15-1 with $\eta = 0.1 \text{and} \alpha = 0.9$. Figure 6.3 shows the mean square error in training and testing with number of iteration. It could be observed from the figure 6.4 that the flank wear predicted by the present radial basis function network lie within $\pm 14\%$ of the actual values.

Table 6.3 Training errors for SOFM network

Center vector	η	α	MSE Training	MSE Testing	Iteration	Maximum % testing error	Strategy
10	0.6	0.9	0.002999	0.001703	842	18.3453	S I
10	0.6	0.1	0.00703	0.009292	4205	18.3453	
15	**0.1**	**0.9**	**0.003255**	**0.001354**	**730**	**13.9997**	
15	0.3	0.9	0.002751	0.001988	268	16.1639	
15	0.6	0.9	0.002576	0.001705	125	16.0106	
20	0.1	0.9	0.002975	0.001621	119	20.4329	
20	0.6	0.9	0.003013	0.001603	41	16.3855	
25	0.1	0.9	0.002537	0.002086	182	26.9768	
35	0.3	0.9	0.002336	0.001717	91	29.8228	
35	0.6	0.9	0.002377	0.001853	130	23.6878	

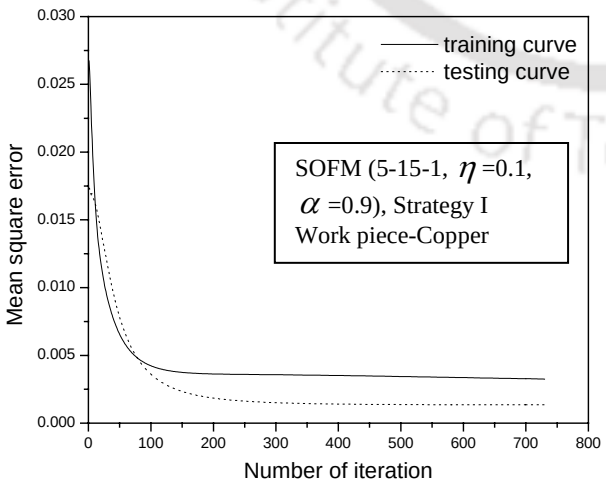

Figure 6.3 Variation of MSE with iteration

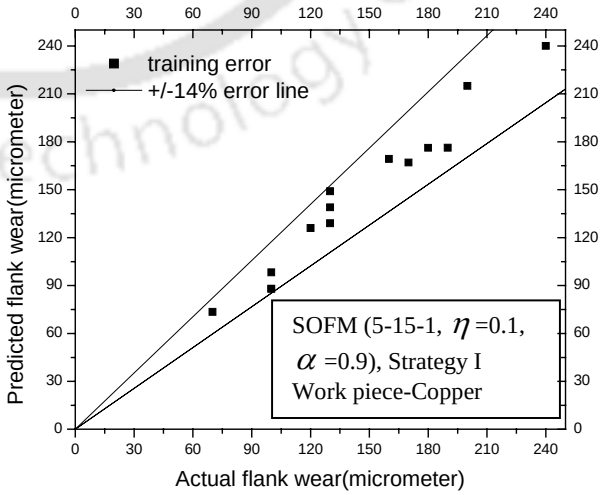

Figure 6.4 Comparison of predicted value with actual values of flank wear

6.2.3 Summary of wear prediction in drilling copper work piece

It has been observed that ANN based drill wear prediction methods developed could predict the drill wear while tested with unknown data sets. It has also been observed that RBFN using SOFM shows better accuracy compared to BPNN in predicting drill wear and it also converges much faster.

6.3 Wear prediction in drilling holes in cast iron (CI) work piece by HSS drill

TCM strategies I, III and V (according to table 6.1(b)) have been tried to develop ANN based drill wear prediction system. Two different types of ANN architectures have been used and the comparative performances of three TCM strategies have been studied. As described in chapter 5, 64 different drilling operations have been conducted at different cutting conditions. These 64 sets of data are randomly divided into training set (40 sets), testing set (14 sets) and validation set (10 sets). These data sets have been normalized before presenting to network as discussed earlier.

6.3.1 Wear prediction by BPNN

Large number of BPNN architectures has been tried and best network architecture (i.e. number of hidden layer, number of neurons in the hidden layers, learning rate and momentum coefficient) has been obtained by heuristically optimizing the ANN parameters. Large numbers of runs were given for selecting the best architecture and table 6.4 shows some of them along with the number of neuron in the hidden layer, MSE for training, MSE for testing, number of iteration and corresponding percentage of error while validating the sample.

Table 6.4 Network architecture for back propagation network

Network Architectures	η	α	MSE training	MSE testing	Iteration	Maximum validation error (%)	TCM Strategy
5-5-1	0.3	0.2	0.000759	0.000458	3066	6.897112	
5-5-1	0.3	0.5	0.000752	0.000455	2029	6.975593	
5-5-1	0.3	0.9	0.000492	0.00049	3200	8.462943	
5-5-1	0.8	0.9	0.000104	0.000431	1709	7.28288	
5-7-1	**0.3**	**0.9**	**0.000221**	**0.000487**	**922**	**5.16795**	
5-7-1	0.5	0.9	0.000103	0.000435	6489	5.43009	
5-10-1	0.3	0.9	0.000267	0.000524	8478	9.34441	I
5-13-1	0.3	0.9	0.000282	0.000477	2431	6.811886	
5-13-1	0.5	0.8	0.000303	0.000507	7368	8.16804	
5-3-1	0.3	0.2	.000946	0.000484	1143	7.79279	
5-3-1	0.3	0.9	0.00054	0.000503	3762	7.139887	
5-1-1	0.6	0.6	0.003813	0.00748	318	11.67687	
5-1-1	0.1	0.1	0.003817	0.00748	2124	11.68429	

6-3-1	0.1	0.1	0.001202	0.000477	317	6.19631	
6-3-1	0.1	0.3	0.001204	0.000478	246	7.26558	
6-3-1	0.1	0.9	0.000657	0.000481	1665	8.81751	
6-3-1	**0.3**	**0.1**	**0.000179**	**0.000444**	**3955**	**5.02308**	
6-3-1	0.3	0.3	0.0007	0.000456	2954	5.6988	
6-3-1	0.3	0.9	0.000665	0.000493	718	10.1467	
6-3-1	0.6	0.3	0.000672	0.000546	1776	8.55762	
6-3-1	0.6	0.6	0.000671	0.000556	997	9.701685	
6-3-1	0.6	0.9	0.000295	0.000482	3561	7.555715	
6-3-1	0.9	0.1	0.000692	0.000515	1379	8.19377	III
6-3-1	0.9	0.6	0.000668	0.00046	672	5.63197	
6-6-1	0.1	0.1	0.001164	0.000379	237	5.89929	
6-6-1	0.1	0.9	0.000471	0.00049	6552	7.228993	
6-6-1	0.6	0.3	0.000504	0.000464	8066	6.924548	
6-6-1	0.6	0.6	0.000482	0.000459	4094	6.449316	
6-6-1	0.6	0.9	0.000179	0.000364	3955	5.48346	
6-6-1	0.9	0.1	0.00057	0.000514	6782	7.585417	
6-6-1	0.9	0.3	0.000543	0.000513	5417	7.310674	
6-6-1	0.9	0.6	0.000491	0.000527	4051	8.261138	
7-5-1	0.3	0.2	0.000373	0.000484	21637	7.43868	
7-5-1	0.3	0.5	0.000373	0.000482	13164	7.40353	
7-5-1	0.3	0.9	0.000314	0.000492	2908	7.680717	
7-5-1	0.5	0.5	0.000369	0.000485	8437	7.3945	
7-5-1	0.4	0.6	0.00037	0.000494	8370	7.36871	
7-7-1	0.3	0.3	0.000416	0.000495	7671	7.4477	
7-7-1	0.3	0.5	0.000414	0.000485	5568	7.47604	
7-7-1	0.4	0.7	0.000417	0.000487	2485	7.3409	
7-10-1	0.3	0.3	0.000676	0.000462	957	5.996261	V
7-10-1	0.3	0.9	0.000267	0.00046	4208	5.26482	
7-10-1	0.5	0.9	0.000308	0.000482	1697	7.558863	
7-13-1	0.2	0.9	0.000367	0.000488	1381	7.076556	
7-13-1	0.5	0.9	0.000253	0.000488	2142	7.296985	
7-10-1	**0.6**	**0.9**	**0.000201**	**0.000356**	**5404**	**4.5308**	
7-5-1	0.8	0.9	0.00028	0.000498	2623	7.733337	
7-5-1	0.1	0.9	0.000379	0.000526	14299	8.178653	
7-8-1	0.6	0.9	0.000314	0.000399	351	4.90103	

It could be observed from table 6.4 that in the present case strategy V gives the best result in terms of validation error. However strategy I provide the fastest convergence even through the validation error is slightly higher. Therefore it could be inferred here that inclusion of two vibration signals (along with thrust force, torque, drill diameter, spindle speed and feed rate) in the TCM strategy leads to better learning of the BPNN but at more number of iteration. Figures 6.5 (a, b), 6.6 (a, b) and 6.7(a, b) show the learning curves and the comparison of predicted and actual values of flank wear for the three strategies considered.

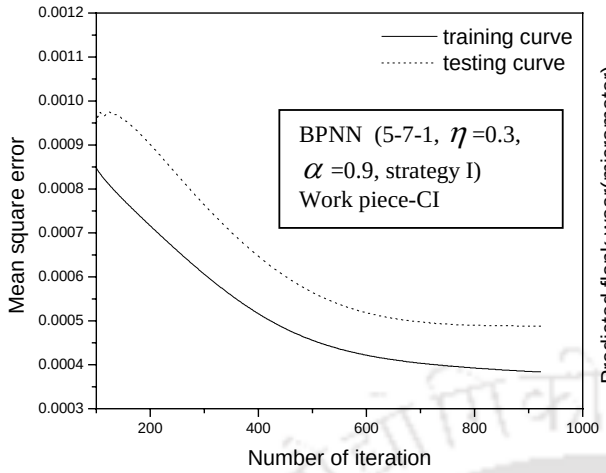

Figure 6.5(a) Variation of MSE with iteration

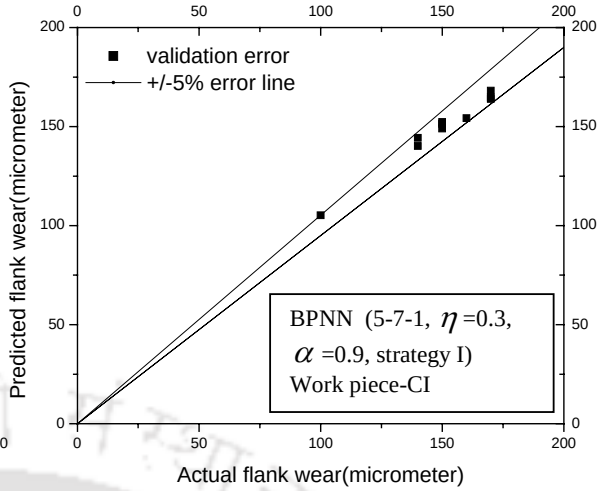

Figure 6.5(b) Comparision of predicted values with actual value of flank wear

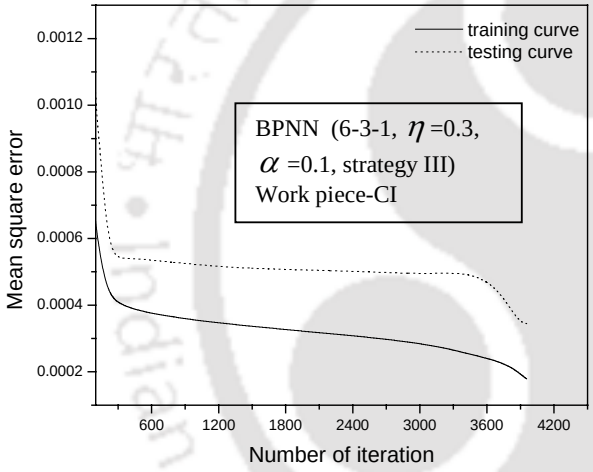

Figure 6.6(a) Variation of MSE with iteration

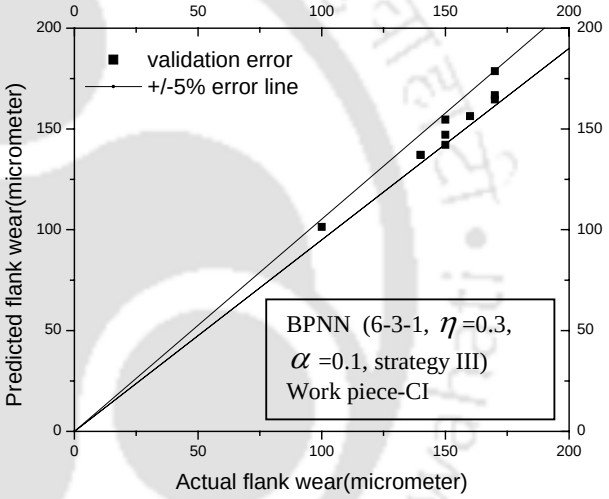

Figure 6.6(b) Comparision of predicted values with actual value of flank wear)

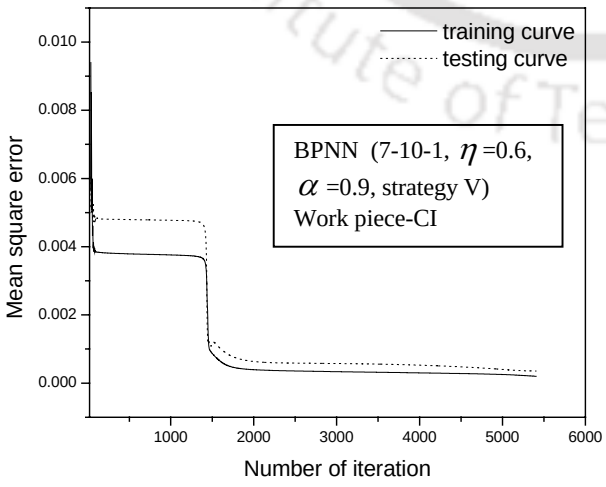

Figure 6.7(a) Variation of MSE with iteration

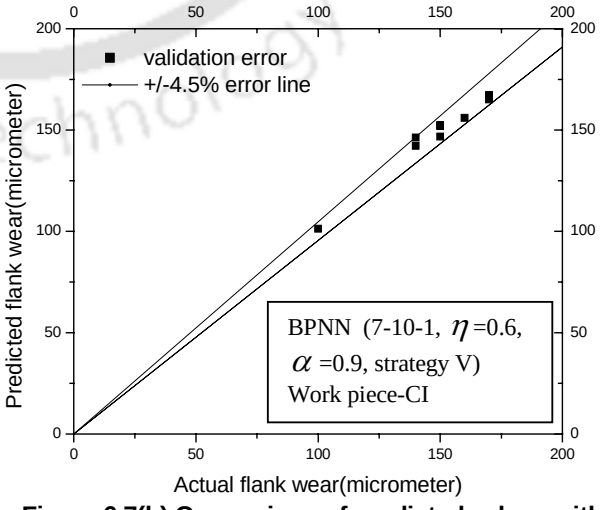

Figure 6.7(b) Comparison of predicted values with actuals values of flank wear

6.3.2 Wear prediction by RBFN using self organizing feature map

With an expectation of faster learning SOFM networks have been trained following the TCM strategies on I, III and V for predicting drill wear with cast iron as work piece. In this case also large number of network architectures have been tried in each of the strategies to arrive at the best architectures. Table 6.5 shows only a few of the architectures tried corresponding to each of the three strategies along with MSE training, MSE testing, number of iteration and maximum validation error for the architectures. It could be observed from the table 6.5 that strategy V (thrust force, torque, feed vibration, radial vibration along with drill diameter, spindle speed and feed rate as input) provides the best drill wear prediction system using SOFM both in terms of validation error (7.97%) as well as minimum number of iterations (435 iteration). Figures 6.8 (a, b), 6.9(a, b) and 6.10(a, b) show the learning curves and the validation error for the best SOFM network corresponding to strategies I, III and V respectively.

Table 6.5 Network architectures for SOFM

Network architectures	η	α	MSE training	MSE testing	Iteration	Maximum validation error (%)	Strategy
5-30-1	0.3	0.5	0.00523	0.000643	3519	18.34707	I
5-30-1	0.1	0.7	0.005461	0.000661	1102	18.9203	
5-30-1	0.3	0.9	0.00595	0.000645	643	18.10457	
5-40-1	0.6	0.6	0.00492	0.000622	927	16.33737	
5-40-1	0.5	0.1	0.005811	0.0005811	3642	16.32767	
5-40-1	**0.6**	**0.9**	**0.00628**	**0.000598**	**614**	**16.0579**	
6-30-1	0.5	0.3	0.00623	0.000773	1694	19.57	III
6-30-1	0.3	0.6	0.006461	0.000791	1124	20.26	
6-30-1	0.3	0.7	0.00655	0.000764	917	19.94	
6-40-1	0.6	0.9	0.00592	0.000612	886	15.26	
6-40-1	0.9	0.6	0.005214	0.0004841	1254	14.84	
6-40-1	**0.1**	**0.9**	**0.000591**	**0.000492**	**759**	**14.04**	
7-20-1	0.1	0.6	0.003791	0.000439	4426	14.0509	V
7-20-1	0.1	0.9	0.001786	0.000486	1956	15.1858	
7-30-1	0.6	0.6	0.005112	0.000767	927	18.33737	
7-30-1	0.9	0.6	0.005101	0.000767	622	18.32767	
7-40-1	0.1	0.9	0.001812	0.000392	1374	8.46373	
7-40-1	**0.3**	**0.9**	**0.001827**	**0.000393**	**435**	**7.97777**	

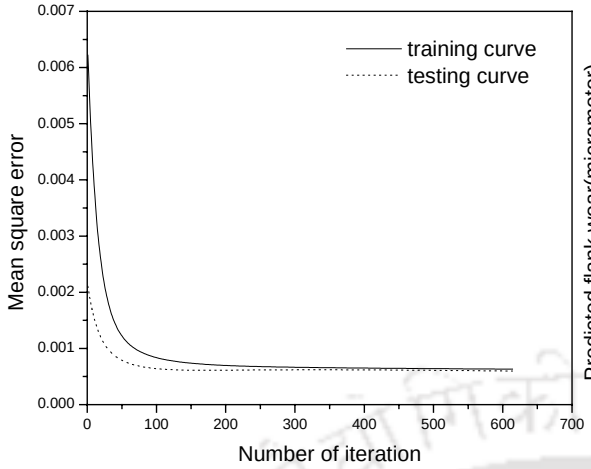

Figure 6.8(a) Variation of MSE with iteration

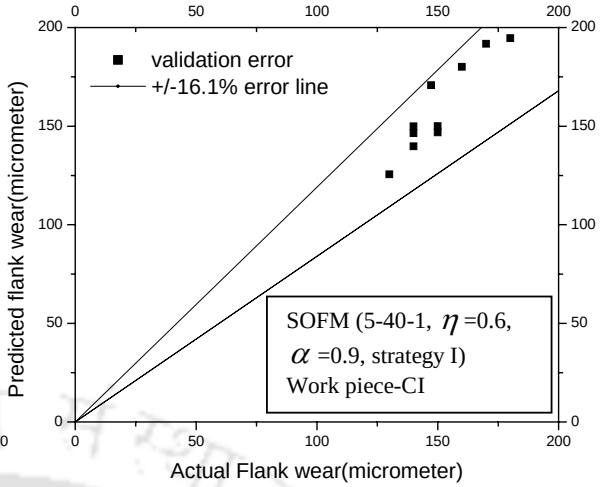

Figure 6.8(b) Comparison of predicted values of flank wear with actual values

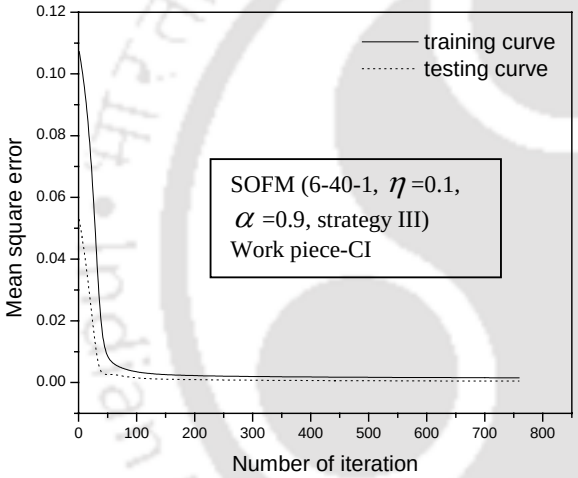

Figure 6.9(a) Variation of MSE with iteration

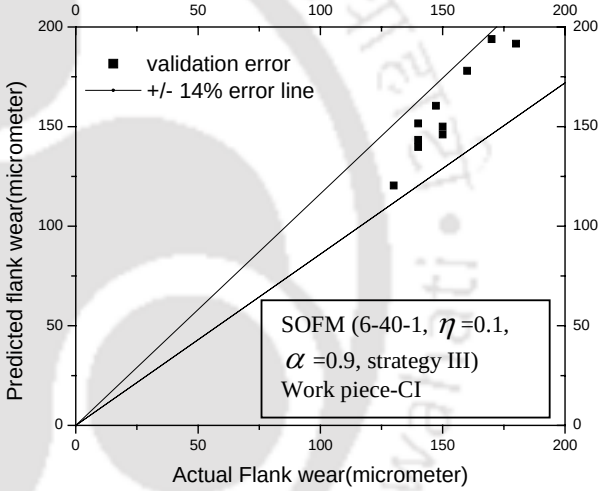

Figure 6.9(b) Comparison of predicted values of flank wear with actual values

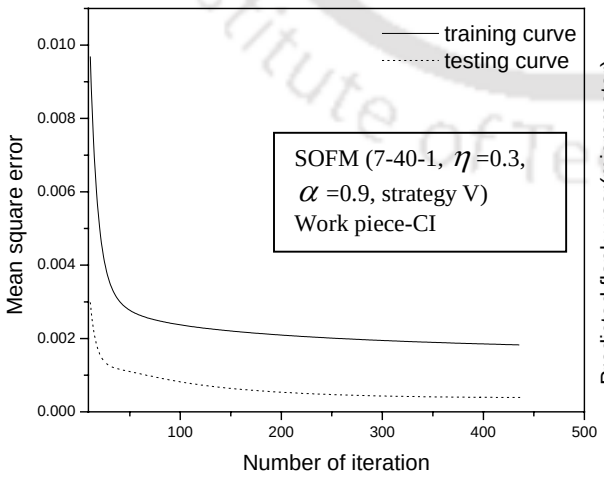

Figure 6.10(a) Variation of MSE with iteration

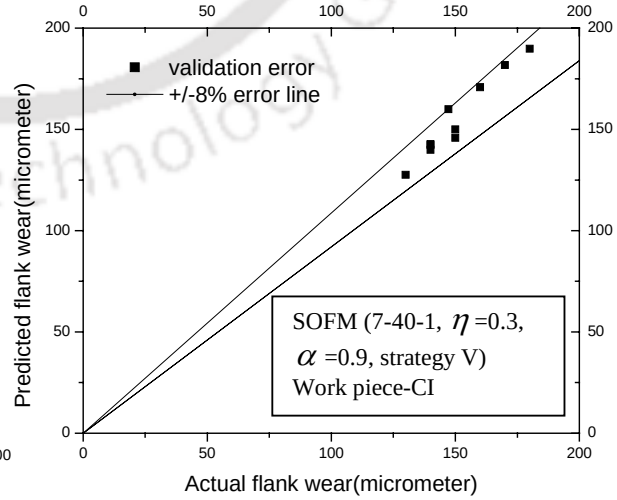

Figure 6.10(b) Comparison of predicted value with actual values of flank wear

6.3.3 Summary of wear prediction in drilling cast iron work piece

It has been observed that ANN based drill wear prediction methods developed could predict the drill wear while tested with unknown data sets. RBFN using SOFM shows better accuracy compared to BPNN in predicting drill wear and it also converges much faster. It has also been observed that inclusion of vibration signals as inputs to ANN leads to better prediction of drill wear.

6.4 Wear prediction in drilling a hole in mild steel work piece by HSS drill

In drilling holes on mild steel (MS) with HSS drills, four sensor signals (thrust force, torque, radial vibration and feed vibration) have been recorded like that in case of drilling holes in cast iron (CI). In addition to this, chip thickness and surface roughness of the holes were also measured corresponding to each cutting condition. Therefore, eleven different TCM strategies (I to XI according to table 6.1(a)) have been tried to develop an ANN based drill wear prediction system.

6.4.1 Wear prediction by BPNN

Large number of architectures has been tried corresponding to each of the strategies to arrive at the best drill wear prediction system using BPNN. Table 6.6 shows only the best and the second best network in terms of the validation error and the number of iteration corresponding to each strategy.

Table 6.6 BPNN network architecture

Architecture L-M-N	η	α	Iteration	MSE training	MSE testing	Maximum validation error (%)	Strategy
5-3-1	0.9	0.7	895	0.000332	0.000599	5.9357	I
5-5-1	**0.1**	**0.1**	**19814**	**0.000299**	**0.000534**	**5.0772**	
5-5-1	**0.1**	**0.5**	**19849**	**0.000293**	**0.000452**	**5.2618**	II
5-8-1	0.9	0.9	2177	0.000155	0.00039	5.9784	
6-3-1	**0.1**	**0.5**	**19830**	**0.000319**	**0.000557**	**5.0577**	III
6-8-1	0.5	0.3	6811	0.000241	0.00042	6.8109	
6-3-1	**0.3**	**0.3**	**19460**	**0.000254**	**0.000367**	**4.6904**	IV
6-5-1	0.5	0.9	870	0.000233	0.000478	5.3619	
7-12-1	**0.5**	**0.7**	**5636**	**0.00017**	**0.000319**	**4.8929**	V
7-12-1	0.9	0.3	565	0.00034	0.000575	6.2404	
6-3-1	0.3	0.7	4101	0.000273	0.000506	5.1334	VI
6-5-1	**0.1**	**0.7**	**19707**	**0.000231**	**0.000516**	**4.89**	
6-3-1	**0.9**	**0.5**	**9612**	**0.000294**	**0.000353**	**4.678**	VII
6-8-1	0.7	0.7	2837	0.000224	0.000393	5.3707	

7-3-1	**0.1**	**0.3**	**19826**	**0.000288**	**0.000485**	**4.5703**	VIII
7-8-1	0.7	0.7	8994	0.000102	0.000239	6.4241	
7-5-1	**0.1**	**0.1**	**19952**	**0.000289**	**0.000472**	**4.4593**	IX
7-5-1	0.7	0.9	3387	0.000197	0.000394	6.336	
8-5-1	0.9	0.3	4060	0.000251	0.000414	5.3678	X
8-8-1	**0.5**	**0.3**	**14363**	**0.000157**	**0.000262**	**4.2557**	
9-8-1	**0.5**	**0.7**	**8703**	**0.000131**	**0.000158**	**3.2197**	XI
9-8-1	0.9	0.3	1736	0.00023	0.000333	6.1009	

It could be observed from the table that fusion of vibration signals (in strategy III, IV and V) along with force signals (thrust force and torque) and process parameters (spindle speed, drill diameter and feed rate) leads to better drill wear prediction in terms of validation error compared to that using only force signals or only vibration signals. It is also observed that validation error is minimum in case of strategy IV with inputs as torque, feed vibration and radial vibration along with three process parameters. However in terms of number of iterations strategy V achieves the fastest learning (with 565 iterations). It has been observed that inclusion of chip thickness along with other sensor signals leads to reduction in validation error of the drill wear prediction system. From table it could be observed that strategy X lead to the minimum validation error where chip thickness has been combined with two force signals (thrust force and torque), two vibration signals and three process parameters. Finally, inclusion of surface roughness (strategy XI) leads to drastic reduction of validation error (3.2%) and the network has been trained at 8703 iterations only. Figures 6.11 to 6.21 show the learning curves and validation error corresponding to the best network in each of the eleven strategies.

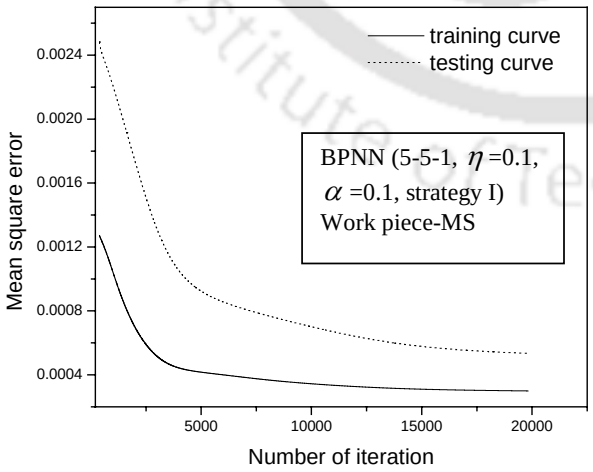

Figure 6.11(a) Variation of MSE with iteration

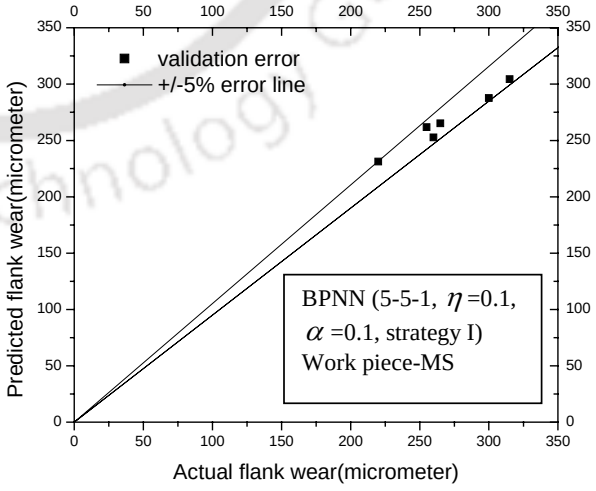

Fig 6.11(b) Comparison of predicted values with actual values of flank wear

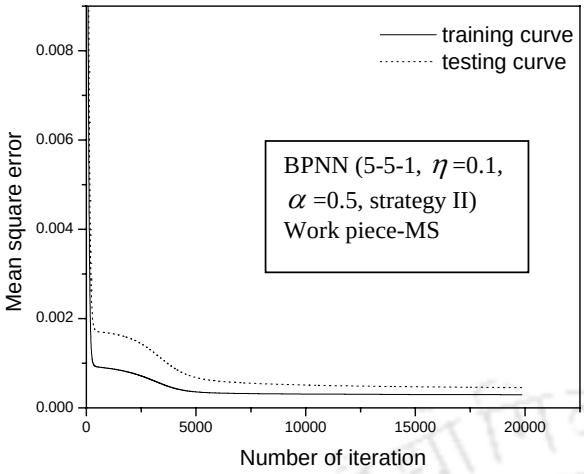

Figure 6.12(a) Variation of MSE with iteration

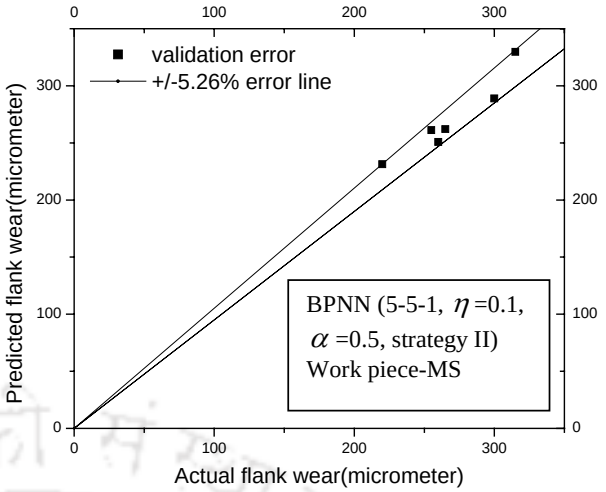

Fig 6.12(b) Comparison of predicted values with actual values of flank wear

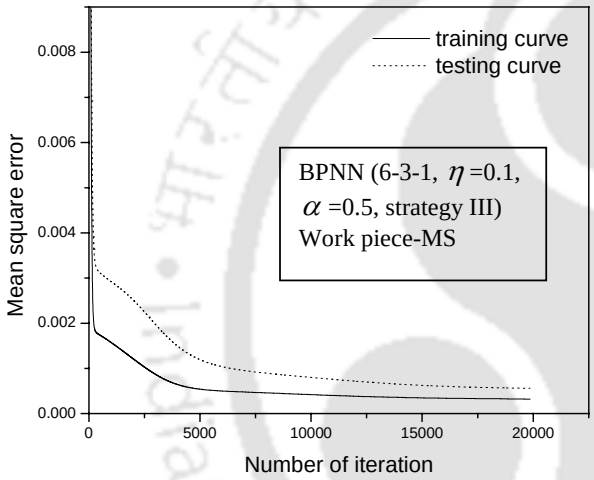

Figure 6.13(a) Variation of MSE with iteration

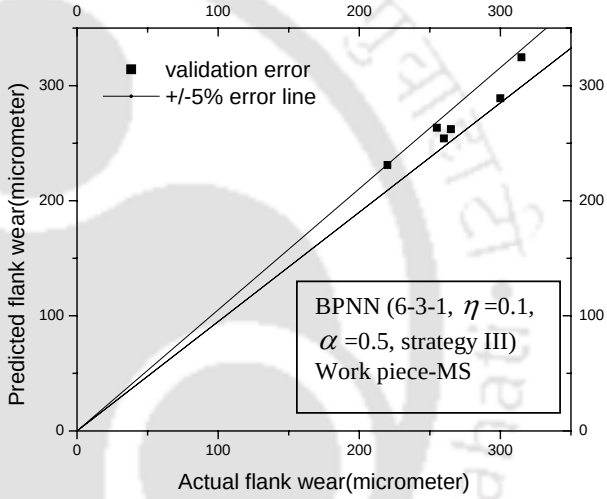

Fig 6.13(b) Comparison of predicted values with actual values of flank wear

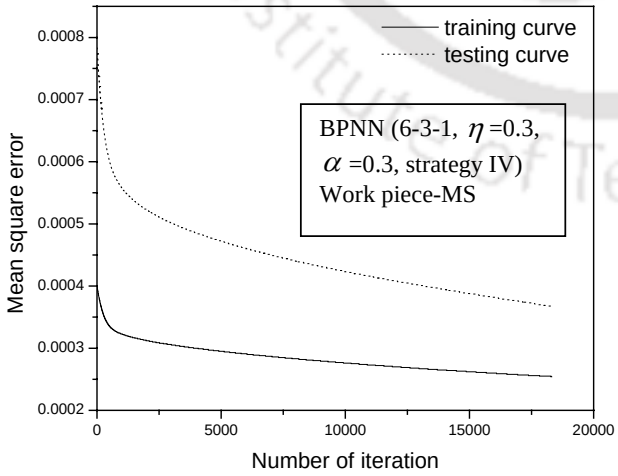

Figure 6.14(a) Variation of MSE with iteration

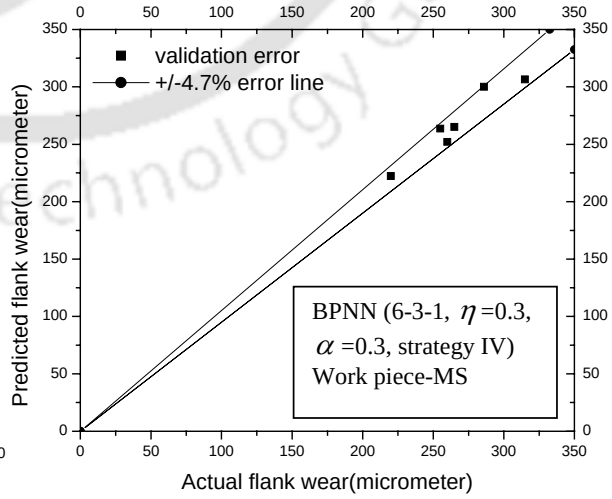

Fig 6.14(b) Comparison of Predicted value with actual values of flank wear

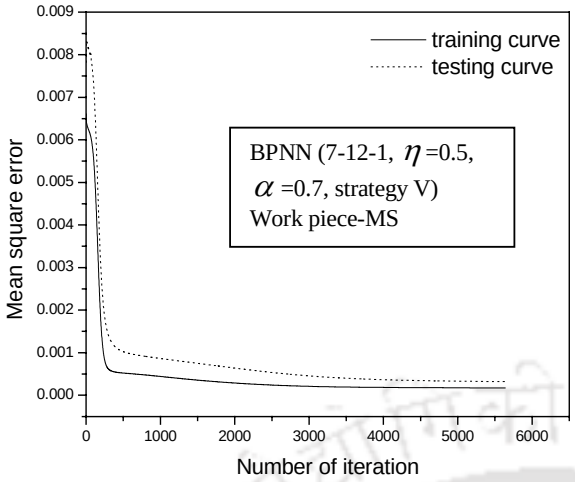

Figure 6.15(a) Variation of MSE with iteration

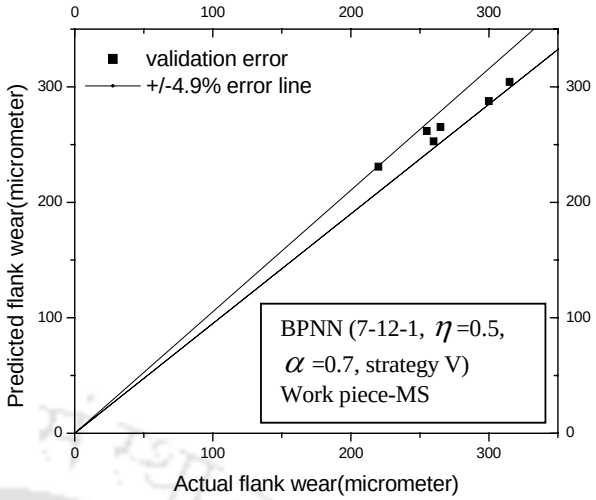

Fig 6.15(b) Comparison of predicted values with actual values of flank wear

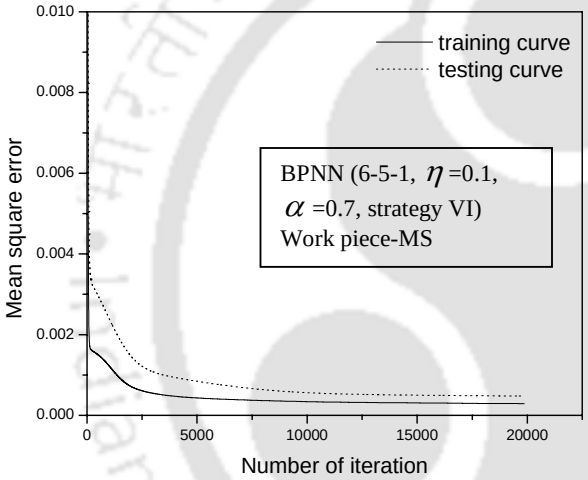

Figure 6.16(a) Variation of MSE with iteration

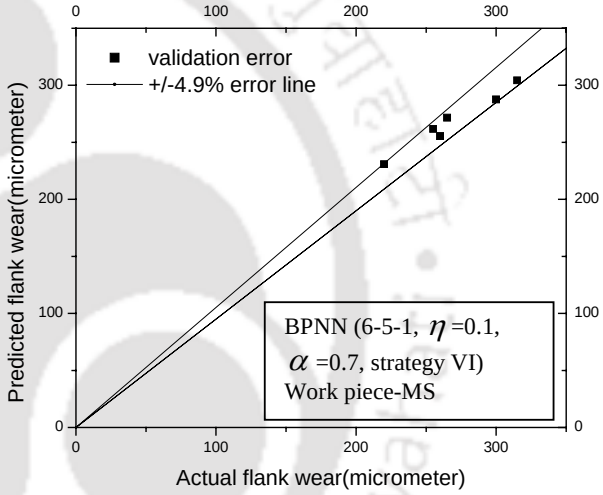

Fig 6.16(b) Comparison of predicted values with actual values of flank wear

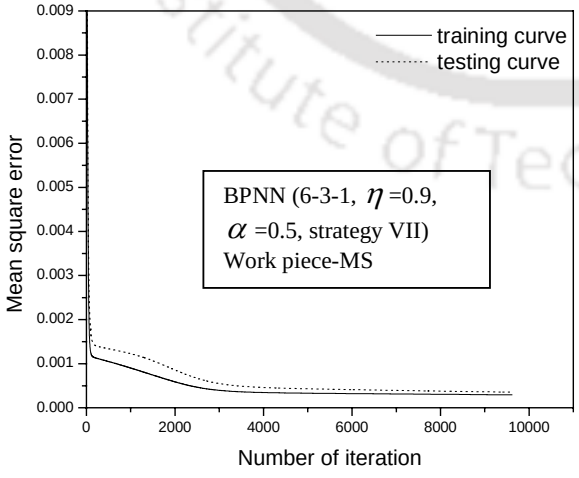

Figure 6.17(a) Variation of MSE with iteration

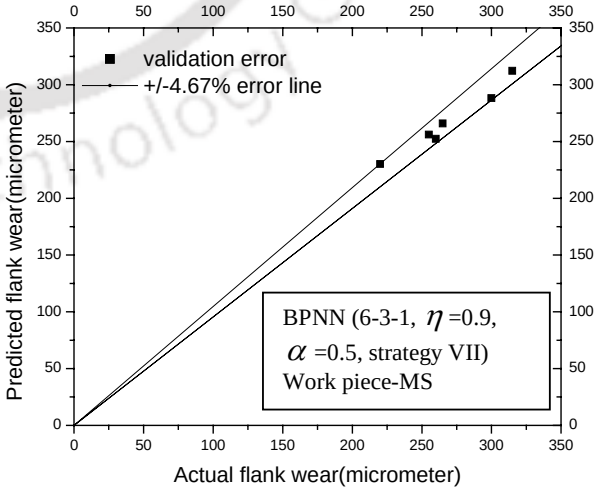

Fig 6.17(b) Comparison of predicted values with actual values of flank wear

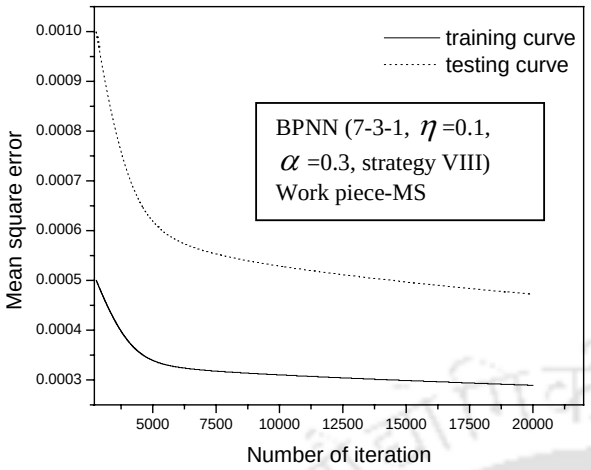

Figure 6.18(a) Variation of MSE with iteration

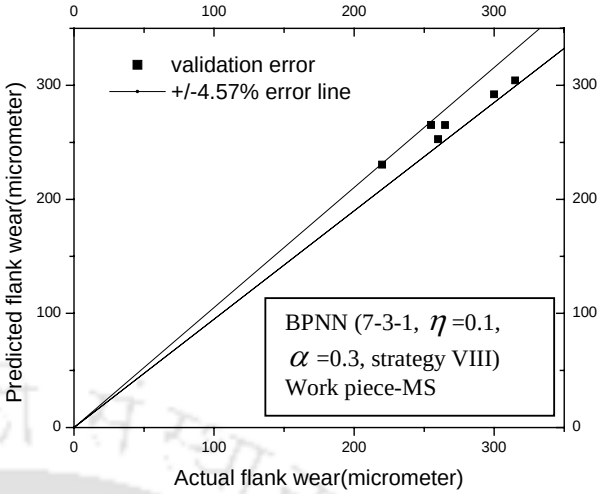

Fig 6.18(b) Comparison of predicted values with actual values of flank wear

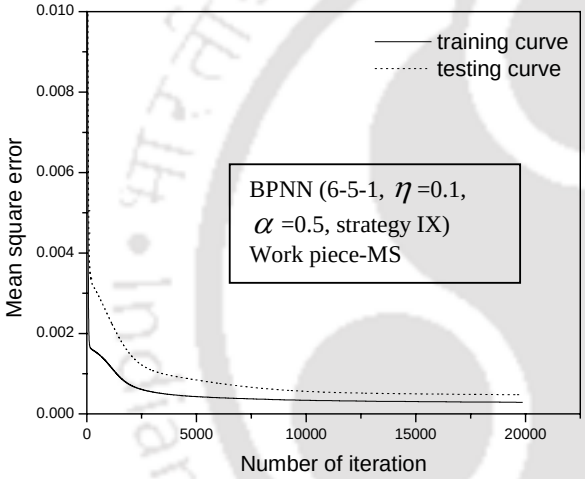

Figure 6.19(a) Variation of MSE with iteration

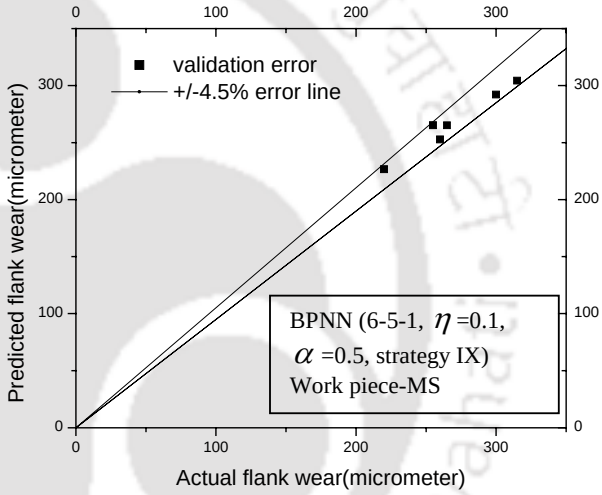

Fig 6.19(b) Comparison of predicted values with actual values of flank wear

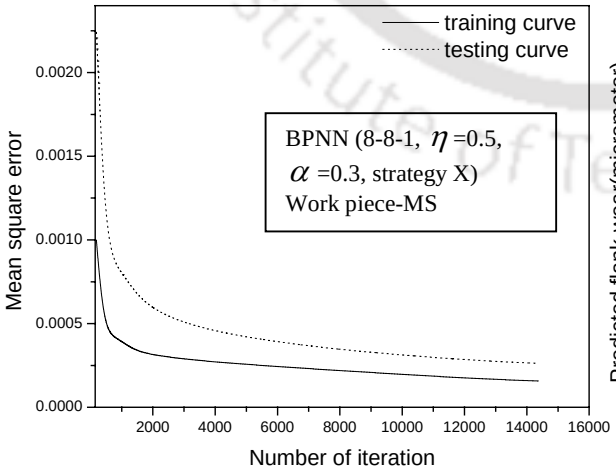

Figure 6.20(a) Variation of MSE with iteration

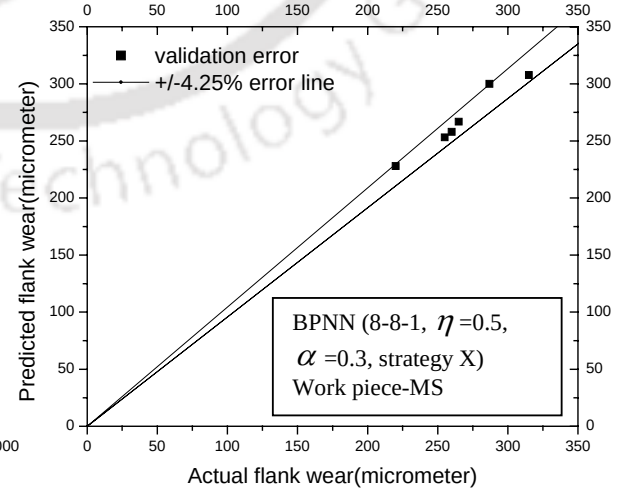

Figure 6.20(b) Comparison of predicted values with actual values of flank wear

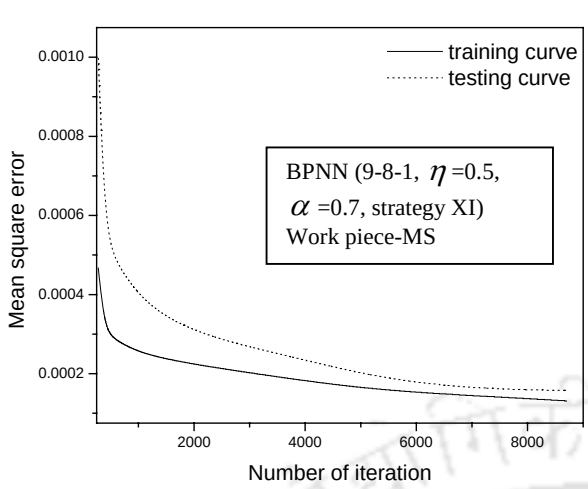

Figure 6.21(a) Variation of MSE with iteration

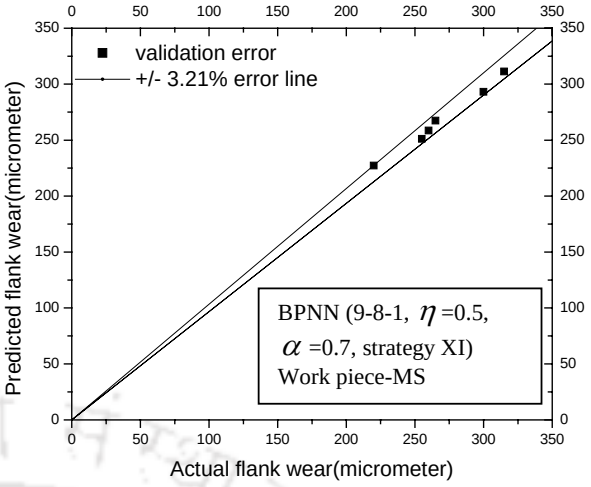

Figure 6.21(b) Comparison of Predicted value with actual values of flank wear

6.4.2 Wear prediction by RBFN using self organizing feature map

SOFM network has been tried for development of drill wear prediction system in drilling holes in mild steel work piece. All the eleven strategies, which have been tried in the case of BPNN, have been tried in this case also. Large number of network architectures has been tried for each of the strategies in order to arrive at the best possible drill wear prediction system. Table 6.7 shows the best architectures corresponding to each of the strategies along with MSE training, MSE testing, validation error and number of iterations. It could be observed from the table that like BPNN, inclusion of vibration signals along with force signal (strategy IV) leads to better prediction accuracy compared to only force or vibration signals (strategy I and II). Inclusion of chip thickness along with force as well as vibration signals (strategy X) leads to best drill wear prediction system using SOFM not only in terms of validation error but also the in terms of minimum number of iterations required for training. Inclusion of surface roughness information (strategy XI) leads to further reduction in validation error marginally however, the number of iterations increases. Figures 6.22 to 6.32 show the learning curves and validation error corresponding to the best network in each of the eleven strategies.

Table 6.7 Network Architecture for SOFM

Architecture L-M-N	η	α	Iteration	MSE training	MSE testing	Maximum validation error (%)	Strategy
5-30-1	0.1	0.1	908	0.000908	0.00136	11.1167	I
5-30-1	0.3	0.7	439	0.000472	0.001119	11.4225	II
6-30-1	0.5	0.7	733	0.000856	0.002712	12.24	III
6-25-1	0.5	0.7	1774	0.000524	0.000963	8.8013	IV
7-40-1	0.5	0.5	1924	0.000732	0.002334	13.89	V
6-30-1	0.5	0.1	987	0.00045	0.001637	10.4958	VI
6-30-1	0.3	0.3	773	0.000645	0.000904	10.9455	VII
7-25-1	0.7	0.7	10000	0.000318	0.001251	9.7599	VIII
7-30-1	0.5	0.5	1607	0.000443	0.001215	9.9146	IX
8-25-1	0.7	0.9	291	0.000427	0.001323	7.9827	X
9-25-1	0.3	0.9	708	0.000482	0.001762	7.12	XI

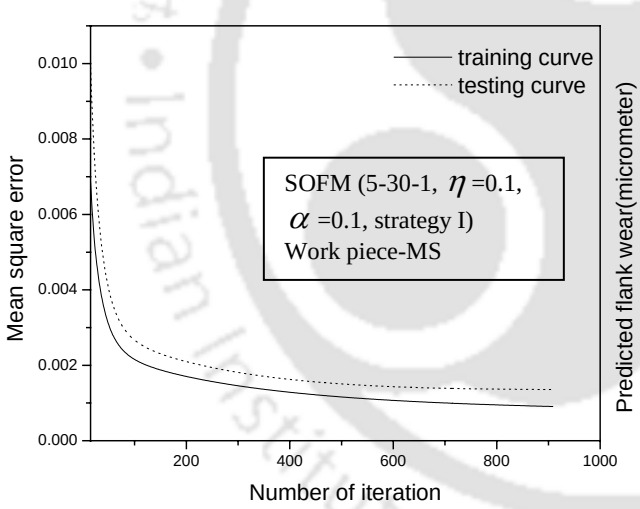

Figure 6.22(a) Variation of MSE with iteration

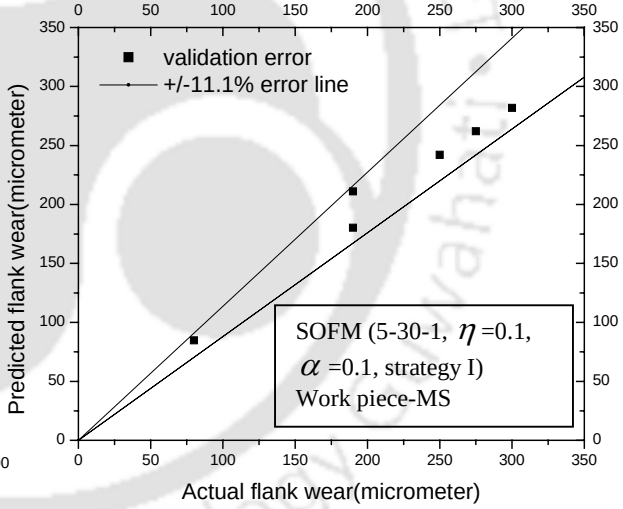

Figure 6.22(b) Comparison of actual values with predicted values of flank wear

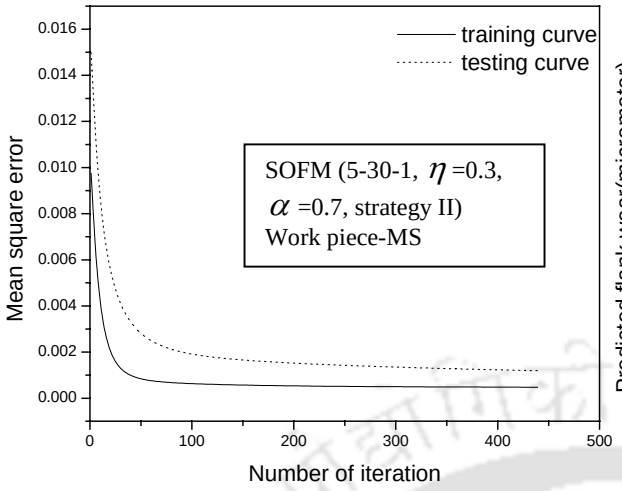

Figure 6.23(a) Variation of MSE with iteration

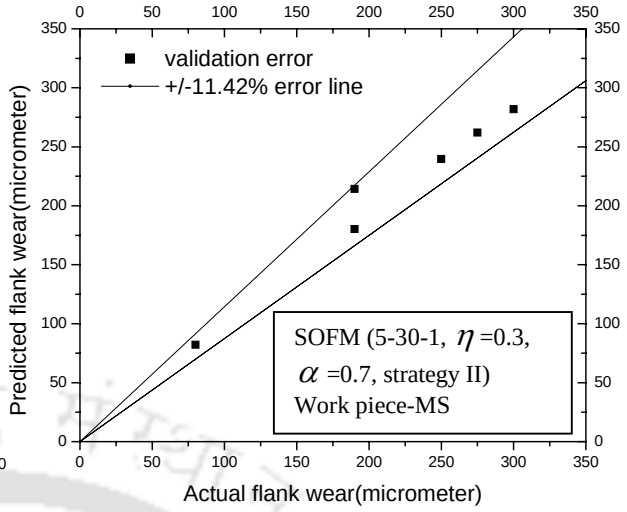

Figure 6.23(b) Comparison of actual values with predicted values of flank wear

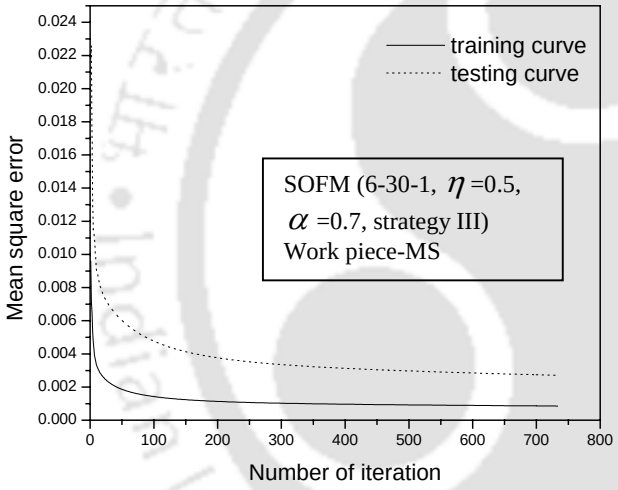

Figure 6.24(a) Variation of MSE with iteration

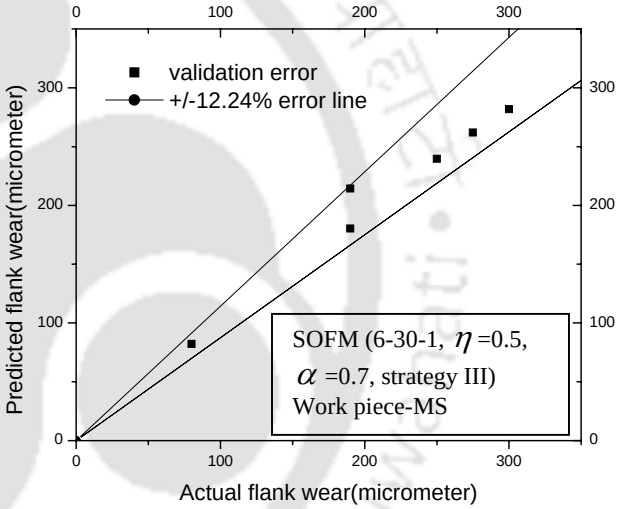

Figure 6.24(b) Comparison of actual values with predicted values of flank wear

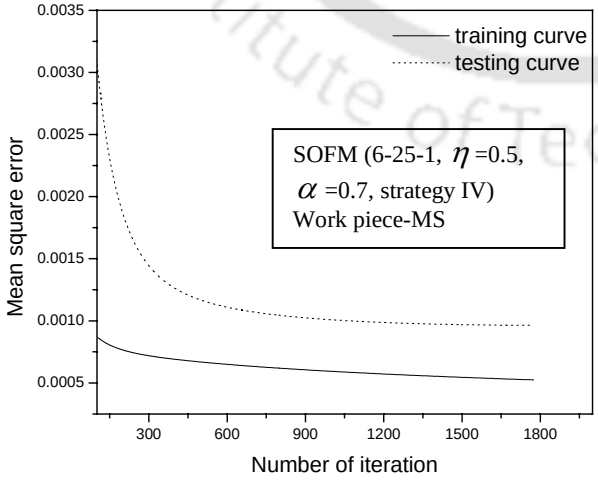

Figure 6.25(a) Variation of MSE with iteration

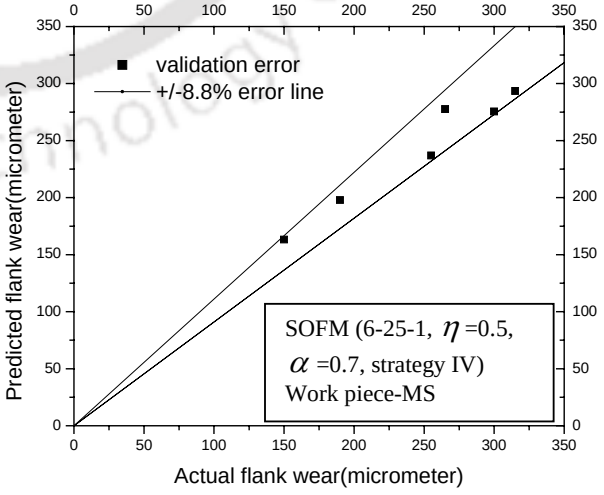

Figure 6.25(b) Comparison of actual values with predicted values of flank wear

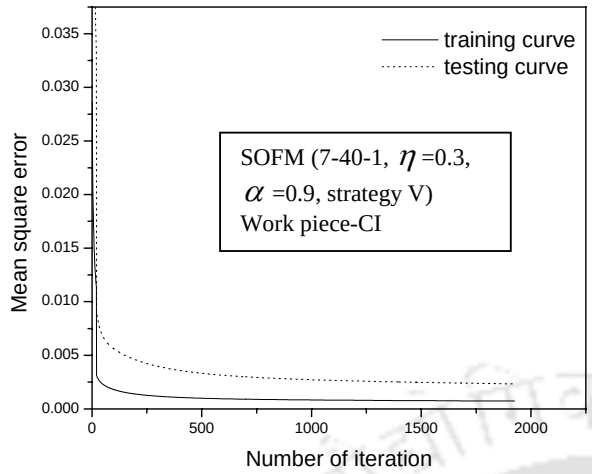

Figure 6.26(a) Variation of MSE with iteration

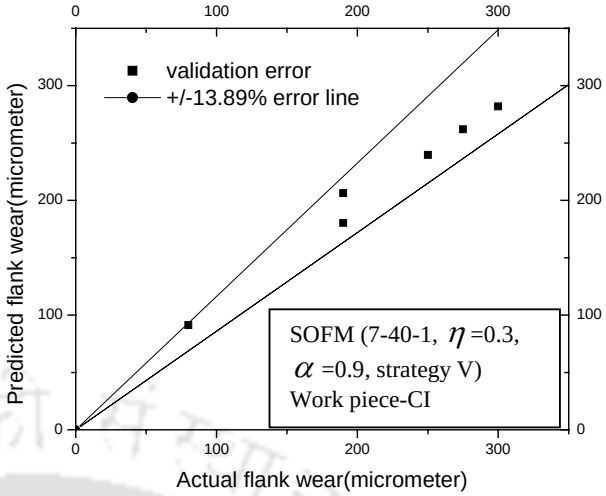

Figure 6.26(b) Comparison of actual values with predicted values of flank wear

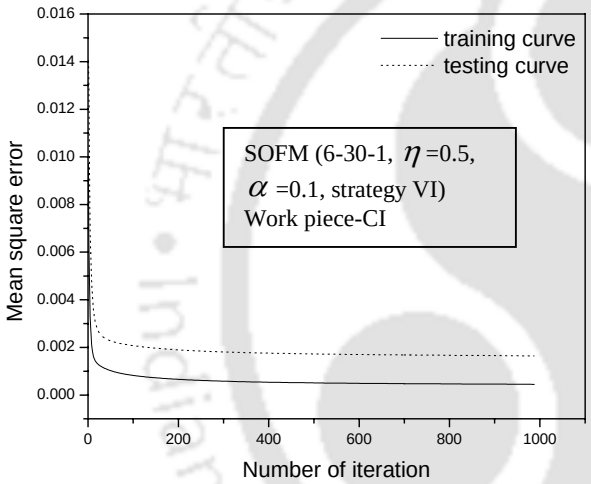

Figure 6.27(a) Variation of MSE with iteration

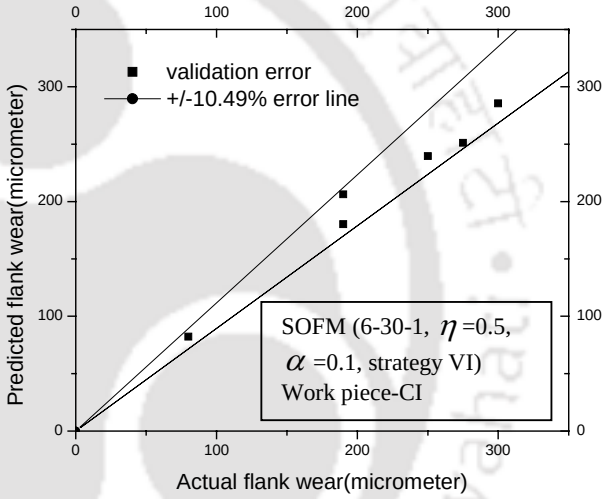

Figure 6.27(b) Comparison of actual values with predicted values of flank wear

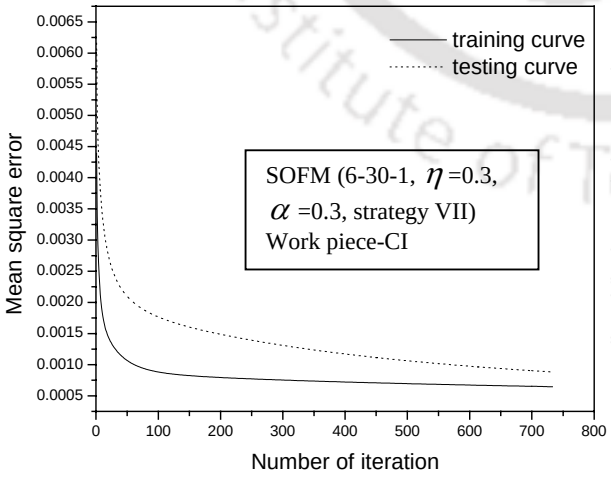

Figure 6.28(a) Variation of MSE with iteration

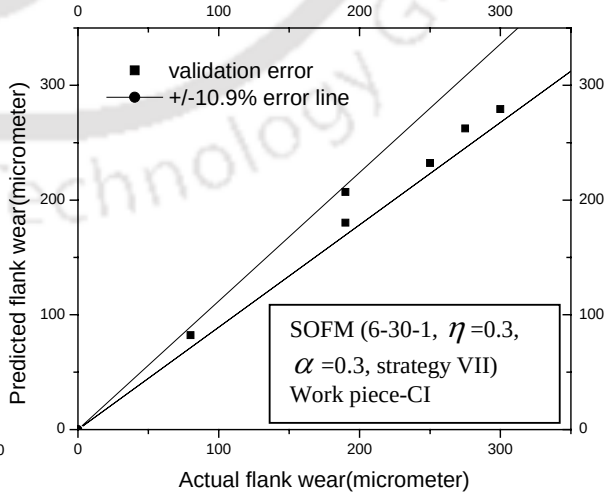

Figure 6.28(b) Comparison of actual values with predicted values of flank wear

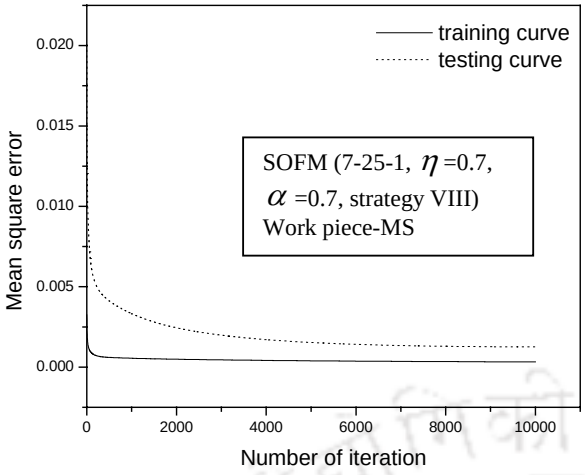

Figure 6.29(a) Variation of MSE with iteration

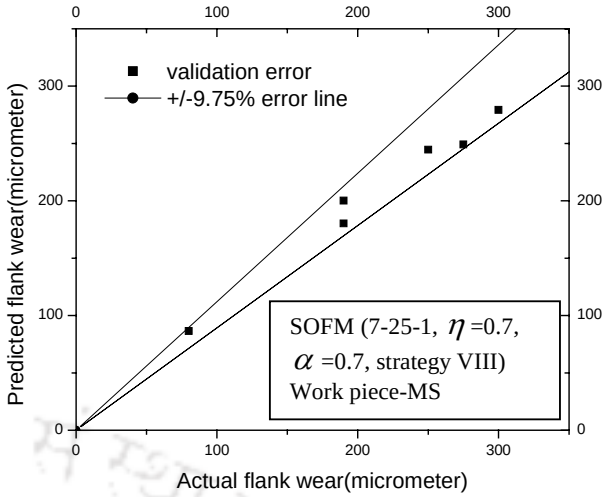

Figure 6.29(b) Comparison of actual values with predicted values of flank wear

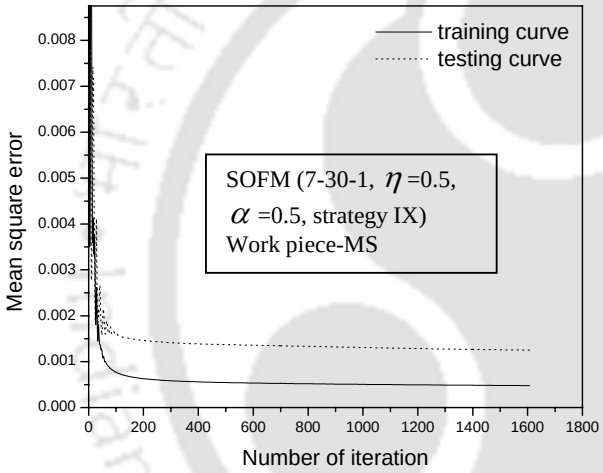

Figure 6.30(a) Variation of MSE with iteration

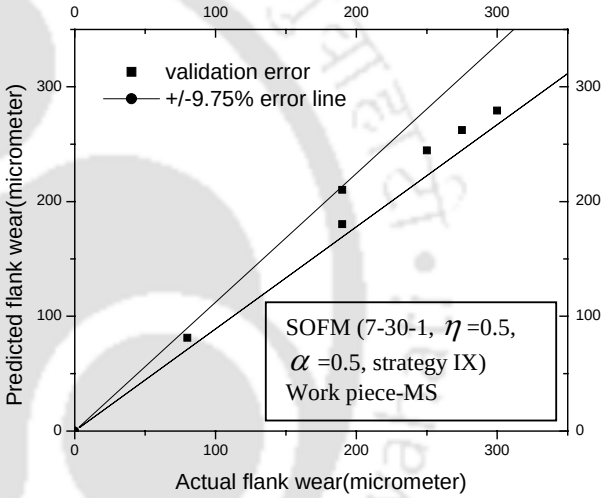

Figure 6.30(b) Comparison of actual values with predicted values of flank wear

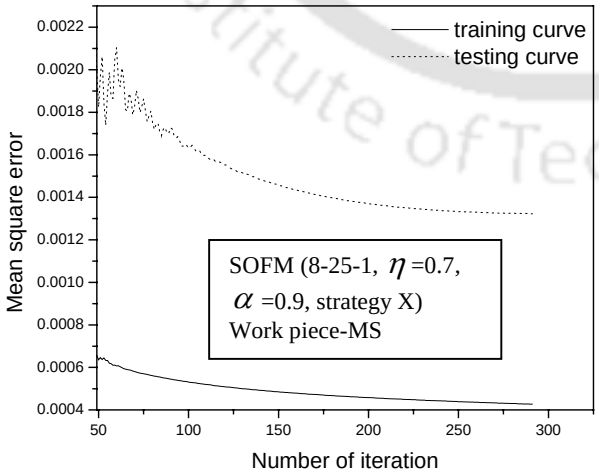

Figure 6.31(a) Variation of MSE with iteration

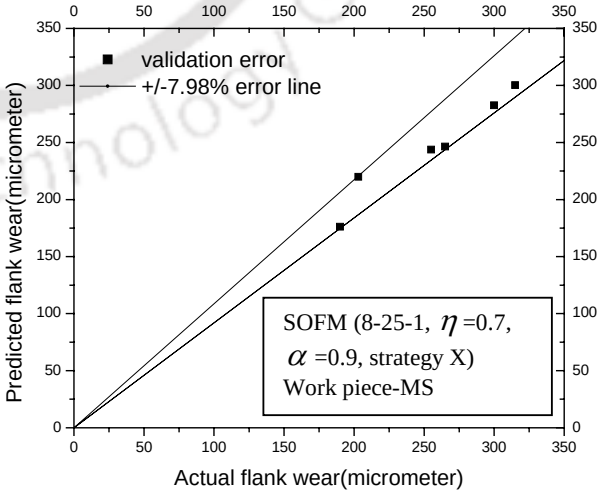

Figure 6.31(b) Comparison of actual values with predicted values of flank wear

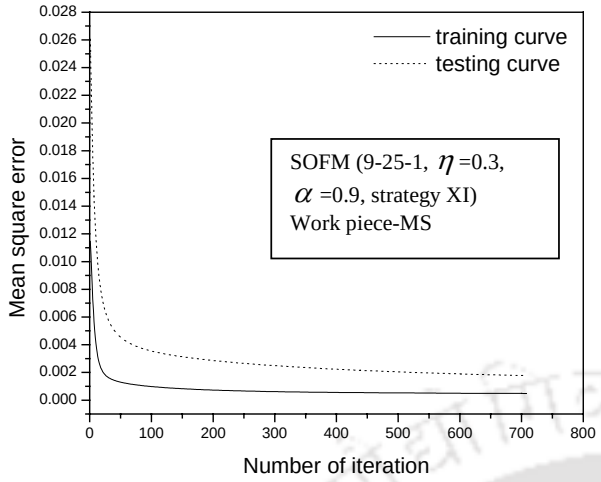

Figure 6.32(a) Variation of MSE with iteration

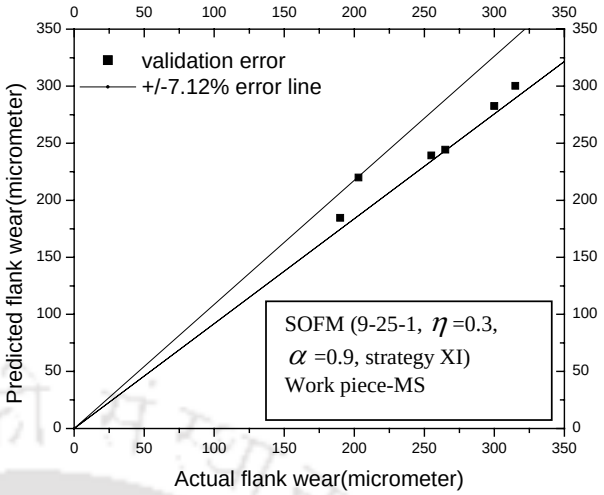

Figure 6.32(b) Comparison of actual values with predicted values of flank wear

6.4.3 Summary of wear prediction in drilling mild steel work piece

It has been observed that in both the cases of drill wear prediction systems (using BPNN as well as SOFM) strategy X (thrust force, torque, feed vibration, radial vibration, chip thickness along with drill diameter, spindle speed and feed rate as input to network) leads to the minimum validation error. However BPNN based drill wear prediction system is more accurate (4.25% validation error) compared to SOFM based drill wear prediction system (7.98% validation error). In terms of number of iterations required for training, SOFM based system is much faster (291 iteration) compared to BPNN based system (14363 iteration).

CHAPTER 7

DRILL WEAR PREDICTION USING FUZZY NEURAL NETWORK

Some times it becomes advantageous to express some of the parameters as fuzzy linguistic variables instead of quantifying them. In those cases, a fuzzy neural network based prediction model becomes more useful in TCM. This chapter describes the application of such a fuzzy neural network model in prediction of drill wear. Here chip thickness has been expressed as fuzzy linguistic variable to be used as an input to the ANN. Computer codes have been developed in C for Fuzzy BPNN (FBPNN) and Fuzzy SOFM (FSOFM) network. FBPNN and FSOFM networks have been tried to develop drill wear prediction system in drilling a mild steel work piece. Finally comparative performances of different TCM strategies along with different ANN architectures tried in the present work for development of a drill wear prediction systems have been presented at the end of this chapter.

7.1 Wear prediction by FBPNN

In the present model, chip thickness has been used as a fuzzy input, and spindle speed, feed rate, drill diameter, thrust force, torque, feed vibration and radial vibration are used as crisp input for the fuzzy back propagation neural network. All the crisp data sets are converted into LR (Left and Right) type fuzzy number by assigning zero to left and right spread. A triangular membership function has been used to describe chip thickness as fuzzy input parameter. Fuzzy sets of chip thickness are overlapped by the adjacent one by 25 percent as shown in figure 7.1. In the drilling operation with mild steel, (referring to table 4.4), it has been observed that the maximum chip thickness was 1.36 mm, and hence fuzzy set of low (L), medium (M) and high (H) chip thickness has been assigned in the range of 0-1.36 mm as shown in figure 7.1. Six TCM strategies (strategy VI to strategy XI) have been used and a large number of network architectures have been tried in order to search for the optimum network corresponding to each of the strategies. Table 7.1 shows the best network architectures in

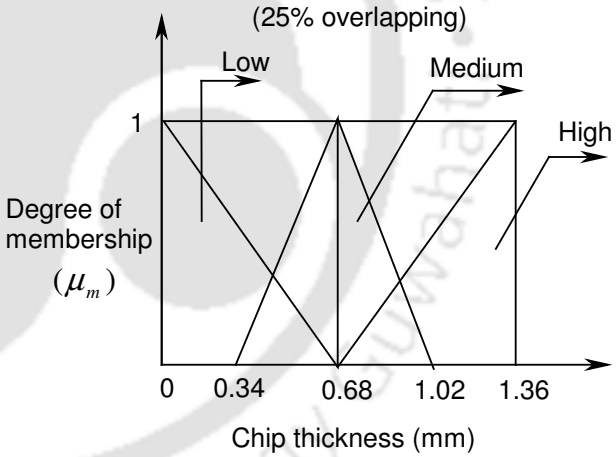

Figure 7.1 Percentage of overlapping of triangular membership function

terms of validation error corresponding to each strategy along with MSE (training and testing) and validation error. It could be observed from table 7.12, that the strategy X (thrust force, torque, feed vibration, radial vibration, chip thickness along with drill diameter, spindle speed and feed rate) leads to the best TCM strategy for drill wear prediction using FBPNN in terms of the validation error. However strategy IX (torque, feed vibration, radial vibration, chip thickness along with drill diameter, spindle speed and feed rate) performs with marginally higher validation error but at a much less number of iteration for learning compared to strategy X. Further, inclusion of surface roughness (strategy XI) leads to even less validation error, however the number of iteration increases. Figures 7.2 to 7.7 show the learning curves and validation error corresponding to the best network in each of the six strategies.

Table 7.1 Network architecture for fuzzy BPNN

Architecture L-M-N	η	α	Iteration	MSE training	MSE testing	Maximum validation error (%)	Strategy
6-12-1	0.1	0.5	19548	0.000238	0.000505	5.9358	VI
6-12-1	0.1	0.7	5064	0.000279	0.000561	4.7618	VII
7-8-1	0.9	0.1	5241	0.000197	0.000529	6.0084	VIII
7-16-1	0.5	0.7	702	0.000317	0.000516	4.4004	IX
8-12-1	0.5	0.5	1775	0.000292	0.000572	4.2895	X
9-12-1	0.3	0.7	2849	0.000292	0.000511	3.89	XI

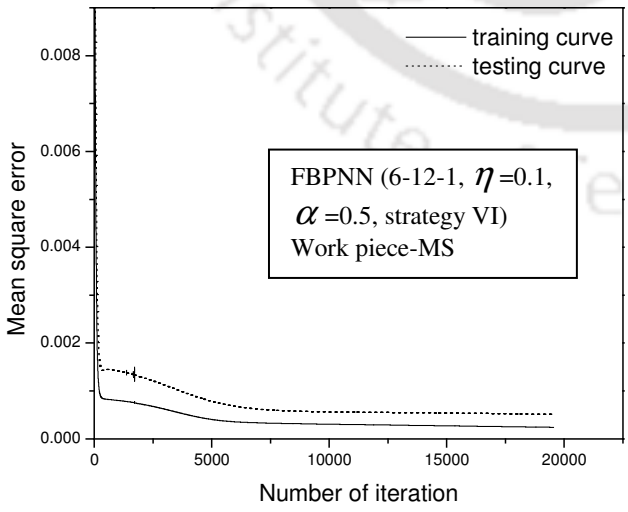

Figure 7.2(a) Variation of MSE with iteration

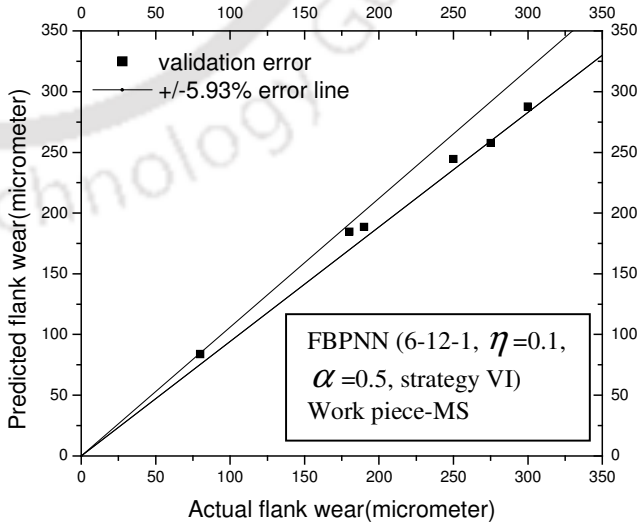

Figure 7.2(b) Comparison of predicted values with actual values of flank wear

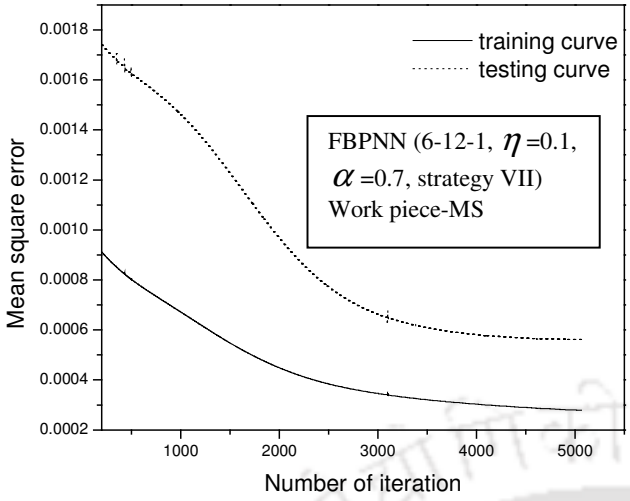

Figure 7.3(a) Variation of MSE with iteration

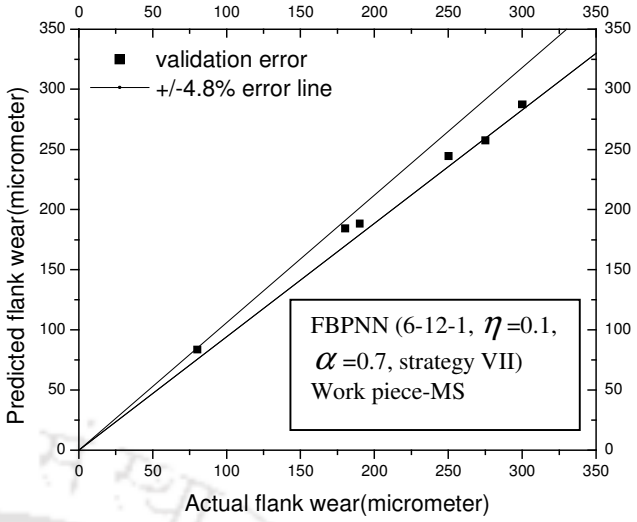

Figure 7.3(b) Comparison of predicted values with actual values of flank wear

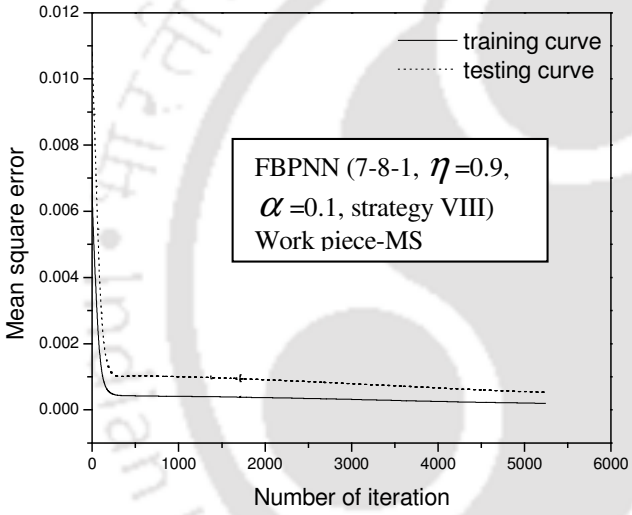

Figure 7.4(a) Variation of MSE with iteration

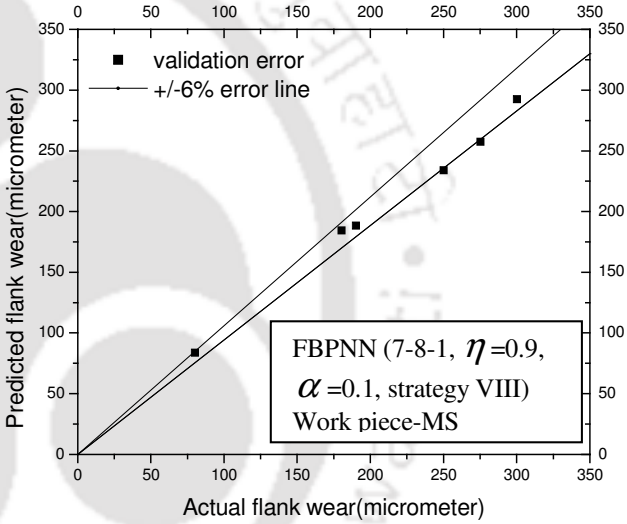

Figure 7.4(b) Comparison of predicted values with actual values of flank wear

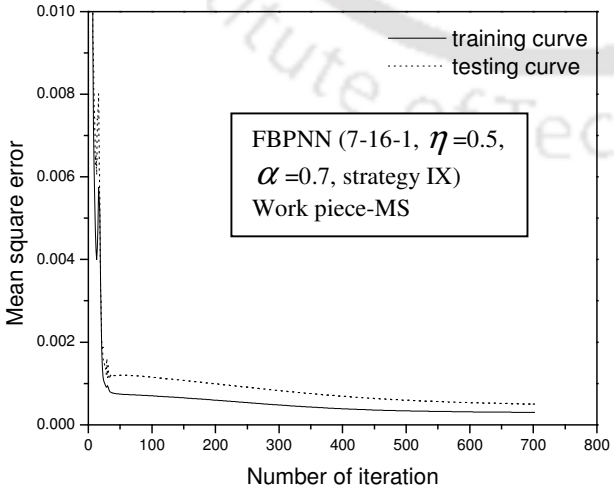

Figure 7.5(a) Variation of MSE with iteration

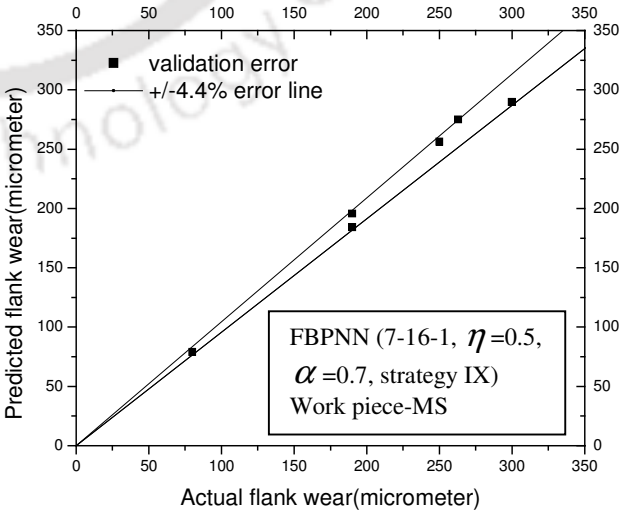

Figure 7.5(b) Comparison of predicted values with actual values of flank wear

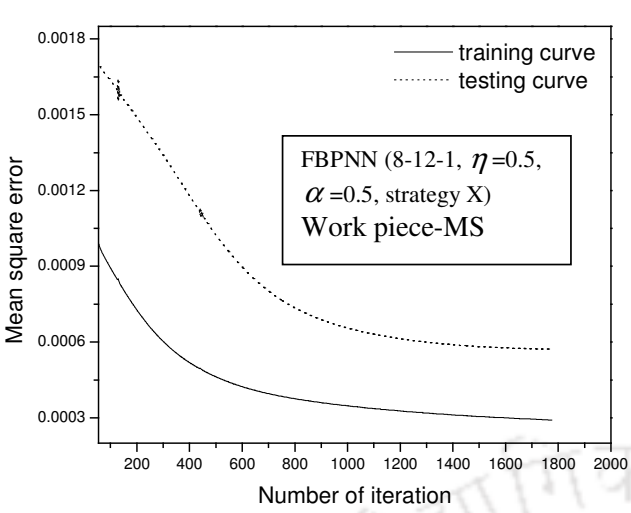

Figure 7.6(a) Variation of MSE with iteration

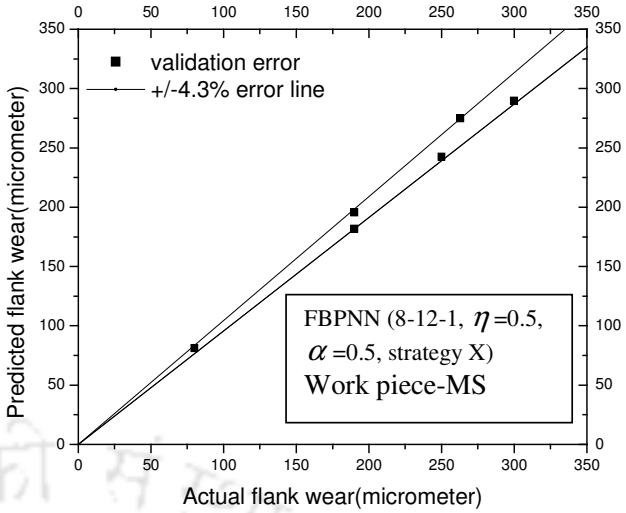

Figure 7.6(b) Comparison of predicted values with actual values of flank wear

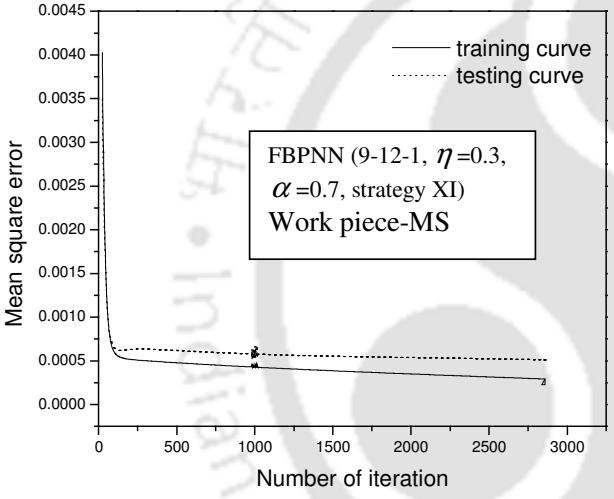

Figure 7.7(a) Variation of MSE with iteration

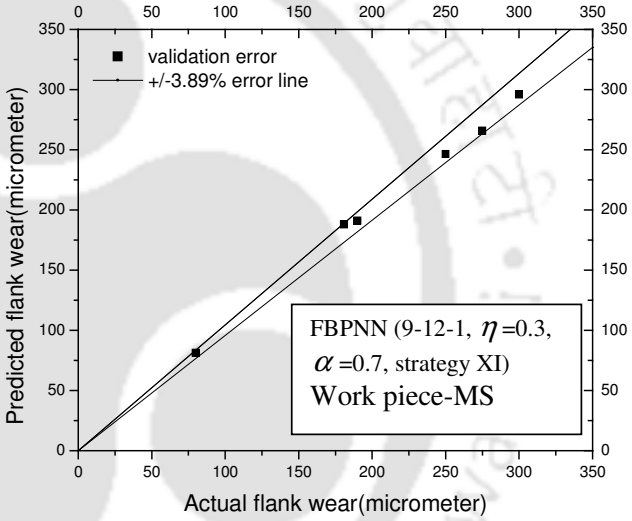

Figure 7.7(b) Comparison of predicted values with actual values of flank wear

7.2 Wear prediction by FSOFM

Six TCM strategies (strategy VI to strategy XI) have been tried for the development of a drill wear prediction systems using FSOFM. Table 7.2 shows the best network architectures in terms of validation error corresponding to each strategy along with MSE (training and testing) and validation error. It could be observed from table 7.2 that the strategy X (thrust force, torque, feed vibration, radial vibration along with spindle speed, feed rate and drill diameter) leads to the best TCM strategy for drill wear prediction using FBPNN. Further, inclusion of surface roughness (strategy XI) leads to even further reduction in validation error, however the number of iteration increases. Figures 7.8 to 7.13 show the learning curves and validation error corresponding to the best network in each of the six strategies.

Table 7.2 Network architectures for FSOFM

Network architecture	η	α	Iteration	MSE training	MSE testing	Maximum validation error (%)	Strategy
6-30-1	0.3	0.5	312	0.000888	0.001553	11.42	S-VI
6-25-1	0.3	0.5	141	0.00089	0.001351	12.84	S-VII
7-25-1	0.1	0.9	2198	0.000438	0.001309	10.44	S-VIII
7-20-1	0.9	0.9	475	0.0005	0.001203	12.90	S-IX
8-25-1	0.5	0.9	325	0.000279	0.001333	9.14	S-X
9-25-1	0.5	0.3	817	0.000348	0.001453	7.91	S-XI

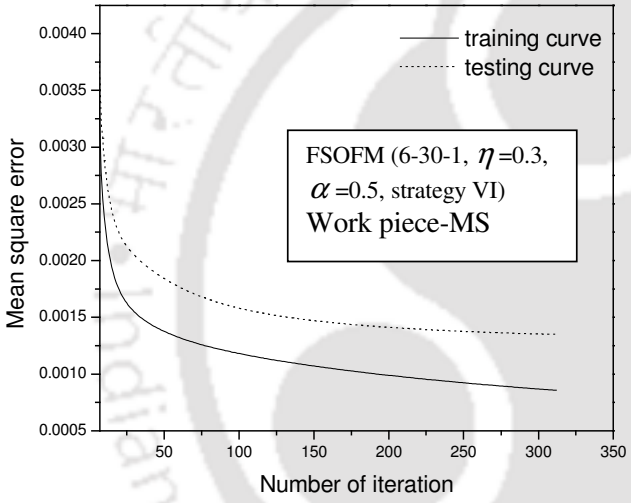

Figure 7.8(a) Variation of MSE with iteration

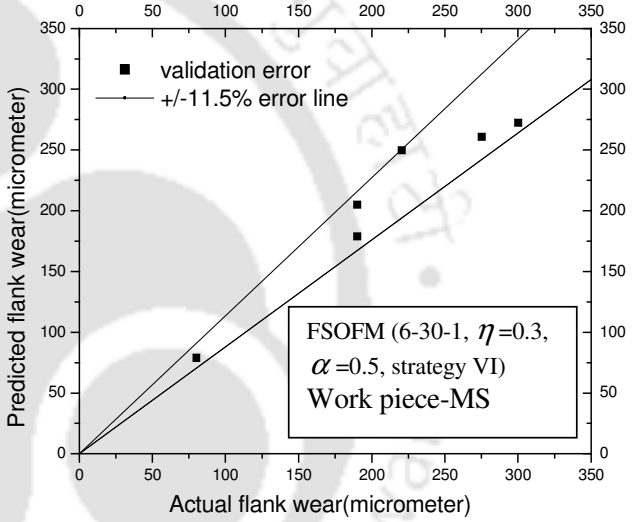

Figure 7.8(b) Comparison of predicted values with actual values of flank wear

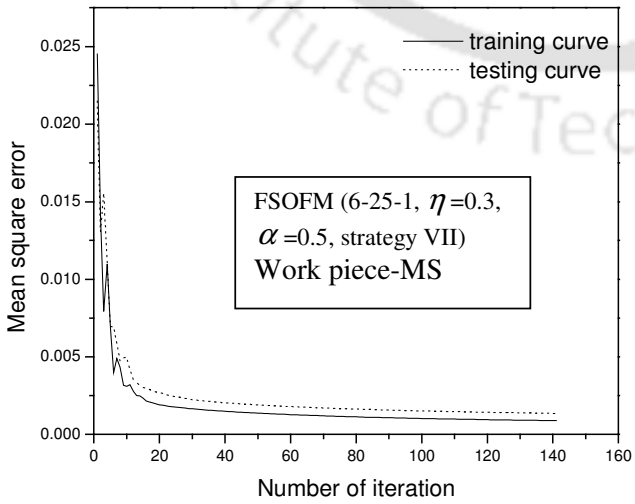

Figure 7.9(a) Variation of MSE with iteration

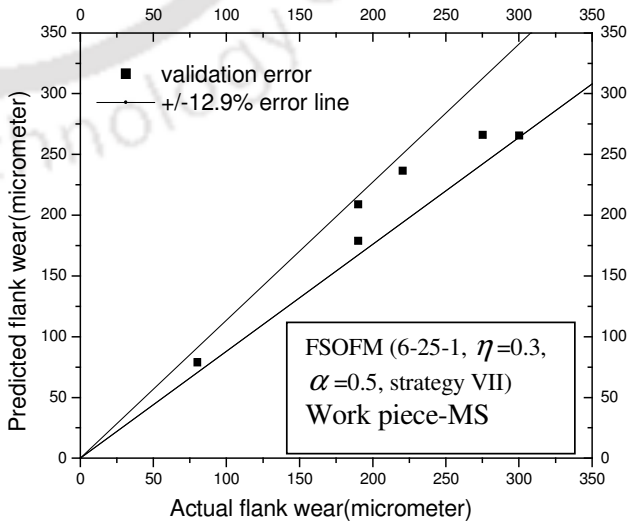

Figure 7.9(b) Comparison of predicted values with actual values of flank wear

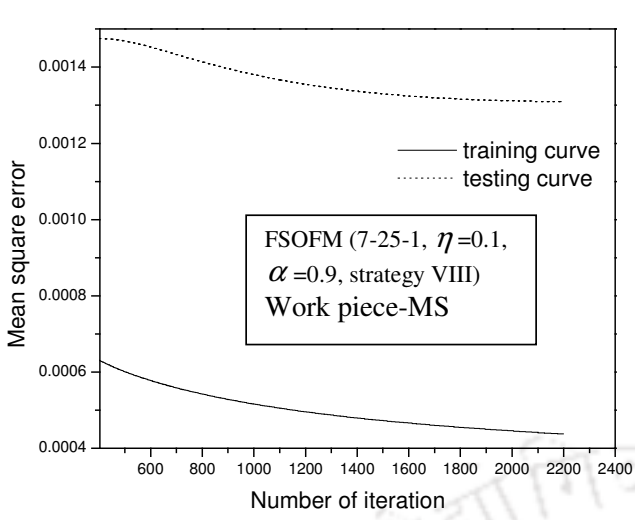

Figure 7.10(a) Variation of MSE with iteration

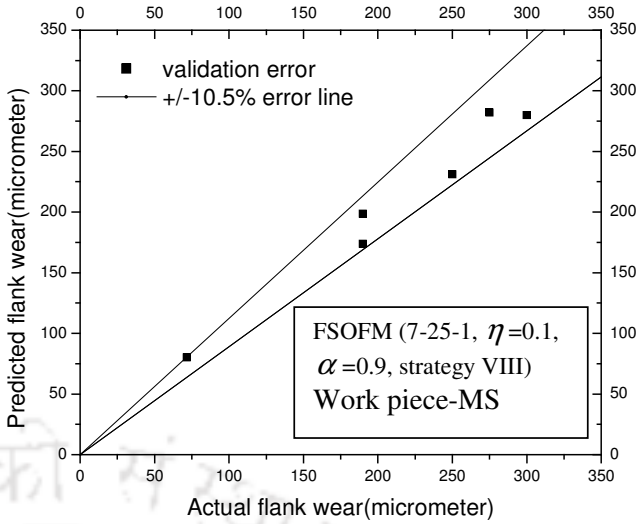

Figure 7.10(b) Comparison of predicted values with actual values of flank wear

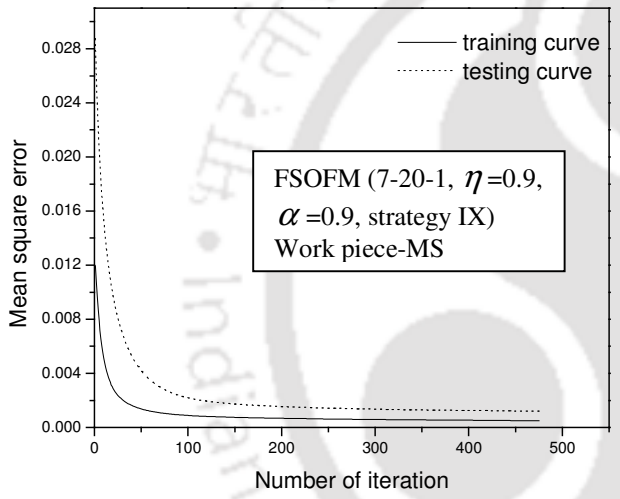

Figure 7.11(a) Variation of MSE with iteration

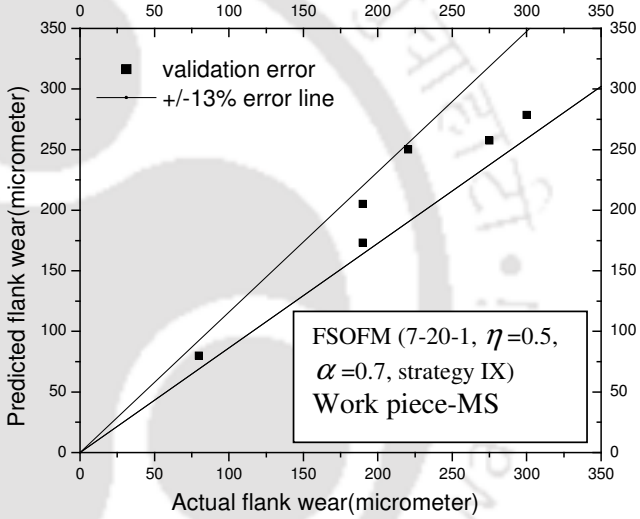

Figure 7.11(b) Comparison of predicted values with actual values of flank wear

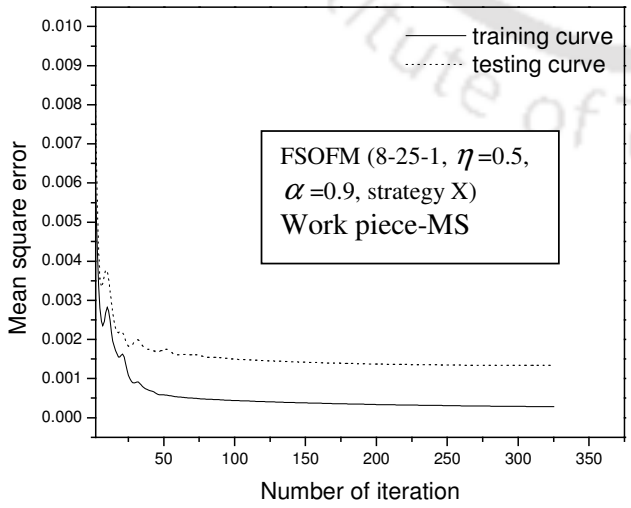

Figure 7.12(a) Variation of MSE with iteration

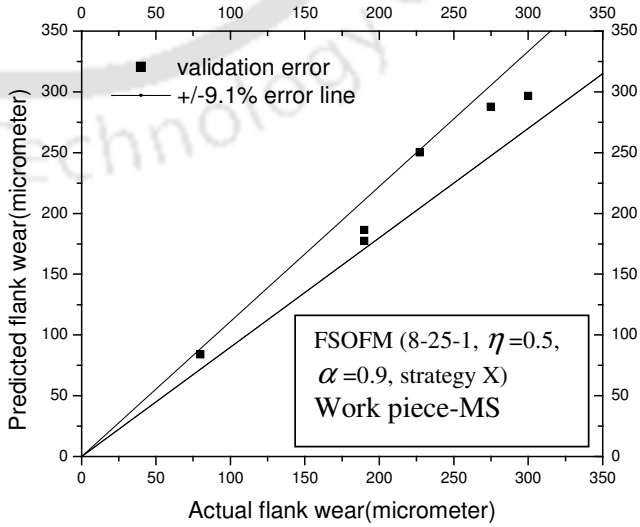

Figure 7.12(b) Comparison of predicted values with actual values of flank wear

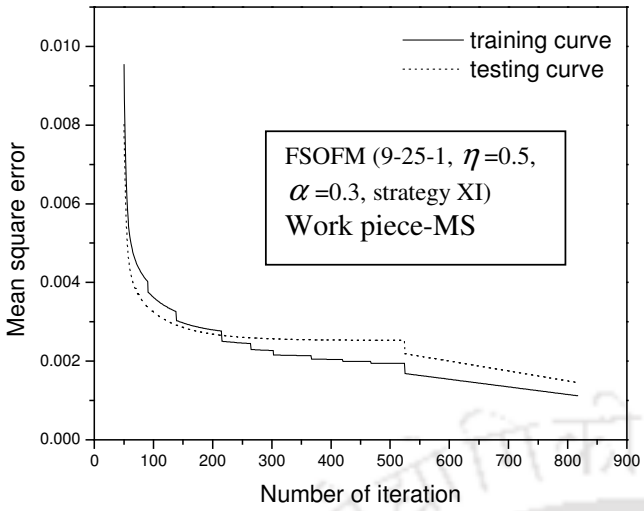

Figure 7.13(a) Variation of MSE with iteration

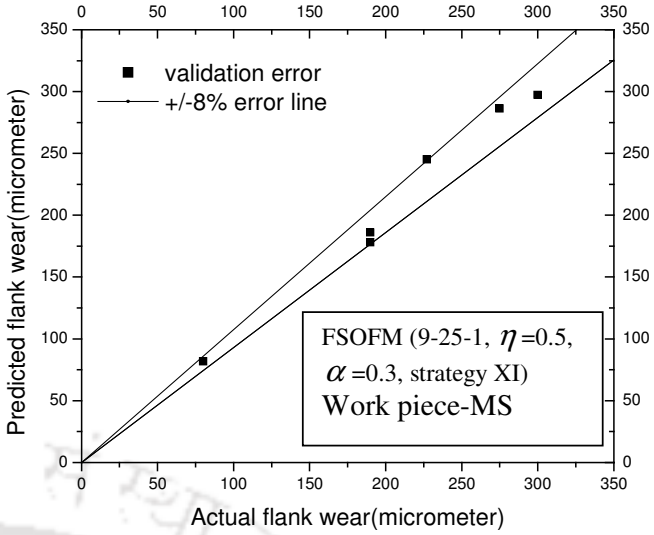

Figure 7.13(b) Comparison of predicted values with actual values of flank wear

7.3 Summary of wear prediction using fuzzy neural network

Here fuzzy neural network based drill wear prediction system has been developed where chip thickness has been used as a fuzzy linguistic variable in the neural network. It has been observed that both FBPNN and FSOFM based prediction system could learn and predict drill wear successfully. In both the cases the best network has been attained corresponding to strategy X, but the convergences is much faster in case of FSOFM compared to that in case of FBPNN.

7.4 Comparative performances of different ANN based drill wear prediction strategies

7.4.1 Drilling in copper

Only one TCM strategy has been tried here with only two sensor signals fused with three process parameters and it was observed that (table 7.3) SOFM converge at a much faster rate and achieving a validation error of 13.99 % which is much less compared to that in BPNN based model.

Table 7.3 Comparative performances of ANN based drill wear prediction in drilling copper work piece

Strategy	ANN	Network architectures	Iterations	Validation error (%)
I	BPNN	5-3-1	4141	25.082
	SOFM	5-15-1	730	13.99

7.4.2 Drilling in cast iron

Here three strategies have been tried and table 7.4 shows that strategy V happened to be the best one. This clearly shows that incorporation of more sensor signals (thrust force, torque, feed vibration and radial vibration) along with process parameters leads to more accurate

prediction by the ANN based drill wear prediction system. It could also be observed in the present case that SOFM converges at a much faster rate compared to BPNN but with an increased validation error level.

Table 7.4 Comparative performances of ANN based drill wear prediction in drilling cast iron work piece

Strategy	ANN	Network architectures	Iterations	Validation error (%)
I	BPNN	5-7-1	922	5.167
	SOFM	5-40-1	614	16.05
III	BPNN	6-3-1	3955	5.02
	SOFM	6-40-1	759	14.04
V	BPNN	7-10-1	5404	4.53
	SOFM	7-40-1	435	7.97

7.4.3 Drilling in mild steel

Out of the eleven different strategies tried here, strategy XI was observed to be the best followed by strategy X. Table 7.5 shows the comparative performances of six different strategies along with four different ANN architectures for development of drill wear prediction systems. It was observed that incorporation of chip thickness along with sensor signals and process parameters as inputs to the ANN leads to more accurate drill wear prediction system with a faster convergence. Inclusion of surface roughness information leads to further reduction of validation error of the prediction systems. It has also been observed that while BPNN and FBPNN based prediction systems predict drill wear with almost same range of validation error, FBPNN is much faster in convergence compared to BPNN in all the cases. In general it was observed in the present study, SOFM based prediction systems achieve convergence much faster compared to BPNN but with a higher validation error level. In particular FSOFM based prediction systems converge much faster compare to SOFM based prediction systems achieving the same level of validation error.

Table 7.5 Comparative performances of ANN based drill wear prediction in drilling mild steel work piece

Strategy	ANN	Network architectures	Iterations	Validation error (%)
VI	BPNN	6-5-1	19707	4.89
	SOFM	6-30-1	987	10.49
	FBPNN	6-12-1	19548	5.93
	FSOFM	6-30-1	312	11.42
VII	BPNN	6-3-1	9612	4.67

Table 7.5 contd.

	SOFM	6-30-1	733	10.94
	FBPNN	6-12-1	5064	4.76
	FSOFM	6-25-1	141	12.84
VIII	BPNN	7-3-1	19826	4.57
	SOFM	7-25-1	10000	9.75
	FBPNN	7-8-1	5241	6.0
	FSOFM	7-25-1	2198	10.44
IX	BPNN	7-5-1	19952	4.45
	SOFM	7-30-1	1607	9.91
	FBPNN	7-16-1	702	4.4
	FSOFM	7-20-1	475	12.90
X	BPNN	8-8-1	14363	4.25
	SOFM	8-25-1	291	7.98
	FBPNN	8-12-1	1775	4.28
	FSOFM	8-25-1	325	9.14
XI	BPNN	9-8-1	8703	3.21
	SOFM	9-25-1	708	7.12
	FBPNN	9-12-1	2849	3.89
	FSOFM	9-25-1	817	7.91

CHAPTER 8

CONCLUSIONS AND SCOPE OF FURTHER WORK

In the present work large number of drilling operations have been conducted and subsequently attempts have been made for development of ANN based drill flank wear prediction systems using the experimental data. Conclusions drawn from the present work have been categorized as

(i) Conclusions based on experimental observations and

(ii) Conclusions based on development of ANN based drill wear prediction systems.

(i) Conclusions based on experimental observations

Various responses in drilling under different cutting conditions have been studied in order to correlate them with drill wear for three different materials viz. copper, cast iron and mild steel. These responses along with other process parameters have been used to study the possibilities of different combinations of them leading to possible drill wear monitoring strategies. From the experiments the following important observation have been made

1. Effect of process parameters on drill wear
   - (i) Increase in drill diameter leads to increase in drill wear
   - (ii) Increase in feed rate leads to increase in drill wear
   - (iii) Spindle speed has negligible effect on the extent of drill wear
2. Influence of drill wear on sensor signals and other measured parameters
   - (iv) Thrust force increases with the increase in extent of drill wear
   - (v) Torque increases with the increase in extent of drill wear
   - (vi) Vibration amplitude increases with the initial progress of wear and then decreases rapidly due to reduction in mass of work piece
   - (vii) Chip thickness increases with the increase in the extent of drill wear
3. Effect of process parameters on sensor signals and other measured parameters
   - (viii) Thrust force and torque increases with increase in feed rate and drill diameter
   - (ix) Spindle speed has negligible effect on thrust force and torque
   - (x) Amplitude of vibration decreases with increase in feed rate
   - (xi) Amplitude of vibration increases with increase in feed rate and drill diameter
   - (xii) Surface roughness of drilled holes increases with increase in feed rate and drill diameter
   - (xiii) Spindle speed has negligible effect on surface roughness

(xiv) Chip thickness increases with increase in feed rate

(xv) Spindle speed and drill diameter have negligible effect on chip thickness

4. Correlation of drill wear with time domain and frequency domain signals

(xvi) Both time domain as well as frequency domain representation of force and vibration signals were observed to have strong correlations with drill wear. However time domain representations have marginally better correlations with drill wear compared to that of frequency domain representations

(ii) Conclusions based on development of ANN based drill wear prediction systems

Different TCM strategies have been tried in conjunction with four different types of ANN architectures namely BPNN, SOFM, FBPNN and FSOFM leading to the study of many possible drill wear prediction systems. From the performance analysis of all these prediction systems the following important conclusions have been drawn

(i) RMS values of measured thrust force, torque and vibration signals have been good indicators of drill wear

(ii) Inclusion of one vibration signal (feed or radial vibration) does not improve the prediction accuracy of the ANN based drill wear prediction systems much but, the convergence is slowed down

(iii) Inclusion of both the vibration signals increases the prediction accuracy of drill wear but number of iteration for convergence is more

(iv) Fusion of both force and vibration signals leads to better drill wear prediction compared to only force and only vibration signals

(v) Inclusion of chip thickness information, leads to more accurate prediction of drill wear when used with force as well as vibration signals and process parameters.

(vi) It has been observed that in case of FBPNN based drill wear prediction systems (where the chip thickness is expressed as fuzzy variable), much faster convergence could be achieved compared to that of BPNN based drill wear prediction systems with almost the same levels of prediction errors. BPNN as such is slow in convergence

(vii) Incorporation of surface roughness information to the ANN along with chip thickness and other sensor signals leads to much better prediction of drill wear along with faster convergence

(viii) In all the cases studied here, SOFM based prediction systems achieves faster convergence compared to BPNN based system but with higher levels of prediction errors

(ix) FSOFM though faster compared to SOFM, FBPNN and BPNN, leads to higher levels of prediction error in all the strategies studied here

Scope for further work

In the present work the training of the neural network architectures has been accomplished off-line. However on-line learning and prediction methodology using different architectures could be undertaken. In addition, other sensor signals such as acoustic emission, sound and chip colour could also be used for fusing into ANN for better prediction of drill flank wear.

List of Publications

1. Panda S.S., Singh A.K., Pal S.K., Chakraborty D., Predicting drill wear using an artificial neural network, International Journal of Advance Manufacturing Technology (2006), 28, 456-462.
2. Panda S.S., Singh A.K., Pal S.K., Chakraborty D., Drill Wear Monitoring using Back Propagation Neural Network, Journal of Material Processing Technology (2006), 172, 283–290.
3. Panda S.S, Chakraborty D, Pal S.K., International Journal of Advance Manufacturing Technology, Monitoring of drill flank wear using fuzzy back propagation neural network (2007), 34(3-4), 227-235
4. Panda S. S., Chakraborty D., Pal S. K., Flank wear prediction in drilling cast iron using Back Propagation Neural Network and Radial Basis Function Network, Journal of Applied Soft Computing, (2008), 8(2), 858-871
5. Panda S.S., Chakraborty D., Pal S.K., Efficacies of sensor integration on drill wear prediction of Mild Steel specimen, under revision in Journal of Advanced Manufacturing Technology (2007).
6. Panda S.S., Chakraborty D., Pal S.K., Comparison of Different Neural Network Architectures for Predicting Drill Wear in Machining Mild Steel, submitted after revision in Journal of Material Processing Technology (2007).
7. Panda S.S., Chakraborty D., Pal S.K., Prediction of drill flank wear using radial basis function neural network, National conference on Soft Computing technique in engineering application (2006), Rourkela.

REFERENCES

[1] M. P. Groover, Fundamentals of Modern Manufacturing (materials, processes, and systems), 2nd edition, John Wiley & Sons, Inc, New York (2002)

[2] M. C. Shaw, Metal cutting principles, New Delhi, CBS Publishers (2002)

[3] K. Subramanian and N. H. Cook, Sensing of drill wear and prediction of drill life (1), Journal of Engineering Industries (1977), 101, 295–301

[4] A. Bhattacharyya, Metal Cutting Theory and Practice, Calcutta, New Central Book (1984)

[5] B. L Juneja, G. S Sekhon and N. Seth, Fundamentals of metal cutting and machine tools, New Delhi, New Age International Pvt Ltd Publication (2003)

[6] A. Ghosh and A. K Mallick, Manufacturing Science, New Delhi, EWP Pvt Limited Publication (2003)

[7] E.J.A. Armarego and R.H. Brown, The Machining of Metals, Prentice-Hall, Inc., 1969

[8] D. A. Stephenson and J. S. Agapiou, Metal Cutting Theory and Practice, Marcel Dekker, Inc., 1997

[9] http://www.mame.mu.oz.au/manuf-sci3/436413/tool_wear.htm

[10] M. Kanai and Y. Kanda, Statistical characteristic of drill wear and drill life for standardized performance tests, Annals of CRIP (1978), 27(1), 61-66.

[11] A. Walsh Ronald, Machining and metal working handbook, New York, MGH Publication (1994)

[12] A. G. Rehorn, J. Jiang and P. E. Orban, State-of-the-art methods and results in tool condition monitoring: a review, International Journal of Advance Manufacturing Technology (2005), 26, 693–710.

[13] M. E. R. Bonifacio, A. E. Dinz, Correlating tool wear, tool life, surface roughness and tool vibration in finish turning with coated carbide tools, Wear (1994), 173, 137-144.

[14] S. B. Rao, Tool wear monitoring through the dynamics of stable turning, Journal of Engineering for Industry (1986), 108, 184-189.

[15] TI El-Wardany, D Gao, MA Elbestawi, Tool condition monitoring in drilling using vibration signature analysis, International Journal of Machine Tools and Manufacture (1996), 36(6), 687–711.

[16] A. Thangaraja and P.K. Wright, Computer assisted prediction of drill failure using in process measurements of thrust force, Journal of Engineering for Industries (1988), Transaction of ASME, 110, 192-200.

[17] I. Inasaki, Application of acoustic emission sensor machining processes, Ultrasonic (1998), 36, 273-281.

[18] S. Y. Hong, Knowledge-based diagnosis of drill conditions, Journal of Intelligent Manufacturing (1993), 4, 233-241.

[19] C. Rubenstein, The torque and thrust force in twist drilling-I: theory, International Journal of Machine and Tools Manufacture (1991), 31(4), 481-89.

[20] C. Chungchoo and D. Saini, A computer algorithm for flank and crater wear estimation in CNC turning operations, International Journal of Machine Tools and Manufacture (2002), 42, 1465–1477.

[21] W. Haili, S. Hua, C. Ming and H. Dejin, On-line tool breakage monitoring in turning, Journal of Materials Processing Technology (2003), 139, 237–242.

[22] M. Nouari, G. List, F. Girot and D. Coupard, Experimental analysis and optimization of tool wear in dry machining of aluminium alloys, Wear (2003), 255, 1359–1368.

[23] V. T. S. Elanayar and Y. C. Shin, Design and implementation of tool wear monitoring with radial basis function neural networks, Proceedings of the American Control Conference, Seattle, Washington (1995), TA8-9: 55.

[24] T. R. Lin, Cutting behavior using variable feed and variable speed when drilling stainless steel with TiN-coated carbide drills, International Journal of Advance Manufacturing Technology (2002), 19, 629–636.

[25] M.Z. Zhang, Y.B. Liu and H. Zhou, Wear mechanism maps of uncoated HSS tool drilling die cast aluminium alloy, Tribology International (2001), 34, 727-731.

[26] S. K. Choudhury, G. Raju, Investigation into crater wear in drilling, International Journal of Machine Tools and Manufacture (2000), 40, 887–898.

[27] E. Morin, J. Masounave and E.E. Laufer, Effect of drill wear on cutting forces in the drilling of metal-matrix composites, Wear (1995), 184, 11-16.

[28] J. M. Zhou, M. Andersson, and J. E. Stahl, The monitoring of flank wear on the CBN tool in the hard turning process, International Journal of Advance Manufacturing Technology (2003), 22, 697–702.

[29] C.H. Gao, K. Cheng and D. Kirkwood, The investigation on the machining process of BTA deep hole drilling, Journal of Materials Processing Technology (2000), 107, 222-227.

[30] H. Konrad, R. Isermann and H. U. Oette, Supervision of tool wear and surface quality during end milling operations, Intelligent Manufacturing System (1994), 507–513

[31] G. Byrne, D. Dornfeld, I. Inasaki, G. Ketteler, W. Konig and R. Teti, Tool condition monitoring (TCM)–the status of research and industrial application, Ann CIRP (1995), 44(2), 541–567

[32] S. H. Yeo, L. P. Khoo and S. S. Neo, Tool condition monitoring using reflectance of chip surface and neural network, Journal of Intelligent Manufacturing (2000), 11, 507–514

[33] C. F. Micheletti, W. Koenig and H. R. Victor, In-process tool wear sensors for cutting operations. Ann CIRP (1976), 25, 483–496

[34] R. Azouzit and M. Guillot, On-line prediction of surface roughness and dimensional deviation using neural network based sensor fusion, International Journal of Machine Tools and Manufacture (1997), 37 (9), 1201-1217

[35] A. Thangaraj and P. K. Wright, Computer assisted prediction of drill failure using in process measurements of thrust force, Journal of Engineering industries (1988), 110,192–200

[36] S. Braun, E. Lenz and C. L. Wu, Signature analysis applied to drilling, Journal of Mechanical Design (1982), 104, 268–276

[37] J. E. Jokinen, Automated on-line diagnosis of cutting tool condition, International Journal of Flexible Automation & Integrated Manufacturing (1996), 4(3-4),
273–287

[38] X. Li, On-line detection of the breakage of small diameter drills using current signature wavelet transform, International Journal of Machine Tools and Manufacture (1999), 39(1), 157–164

[39] K. Patra, S.K. Pal and K. Bhattacharyya, Artificial neural network based prediction of drill flank wear from motor current, Journal of Applied Soft Computing (2007), 7, 929-935

[40] K. Ramamurthi and C. L. Hough Jr, Intelligent real-time predictive diagnostics for cutting tools and supervisory control of machining operations, Journal of Engineering for Industries (1993), 115, 268–277

[41] M. Elhachimi, S. Torbaty and P. Joyot, Mechanical modeling of high speed drilling 2: predicted and experimental results, International Journal of Machine Tools and Manufacture (1999), 39, 569-581

[42] S. C. Lin and C. J. Ting, Tool wear monitoring in drilling using force signals, Wear (1995), 180, 53–60

[43] E. Brinksmeier, Prediction of tool fracture in drilling, Annal of the CRIP (1990), 39(1), 97-100

[44] G. S. Li, W. S. Lau and Y. Z. Zhang, In-process prediction of drill wear and breakage monitoring for a machining center based on cutting force parameters, International Journal of Machine Tools and Manufacture (1992), 32(6), 855-867

[45] J. E. Jokinen, A summary of methods applied to tool condition monitoring in drilling, International Journal of Machine Tools and Manufacture (2002), 42, 997–1010

[46] L. Wang, E. Kannatey-Asibu Jr. and M. G. Mehrabi, A Method for sensor selection in re-configurable process monitoring, Journal of Manufacturing Science and Engineering (2003), 125, 95-99

[47] S. Kakade, L. Vijayraghavan and R. Krishnamurthy, Monitoring of tool status using intelligent acoustic emission sensing and decision based neural network, IEE, IA&C, (1995), 25-29

[48] D. E. Dimla Snr., The Correlation of vibration signal features to cutting tool wear in a metal turning operation, International Journal of Advance Manufacturing Technology (2002), 19, 705–713

[49] Y. M. Niu, Y. S. Wong and G. S. Hong, An Intelligent sensor system approach for reliable tool flank wear recognition, International Journal of Advance Manufacturing Technology (1998), 14, 77-84

[50] C. Scheffer, H. Engelbrecht and P. S. Heyns, A comparative evaluation of neural networks and hidden Markov models for monitoring turning tool wear, Neural Computing & Application (2005), 14, 325–336

[51] H. Gao and M. Xu, Intelligent tool condition monitoring system for turning operations, ISNN 2005, Springer-Verlag Berlin Heidelberg 2005, LNCS 3498, 883-889

[52] S.C. Lin and C.J. Ting, Drill wear monitoring using neural network, International Journal of Machine Tools and Manufacture (1996), 36, 465-475

[53] T. I. Liu and W.Y. Chen, Intelligent detection of drill wear, Journal of Mechanical Systems and Signal Processing (1998), 12(6), 863-873

[54] T. Szecsi, Automatic cutting-tool condition monitoring on CNC lathes, Journal of Materials Processing Technology (1998), 77, 64–69

[55] Z. Wang, W. Lawrenz, R.B.K.N. Rao and Tony Hope, Feature-filtered fuzzy clustering for condition monitoring of tool wear, Journal of Intelligent Manufacturing (1996), 7, 13-22

[56] B. Pena, G. Aramendi and A. Rivero, L. N. L. de Lacalle, Monitoring of drilling for burr detection using spindle torque, International Journal of Machine Tools and Manufacture (2005), 45, 1614–1621

[57] H. Y. Kim, J. H. Ahnn, S. H. Kim and S. Takata, Real-time drill wear estimation based on spindle motor power, Journal of Material Processing Technology (2002), 124, 267–273

[58] Z. Adamczyk, Transient states in drilling process as a source of tool wear knowledge for intelligent tool condition monitoring system, IX workshop on supervising and diagnostic of machine systems manufacturing simulation for industrial use, Prace Naukowe Instytutu Technologii Maszyn I Automatyzacji Politechniki Wroclawskiej (1998), 69(31), 195-204

[59] M. Routio and M. Saynatjoki, Tool wear and failure in drilling of stainless steel, Journal of material processing technology (1995), 52(1), 35-43

[60] R. W Barker, R. A. Kluthe and M. J. Hinich, Monitoring rotating tool wear using higher-order spectral features, Journal of Engineering industries (1993), 115, 23–29

[61] S. A. Kumar, H. V. Ravindra and Y. G. Srinivasa, In-process tool wear monitoring through time series modeling and pattern recognition, International Journal of Production Research (1997), 35, 739-751

[62] S. Damodarasamy and S. Raman, An inexpensive system for classifying tool wear states using pattern recognition, Wear (1993), 170 (2), 149–160

[63] L.C. Lee, K.Y. Lam and X.D. Liu, Characterization of tool wear and failure, Journal of Materials Processing Technology (1994), 40, 143–153

[64] K. Jemielniak, Commercial tool condition monitoring systems, International Journal of Advance Manufacturing Technology (1999), 15, 711–721

[65] L. A. Franco-Gasca, G. Herrera-Ruiz, R. Peniche-Vera, R. de, J. Romero-Troncoso and W. Leal-Tafolla, Sensorless tool failure monitoring system for drilling machines, International Journal of Machine Tools and Manufacture 46 (2006) 381–386

[66] D. Shi, D. A. Axinte and N. N. Gindy, Development of an online machining process monitoring system: a case study of the broaching process, International Journal of Advance Manufacturing Technology (2006), DOI 10.1007/s00170-006-0588-1

[67] I. Abu-Mahfouz, Drilling wear detection and classification using vibration signals and artificial neural network, International Journal of Machine Tools and Manufacture (2003), 43, 707–720

[68] T. J. Ko and D. W. Cho, Cutting state monitoring in milling by a neural network, International Journal of Machine Tools and Manufacture (1994), 24(5), 659-676

[69] X. Li, S. Dong and P. K. Venuvinod, Hybrid Learning for Tool Wear Monitoring, International Journal of Advance Manufacturing Technology (2000), 16, 303–307

[70] S.Y Hong, J. Ni and S.M. Wu, Analysis of drill failure modes by multiple sensors on a robotic and effector, Japan/USA symposium on flexible automation, ASME (1992), 2, 947-956

[71] C. Scheffer and P.S. Heyns, Wear monitoring in turning operations using vibration and strain measurements, Journal Mechanical Systems and Signal Processing (2001), 15(6), 1185-1202

[72] A. Prateepasen, Y.H.J. Au and B .E. Jones, Acoustic emission and vibration for tool wear monitoring in single-point machining using belief network, IEEE Instrumentation and Measurement Technology Conference (2001), Budapest, Hungary, 0-7803-6646-8

[73] S.R. Hayashi, C.E. Thomas and D.G. Wildes, Tool break detection by monitoring ultrasonic vibrations, Annals of the CIRP (1988), 37 (1), 61–64

[74] E.J Weller, H.M Schrier and B. Weichbrodt, Journal of Engineering Industries (1969), 91, 525-534

[75] M. Lee, C.E. Thomas and D.G. Wildes, Review Prospects for in-process diagnosis of metal cutting by monitoring vibration signals, Journal of Material Science (1987), 22, 3821-3830

[76] A.D. Tageia, S. Portunato and P. Toni, An Approach to On-Line Measurement of Tool Wear by Spectrum Analysis, Proceedings of the 7th Machine Tool Design and Research Conference, Manchester University, UK (1976), 141-148.

[77] L. B. Bahr, S. Motavalli and T. Arfi, Sensor fusion for monitoring machine tool conditions, International Journal of Computer Integrated manufacturing (1997), 10, 314–323.

[78] K.W. Yee and D.S. Blomquist, An On-Line Method of Determining Tool Wear by Time Domain Analysis, SME Tech. Paper MR 82-901, Society of Manufacturing Engineers, Dearborn, Michigan (1982).

[79] K. W. Yee and L. Evans, Drill-Up, An Alternative for On-Line Determination of End-Mill Wear, Proceedings of 13th North American Manufacturing Research Conference, CBerkeley, Berkeley, California (1985), 304-309

[80] G.H Lim, Tool wear monitoring in machine turning, Journal of Material Processing technology (1995), 51, 25-36

[81] R. E. Haber, J. E. Jimenez, C. R. Peres and J. R. Alique, An investigation of tool-wear monitoring in a high-speed machining process, Sensors and Actuators (2004), A 116, 539–545

[82] D. E. Dimla, Sensor signals for tool-wear monitoring in metal cutting operations— a review of methods International Journal of Machine Tools and Manufacture (2000), 5 (40), 1073-1098

[83] D. E. Dimla and P. M. Lister, On-line metal cutting tool condition monitoring.: I: force and vibration analyses International Journal of Machine Tools and Manufacture (2000), 40, 739-768

[84] D. E. Dimla and P. M. Lister, On-line metal cutting tool condition monitoring: II: tool state classification using multi-layer perceptron neural networks International Journal of Machine Tools and Manufacture (2000), 5 (40), 769-781

[85] S. Liang and D. Dornfeld, Tool wear detection using time series analysis of acoustic emission, Journal of Engineering Industries (1989), 111 (3), 199–205

[86] S. R. Hayashi, C. E. Thomas and D. G. Wildes, Tool break detection by monitoring ultrasonic vibration, Annal of CRIP (1988), 37(1), 61-64

[87] F. A. Farrelly, A. Petri, L. Pitolli, and G. Pontuale, Statistical properties of acoustic emission signals from metal cutting processes, Journal of Acoustical Society of America (2004), 116 (2), 981–986

[88] C. Beggan, M. Woulfe, P. Young and G. Byrne, Using acoustic emission to predict surface Quality, International Journal of Advance Manufacturing Technology (1999), 15, 737–742

[89] C. E. Everson and S. H. Cheraghi, The application of acoustic emission for precision drilling process monitoring, International Journal of Machine Tools and Manufacture (1999), 39 371–387

[90] E. kannatey-Asibu, On the application of pattern recognition method to manufacturing process monitoring, Proceeding of NAMRC-X, Hamilton, Ontario, Canada (1982), 487-492

[91] W. P Dong, Y. E. Joe Au and A. Mardapittas, Characteristics of acoustic emission in drilling, Tribology (1994), 27(3), 169–170

[92] W. Koenig, K. Kutzner and U. Schehl, Tool monitoring of small drills with acoustic emission, International Journal of Machine Tools and Manufacture ((1992), 32 (4), 487–493

[93] K. Kojima, I. Inasaki and R. Miyake, Monitoring of turning process with acoustic emission signals, Nippon Kikai Gakkai Ronbunshu, C Hen (1986), 52 (474), 799–805.

[94] Y. Naerheim and A. Arora, In-process monitoring of machining using acoustic emission, Review of Progress in Quantitative Nondestructive Evaluation, 3 (B), Plenum Press, USA, 1984, 753–762.

[95] R. Heinemann, S. Hinduja and G. Barrow, Use of process signals for tool wear in drilling small deep holes, International Journal of Advance Manufacturing Technology (2005), DOI 10.1007/s00170-006-0459-9

[96] W. Grzesik and S. Brol, Hybrid approach to surface roughness evaluation in multistage machining process, Journal of material processing technology (2003), 134, 265-272

[97] A.A. Houshmand, A dynamic model for tool wear detection using acoustic emission, Mechanical Systems and Signal Processing (1995), 9(4), 415-428

[98] T. Moriwaki and R. Hino, Application of neural network to AE signal processing for automatic detection of cutting tool life, JSPE (1991), 57(7), 1259-1264

[99] E. Goverkar, I. Grabec and H. O. Madsen, Estimation of drill wear from AE signals using self organisms neural network, Proceeding of 4th world meeting on AE/1st, International Conference AE in Manufacturing (1991), 65, ASNT, Boston, MA

[100] S. Y. Liang, Y. K. Kwon and R. Y. Chiou, Modeling the effect of flank wear on machining thrust stability, International Journal of Advance Manufacturing Technology (2004), 23, 857–864

[101] G. Pontuale, F.A. Farrelly, A. Petri and L. Pitolli, A statistical analysis of acoustic emission signals for tool condition monitoring (TCM), Acoustics Research Letters Online (2002), DOI 10.1121/1.1532370

[102] V. B. Jammu, K. Danai and S. Malkin, Unsupervised neural network for tool breakage detection in turning, Annal CIRP (1993), 42(1),67-70

[103] P. Wilkinson and R.L. Reuben, Tool wear prediction from acoustic emission and surface characteristic via an artificial neural network, Mechanical Systems and Signal Processing (1999), 13(6), 955-966

[104] O. Masory, Detection of tool wear using multi sensor reading defined by artificial neural network, Proc SPIE-Int Soc Opt Engng (1991),1469(2),515-520

[105] H. V. Ravindra, Y. G. Srinivasa and R. Krishnamurthy, Acoustic emission for tool condition monitoring in metal cutting, Wear *(*1997), 212, 78-84

[106] T. Obikawa, C. Kaseda, T. Matsumura, W. G. Gong and T. Shirakashi, Tool wear monitoring for optimizing cutting conditions, Journal of Materials Processing Technology (1996), 62, 374-379.

[107] M.A. McPhee, C. Subramanian, K.N. Stratford, T.P. Wilks and L.P. Ward, Evaluation of coated twist-drills using frequency-domain analysis, Surface and Coatings Technology (1995), 71, 215-221

[108] D. E. Dimla Jnr., P. M. Lister and N J Leighton, A multi sensor integration method of signals in metal cutting operation via application of multi layer perceptron neural network, Artificial Neural Networks (1997), Conference Publication No. 440, IEE

[109] T.I EL-Wardany, D. Gao and M.A. Elbestawi, Tool condition monitoring in drilling using vibration signature analysis, International Journal of Machine Tools and Manufacture (1996), 36(6), 687-711.

[110] S. Rangwala and D. Dornfeld, Sensor integration using neural networks for intelligent tool condition monitoring, Journal of Engineering for Industry (1990), 112, 219–228

[111] E. O. Brigham, The Fast Fourier Transform and its Applications, Signal Processing Series (1988), Englewood Cliffs: Prentice-Hall

[112] L. Monostori, A step towards intelligent manufacturing: Modeling and monitoring of manufacturing processes through artificial neural networks, Annals of the CIRP (1993), 42, 485–488.

[113] R. G. Silva, R. L. Rueben, K. J. Baker and S. J. Wilcox, Tool wear monitoring of turning operations by neural network and expert system classification of a feature set generated form multiple sensors, Mechanical Systems and Signal Processing (1998), 12, 319-332

[114] Y. Quan, M. Zhou and Z. Luo, On-line robust identification of tool-wear via multi-sensor neural network fusion, Engineering Applications of Artificial Intelligence (1998), 11, 717-722

[115] I. H. Choi and J. D. Kim, Development of monitoring system on the diamond tool wear, International Journal of Machine Tools and Manufacture (1999), 39, 505-515

[116] H. Chelladurai, V. K. Jain and N. S. Vyas, Development of a cutting tool condition monitoring system for high speed turning operation by vibration and strain analysis, International Journal of Advance Manufacturing Technology (2007), DOI 10.1007/s00170-007-0986-z

[117] E.J.A. Armarego and C.Y. Cheng, Drilling with flat rake face and conventional twist drills-I: Theoretical investigation, International Journal of Machine Tool Design & Research (1972), 12, 17-35.

[118] M. Elhachimi, S. Torbaty and P. Joyot, Mechanical modeling of high speeds drilling 1: Predicting torque and thrust, International Journal of Machine Tools and Manufacture (1999), 39, 553–568.

[119] W. Bouzid-Saı, An investigation of tool wear in high-speed turning of AISI 4340 steel, International Journal of Advance Manufacturing Technology (2004), DOI 10.1007/s00170-003-1991-5.

[120] S. K. Bhattacharya and I. Ham, Analysis of tool wear part-I: theoretical model of flank wear, Journal of Engineering for Industries (1969), 790-798.

[121] E.J.A. Armarego and C.Y. Cheng, Drilling with flat rake face and conventional twist drills-II: experimental investigation, International Journal of Machine Tool Design & Research (1972), 12, 37-54.

[122] K. Gupta, O. B. Ozdoganlar, S. G. Kapoor and R. E. DeVor, Modeling and prediction of hole profile in drilling, Part 1: Modeling drill dynamics in the presence of drill alignment errors, Journal of Manufacturing Science and Engineering (2003), 125, 6-13.

[123] Y. Gong, C. Lin and K. F. Ehmann, Dynamics of initial penetration in drilling: Part 1—Mechanistic model for dynamic forces, Journal of Manufacturing Science and Engineering (2005), 127,280-288.

[124] L.-B. Zhang, L.-J. Wang, X.Y. Liu, H.W. Zhao, X. Wang and H.Y. Luo, Mechanical model for predicting thrust and torque in vibration drilling fiber-reinforced composite materials, International Journal of Machine Tools and Manufacture (2001), 41, 641–657

[125] R. A. Williams, A study of drilling process. J Engineering industries (1974), 96, 1207–1215

[126] D.A. Stephenson and J.S. Agapiou, Calculation of main cutting edge forces and torque for drills with arbitrary point geometries, International Journal of Machine Tools and Manufacture (1992), 32(4), 521-538.

[127] B.Y. Lee, H. S. Liu and Y. S. Tarng, Modeling and optimization of drilling process, Journal of Material Processing Technology (1998), 74, 149–157

[128] H. S. Liu, B. Y. Lee and Y. S. Tarng, In-process prediction of corner wear in drilling operations. Journal of Material Processing Technology (2000), 101, 152–158

[129] G. Chryssolouris and M. Domroese, An experimental studies of strategies for integrating sensor information in machining, Annals of the CRIP, 38(1), 1989, 425-428

[130] H. V. Ravindra, Y. G. Srinivasa and R. Krishnamurthy, modeling tool wear based on cutting forces in turning, wear, 169, 1993, 25-32

[131] S. Spiewak and S. M. Wu, Tool wear monitoring and breakage detection based on intelligent filtering, International Journal of Machine Tools and manufacture, 28(4), 1988, 483-494

[132] A. Noori-Khajavi and R. Komanduri, Frequency and time domain analyses of sensor signal in drilling-I, correlation with drill wear, International Journal of Machine Tools and Manufacture (1995), 35(6), 775-793

[133] A Noori-Khajavi, R Komanduri, Frequency and time domain analyses of sensor signal in drilling-II, investigation on some problems associated with sensor signal. International Journal of Machine Tools and Manufacture (1995), 35(6), 795–815

[134] H. M. Ertunc and C. Oysu, Drill wear monitoring using cutting force signal, Journal of Mechatronics (2004), 14, 533–548

[135] Li Xiaoli and S.K. Tso, Drill wear monitoring based on current signals, Wear (1999), 231, 172-178

[136] S. C. Lin and C. J. Ting, Drill wear monitoring using neural network, International Journal of Machine Tools and Manufacture (1996), 36, 465–475

[137] H. M. Ertunc and K. A. Loparo, A decision fusion algorithm for tool wear condition monitoring in drilling, International Journal of Machine Tools and Manufacture (2001), 41, 1347–1362

[138] S. Das, A.B Chattopadhyay and A.S.R Murthy, Force parameter for on-line tool wear estimation: a neural network approach, Neural Network (1996), 9(9) 1639-1645

[139] L I Xioli and Y. Zhejun, Tool wear monitoring with wavelet packet transform fuzzy clustering method, Wear (1998), 219, 145-154

[140] V. Karri and T. Kiatcharoenpol, Tool condition monitoring in drilling using artificial neural networks, AI 2003, LNAI 2903, 293-301, T.D. Gedeon and L.C.C. Fung (Eds.)

[141] C.C. Tsao, Prediction of flank wear of different coated drills for JIS SUS 304 stainless steel using neural network, Journal of Material Processing Technology (2002), 123, 354-360

[142] T. I. Liu and K. S. Anantharaman, Intelligent classification and measurement of drill wear, Journal of Engineering Industries (1994), 116, 392-397

[143] R. K. Dutta, S. Paul and A. B. Chattopadhyay, The efficacy of back propagation neural network with delta bar delta learning in predicting the wear of carbide inserts in face milling, International Journal of Advance Manufacturing Technology (2006), 31, 434-442

[144] D. E. Dimla, Jnr., P. M. Lister and N. J. Leighton', Investigation of single layer perceptron neural network to tool wear inception in a METM turning process, 1996 The Institution of Electrical Engineers, 311 Printed and published by the IEE, Savoy Place, London WCPR OBL, 1

[145] D. E. Dimla Jnr., P. M. Lister & N. J. Leighton', Tool condition monitoring in metal cutting through application of MLP neural networks, The Institution of Electrical Engineers (1997), Printed and published by the IEE, Savoy Place, London WCSR OBL, UK

[146] T. Szecsi, Cutting force modeling using artificial neural networks, Journal of Materials Processing Technology (1999), 92-93, 344-349.

[147] T. Obikawa and J. Shinozuka, Monitoring of flank wear of coated tools in high speed machining with neural network ART2, International Journal of Machine Tools and Manufacture (2004), 44 1311-1318.

[148] S.V. Wong and A.M.S. Hamouda, Machinability data representation with artificial neural network, Journal of Materials Processing Technology (2003), 138, 538–544

[149] S. Das, R. Roy and A. B. Chottopadhyay, Evaluation of wear of turning carbide inserts using neural network, International Journal of Machine Tools and Manufacture (1996), 36, 789–797

[150] S. K. Choudhury, V. K. Jain and ChVV Rama Rao, On-line monitoring of tool wear in turning using neural network, International Journal of Machine Tools and Manufacture (1999), 39, 489–504

[151] E.O Ezugwu, S.J Arthur and E.L Hines, Tool-wear prediction using artificial neural network, Journal of Material Processing Technology (1995), 49, 255-264

[152] C. Harpham, C. W. Dawson and M. R. Brown, A review of genetic algorithms applied to training radial basis function networks, Neural Computing & Application (2004), 13, 193–201

[153] K. Hashmi, I.D. Graham and B. Mills, Fuzzy logic based data selection for drilling process, Journal of Material Processing Technology (2000), 108, 55-61.

[154] M.A. El Baradie, Fuzzy logic model for machining data selection, International Journal of Machine Tools and Manufacture (1997), 37(9), 1353-1372

[155] S.P. Lo, The application of an ANFIS and grey system method in turning tool-failure detection, International Journal of Advanced Manufacturing Technology (2002), 19, 564-572.

[156] M. Guillot, and A. EI Quafi, Online identification of tool breakage in metal cutting process by use of artificial neural network, Proceeding of ANNIE (1991), St Louis, MO, 701-703

[157] S. Elanayar and Y. C. Shin, Tool wear estimation in turning operation based on radial basis functions, Proceeding of Artificial Neural Network in Engineering, ANNIE (1991), St Louis, MO, 685-692

[158] Y. L. Yao and X. Fang, Assessment of chip forming pattern with tool wear progression in machining via neural networks, International Journal of Machine Tools and Manufacture (1993), 33, 89-102

[159] E. Goverkar and I. Grabec, Self organizing neural network application to drill wear classification, Journal of Engineering Industries (1994), 116, 233-238

[160] S. V. Karmathi, G. S. Sankar and P. H. Cohen and S. R. T. Kumara, Online tool wear monitoring using a Kohonen feature map, Proceeding of Artificial Neural Network in Engineering, ANNIE (1991), St Louis, MO, 639-648

[161] E. Govekar, I.Grabec and H.O. Madsen, Estimation of drill wear from AE signal using self organizing neural network, Proceeding of 14th world meeting on AE/ 1st International conference AE in manufacturing, ASNT, Boston, MA (1991), 65

[162] W. T. Chien and C. S. Tsai, The investigation on prediction of tool wear and the determination of optimum cutting conditions in machining17–4 PH stainless steel, Journal of Material Processing Technology (2003), 140, 340–345

[163] R. J. Kuo and P. H. Cohen, Multi-sensor integration for online tool wear estimation through radial basis function networks and fuzzy neural network, Neural Network (1999), 12, 355–370

[164] E. O. Ezugwu, D. A. Fadare, J. Bonney, R. B. Da Silva and W. F. Sales, Modeling the correlation between cutting and process parameters in high-speed machining of Inconel 718 alloy using an artificial neural network, International Journal of Machine Tools and Manufacture (2005), 45, 1375–1385

[165] R. J. Kuo, Multi-sensor integration for on-line tool wear estimation through artificial neural networks and fuzzy neural network, Engineering Application of Artificial Intelligence (2000), 13, 249–261

[166] J. A. Freeman and D. M. Skapura, Neural networks algorithm, application and programming techniques, Pearson Education (2004), Upper Saddle River, NJ, USA

[167] S. Haykin, Neural networks a comprehensive foundation, 2nd edition. Prentice Hall (2004), NJ, USA

[168] X. Li, S. Dong and P.K. Nenuvinod, Hybrid learning for tool wear monitoring, International Journal of Advanced Manufacturing Technology (2000), 16, 303-307.

[169] M. Balazinski, E. Czogala, K. Jemielniak and J. Leski, Tool condition monitoring using artificial intelligence methods, Engineering application of artificial intelligence (2002), 15, 73-80.

[170] C Chungchoo and D Saini, On line tool wear estimation in CNC turning operation using fuzzy neural network model, International journal of machine tool and manufacturer (2002), 42, 29-40.

[171] G. Huang, Y. Chen, and H. A. Babri, Classification ability of single hidden layer feed forward neural networks, Neural Networks (2000), 11, 799–801

[172] G. B. Huang and H. A. Babri, Upper bounds on the number of hidden neurons in feed forward networks with arbitrary bounded nonlinear activation functions, Neural Networks (1998), 9, 224–229.

[173] B Brophy, K. Kelly and G Byrne, AI-based condition monitoring of the drilling process, Journal of Material Processing Technology (2002), 124, 305-310

[174] R. G. Petersen, Design and analysis of experiments, Marcel Dekker Inc, New York and Basel, 1992

[175] Y. L Yao and X. D Fang, Assessment of chip forming pattern with tool wear progression in machining via neural network, International Journal of Machine Tools and Manufacture (1993), 33(1), 89-102

[176] T. Kohonen, The self-organising map, Neuro-computing (1998), 21, 1-6

[177] Y. X. Yao, X. Li and Z. J. Yuan, Tool wear detection with fuzzy classification and wavelet fuzzy neural network International Journal of Machine Tools and Manufacture (1999), 39, 1525–1538

[178] C. Scheffer, H. Kratz, P.S. Heyns and F. Klocke, Development of a tool wear monitoring system for hard turning, International Journal of Machine Tools and Manufacture (2003), 43, 973–985

[179] S.K. Choudhury and G. Bartarya, Role of temperature and surface finish in predicting tool wear using neural network and design of experiments, International Journal of Machine Tools and Manufacture (2003), 43, 747–753

[180] O. Yumak and H. M. Ertunc, Tool Wear Condition Monitoring in Drilling Processes Using Fuzzy Logic, ICONIP 2006, Part III, LNCS 4234, 508–517

[181] E.O. Ezugwu, D.A. Fadare, J. Bonney, R.B. Da Silva and W.F. Sales, Modeling the correlation between cutting and process parameters in high speed machining of Inconel 718 alloy using an artificial neural network, International Journal of Machine Tools and Manufacture (2005), 45 1375-1385

[182] J. Sun, G.S. Hong, Y.S Wong, M. Rahman and Z.G. Wang, Effective training data selection in tool condition monitoring system, International Journal of Machine Tools and Manufacture (2006), 46 218-224

[183] T.I Liu and K.S. Anantharaman, On-line sensing of drill wear using neural network approach, IEEE Transaction (1993), 0-7803-0999-5/1993

[184] Snr D. E. Dimla, Application of perceptron neural networks to tool-state classification in a metal-turning operation, Engineering Applications of Artificial Intelligence (1999), 4(12), 471-477

[185] G. Chryssolouris and M. Guillot, A comparison of statistical and AI approaches to the selection of process parameters in intelligent machining, Journal of Engineering Industries (1990), 112, 122-131

[186] R. P. Lippmann, An introduction to computing with neural nets, IEEE ASSP (1987), 4-22

[187] P. K. Simpson, Foundations of neural networks, Artificial Neural Network, Paradigms, Application and Hardware Implementations, IEEE Press, 1992.

[188] P.G. Benardos and G.C. Vosniakos, Predicting surface roughness in machining: a review, International Journal of Machine Tools and Manufacture (2003), 43, 833-844

[189] P. Palanisamy, I. Rajendran and S. Shanmugasundaram, Prediction of tool wear using regression and ANN models in end-milling operation, International Journal of Advance Manufacturing Technology (2007), DOI 10.1007/s00170-007-0948-5

[190] R. Quiza, L. Figueira and J. P. Davim, Comparing statistical models and artificial neural networks on predicting the tool wear in hard machining D2 AISI steel, International Journal of Advance Manufacturing Technology (2007), DOI 10.1007/s00170-007-0999-7

[191] T. Ozel and Y. Karpat, Predictive modeling of surface roughness and tool wear in hard turning using regression and neural networks, International Journal of Machine Tools and Manufacture 45 (2005) 467–479

[192] C. Sanjay, M.L. Neema and C.W. Chin, Modeling of tool wear in drilling by statistical analysis and artificial neural network, Journal of Materials Processing Technology (2005), 170, 494–500

[193] S. Rajsekharan and G. A. Vijayalakshmi Pai, Neural networks, Fuzzy Logic, and Genetic algorithms synthesis and applications, New Delhi, PHI Publication (2003)

[194] A. Kaufmann and M. M. Gupta, Introduction to fuzzy arithmetic theory and application, International Thomson computer press (1991)

[195] F. Ham and I. Kostanic, Principles of Neurocomputing for Science and Engineering, New York, Mcgraw-Hill (2001)

[196] M. Bakkal, A. J. Shih, S. B. McSpadden, C.T. Liu and R. O. Scattergood, Light emission, chip morphology, and burr formation in drilling the bulk metallic glass, International Journal of Machine Tools and Manufacture 45 (2005) 741–752

[197] S.A. Batzer, D.M. Haan, P.D. Rao, W.W. Olson and J.W. Sutherland, Chip morphology and hole surface texture in the drilling of cast Aluminum alloys, Journal of Materials Processing Technology 79 (1998) 72–78